Durham University

Durham E-Theses

Relaxation mechanisms in maser materials

Mason, D. R.

How to cite:

Mason, D. R. (1966) *Relaxation mechanisms in maser materials*, Durham theses, Durham University. Available at Durham E-Theses Online: http://etheses.dur.ac.uk/8859/

Use policy

The full-text may be used and/or reproduced, and given to third parties in any format or medium, without prior permission or charge, for personal research or study, educational, or not-for-profit purposes provided that:

- a full bibliographic reference is made to the original source
- a link is made to the metadata record in Durham E-Theses
- the full-text is not changed in any way

The full-text must not be sold in any format or medium without the formal permission of the copyright holders.

Please consult the full Durham E-Theses policy for further details.

Academic Support Office, The Palatine Centre, Durham University, Stockton Road, Durham, DH1 3LE
e-mail: e-theses.admin@durham.ac.uk Tel: +44 0191 334 6107
http://etheses.dur.ac.uk

Relaxation Mechanisms in Maser Materials

by

D. R. Mason, B.Sc.

A thesis submitted in candidature for the degree of

Doctor of Philosophy

University of Durham

June, 1966.

20 OCT 1966
LIBRARY

ABSTRACT

Measurements have been made using a pulse saturation technique at 35 Gc/s of the relaxation times for transitions within the ions of the 'iron group' of transition metal elements placed in various lattices. A microwave spectrometer has been constructed in which the need for a separate local oscillator source has been overcome. A detailed study of the relaxation times and the texture in ruby single crystals has shown that the relaxation depends on the c-axis misorientation within the crystal, but is independent of the mosaic structure. A study of the temperature dependence of the relaxation times from $1.5^{o}K$ to $120^{o}K$ has shown that the chromium ions occupy two types of site within the lattice, one perfect the other distorted. Similar results have been obtained for samples of ruby grown by Verneuil and Czochralski techniques.

The effect of impurities in ruby has been considered and a 'figure of merit' has been empirically devised to describe the effects of cross-relaxation between chromic and ferric ions. X-irradiation of rubies has given indirect evidence for the existence of the Cr^{2+} ion.

A brief examination of the relaxation times in chromium doped spinel and rutile has led to an explanation of the frequency dependence of the relaxation times for

transitions across the lower Kramer's doublet in terms of an Orbach process.

An examination of three alums has supported the suggestion of Kochelaev that the relaxation process in these materials is governed by the vibrations of the water complex surrounding the paramagnetic ion.

ACKNOWLEDGEMENTS

I would like to thank the following organizations and people for their generous help, fiscal and otherwise, without which the present course of study could not have been completed. The Admiralty C.V.D. and the Science Research Council, formerly D.S.I.R., for their financial aid. The Thermal Syndicate Ltd., for their co-operation in supplying samples. Professor D.A. Wright, my supervisor Dr. J.S. Thorp, and the staff of the Department of Applied Physics, for their enthusiasm, help and constant encouragement. Research students and colleagues within the Department, in particular Dr. D.A. Curtis, C.J. Kirkby and G. Brown for their ideas and advice. The technical staff led by Mr. F. Spence for their ingenuity and unfailing efforts to make a practical expression of my ideas. Miss F.Harland who has carefully typed the original manuscript, and the staff of the Examinations Department who copied it using a Xerox machine.

D. R. Mason

CONTENTS

Chapter 7 - continued

Chapter I

Introduction

A considerable amount of effort in physics this century has been devoted to the study of the interaction of electromagnetic radiation with matter. The fundamental work of Einstein (1917) concerning stimulated absorption, stimulated emission and spontaneous emission of radiation led to developments from which the maser resulted. One of Einstein's results was that the probability per unit time of stimulated emission was equal to the probability per unit time of stimulated absorption. Thus the net power absorbed per unit volume by a system of weakly interacting atoms, with energy levels E_1 and E_2, from a radiation field of frequency $\nu = (E_2 - E_1)/h$ is

$$P = h\nu \; w \; (n_1 - n_2)$$

where n_1 and n_2 are the population densities of levels E_1 and E_2, and w is the stimulated absorption probability per unit time. Prior to the advent of the maser, atomic systems had usually been considered to be in thermal equilibrium, with the population distribution

MONTANA STATE UNIVERSITY SCIENCE
20 OCT 1966
SCIENCE LIBRARY

given by the Boltzmann formula :

$$\frac{n_1}{n_2} = \exp(h\nu/kT)$$

so that $n_1 > n_2$. It was recognised that emission may have been possible if the distribution could be suitably disturbed so that $n_2 > n_1$. Bloch (1946) and Purcell and Pound (1951) both achieved stimulated emission in their experiments on atomic nuclei but it was not until 1953 that Weber proposed that an inverted population could be used for amplifying microwaves. One year later Gordon, Zeiger and Townes obtained coherent radiation from the inverted population of two energy levels in an ammonia beam. Similar work was done independently by Basov and Prokhorov, who suggested the three level maser in 1955. The first demonstration of this principle in a solid was by Scovil, Feher and Seidel (1957) who produced oscillations at 9 Gc/s by inverting two paramagnetic spin levels of Gd^{3+} in lanthanum ethyl sulphate. Since this experiment masers and lasers (using the optical levels within the ions) have been used extensively and the need for more efficient devices has made the study of paramagnetically doped materials particularly important.

In a paramagnetic atom the electron distribution is such that there is a residual magnetic dipole. If a small number of such atoms are distributed in a diamagnetic host lattice the magnetic properties of the latter are so weak that the paramagnetic properties of the substituted atoms dominate.

The Zeeman energy levels of a paramagnetic atom built into a solid crystalline lattice are roughly similar to the Zeeman levels of the free atom. There are, however, important differences which result chiefly from the strong crystalline fields between atoms in the crystal lattice. A particularly important result of this is that the overall angular momentum J of an atom depends on the particular lattice in which it is placed. For the iron group atoms, whose paramagnetic properties derive from partially filled 3d shells, the ground state energy levels are widely separated in energy from the upper excited states and the orbital momentum is said to be quenched. In this case J becomes equal to S, the spin angular momentum, and the degeneracy of the levels is then (2S + 1). It must be noted that S may not always be the spin quantum number of the free atom, as in some cases where the number of levels does not equal (2S + 1) an effective spin S' is used such that

the degeneracy condition is satisfied. The energy separation of levels which are split solely by a magnetic field is:

$$E = M\, g\, \beta\, H$$

M = 1 for a doublet of S = 1/2, H is the magnetic field, ß the Bohr magneton and g is homologous to the Lande g-factor. If the levels are due solely to a free spin, g = 2, the value of g is an indication of the degree of quenching of the orbital angular momentum. If the ground state levels are labelled with the spin quantum numbers, transitions may be seen between levels for which such transitions are strictly forbidden by the selection rule $\Delta M = 1$. This is because usually a particular state is a mixture of pure spin states and cannot be described by a single spin quantum number. For example, in an atom with S = 3/2, a particular energy eigenstate is represented as

$$|i\rangle = a_i\ |3/2\rangle + b_i\ |1/2\rangle + c_i\ |-1/2\rangle + d_i\ |-3/2\rangle$$

where

$$|a_i|^2 + |b_i|^2 + |c_i|^2 + |d_i|^2 = 1$$

A particular example of this case is the Cr^{3+} ion in Al_2O_3. If the magnetic field is directed along the

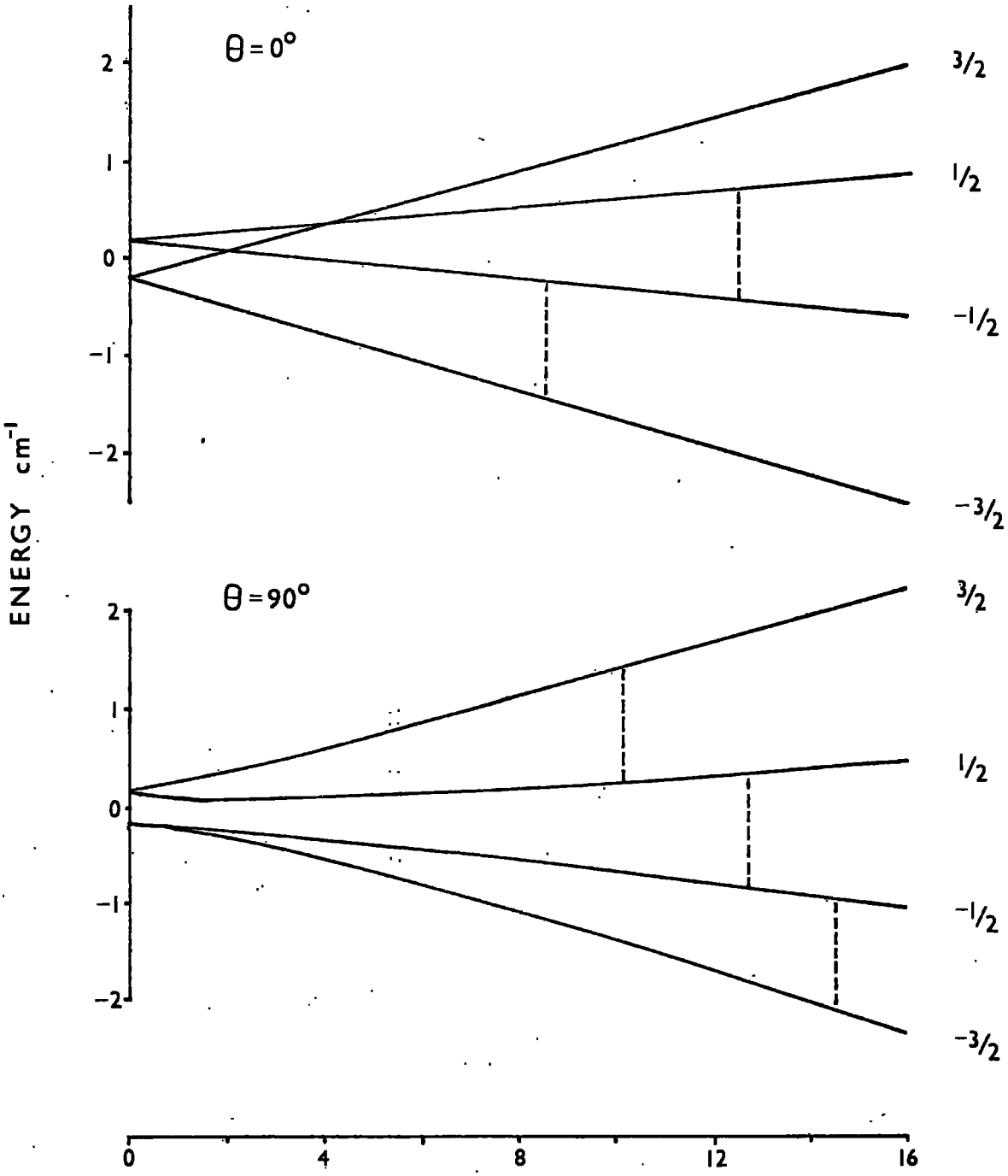

Ground Levels of Cr^{3+} ion in Al_2O_3

Fig. I.I

trigonal axis of the crystal (polar angle $\theta = 0^{o}$) the levels can be described by pure spin values. As θ is varied the degree of mixing of the states changes, and so nominally forbidden transitions are allowed. The Zeeman energy levels for ruby for $\theta = 0^{o}$ and $\theta = 90^{o}$ are shown in fig. 1.1. with the $\Delta M = 1$ transitions at 35 Gc/s marked. The labelling of the levels is after the notation of Schultz-du Bois (1959), and it will be understood from the previous comments that the use of a single quantum number is not strictly valid.

A concise description of the ground state levels is given by the quantum mechanical spin Hamiltonian for an ion. This depends on the particular crystal symmetry but can be generally represented as follows:

$$\mathcal{H}_s = g\,\beta\,\underline{H}.\underline{S} + D\left[S_z^2 - S(S+1)\right] + E\left(S_x^2 - S_y^2\right)$$

The first term describes the orientational energy of

Omit lines 20 - 23

Replace by :

The energy separation of the levels in zero field arises from contributions from the D and E terms in the spin Hamiltonian. In the case when E 0, the zero field splitting is 2D. Additional terms are required if the atom ...

Hamiltonian is sufficient to describe the different materials examined in the present work. The constants for the spin Hamiltonian of ruby are $g_{\perp} = 1.986$ and $g_{/\!/} = 1.984$ indicating that the ground state levels are almost pure spin; $2D = -0.3831\ cm^{-1}$, E is approximately equal to zero. Using the spin Hamiltonian the solutions of the equation

$$\mathcal{H}_s\ |n> = E_n\ |n>$$

can be found in terms of E_n, the energies of particular eigenstates. Consider a simple two energy level system E_1 and E_2, where $E_2 > E_1$, and the populations of the two levels n_1 and n_2 are determined by the Boltzmann formula. If radiation of the correct frequency is present the thermal distribution is disturbed because the stimulated absorption probability is equal to the stimulated emission probability. Purcell (1946) has shown that the spontaneous emission probability is negligible so that another mechanism is necessary to allow the spin system to return to equilibrium when the radiation is removed. In fact the distribution is restored through a relaxation transition probability which is greater for a downward transition than for an upward one, the ratio of the probabilities is :

$$\frac{W_{12}}{W_{21}} = \frac{n_2}{n_1}$$

The small but finite interaction of the spins with the lattice through the spin orbit coupling allows the spins to 'feel' the modulation of the crystalline electric field around the atom due to the thermal vibrations of the lattice, and this is what gives rise to the relaxation probability. Andrew (1958) reports an explanation by Bloembergen of why there is a difference between the upward and downward probability rates. For a simple model suppose that the lattice is simulated by a set of harmonic oscillators whose equally spaced energy levels are separated by $(E_2 - E_1)$, the spin energy level difference. The probability that a spin will make an upward transition by exchanging a quantum of energy $(E_2 - E_1)$ with the lattice is proportional to the probability that the oscillator is in a state other than the lowest energy state, since if it is in this state it cannot give up a quantum of energy. On the other hand for a downward transition the spin gives up a quantum of energy and this can always be accepted by an oscillator.

If we write $n = n_1 - n_2$, the rate of change of n when the populations have been disturbed is given by :

$$\frac{1}{2}\frac{dn}{dt} = n_2 W_{21} - n_1 W_{12}$$

$$= 2 W (n_o - n)$$

where W is the mean of the transition probabilities, and n_o is the value of n when the system is in thermal equilibrium. Thus :

$$n_o - n = (n_o - n_\alpha) \exp. (-2Wt)$$

n_α is the initial value of n. The system returns to equilibrium with a characteristic time constant

$$\tau = \frac{1}{2W}$$

Grant (1964) has shown that in general for a p level system, there are (p - 1) independent equations describing the return to equilibrium of the system and the quantities $1/\tau_i$ are the eigenvalues of the (p - 1) dimensional matrix $M_{SL_{ij}}$ where

$$M_{SL_{ij}} = (W_{ij} - W_{Li}) - \delta_{ij} \sum_{k=1}^{p} W_{ik}$$

i = 1, 2, ...p, and L is the level we have chosen to eliminate by taking only (p - 1) equations.

The presence of other energy levels in the crystal with a similar energy separation to the ones under investigation, whether they arise from the same ion or a different paramagnetic species, will modify the above rate equations. A process known as cross-relaxation

occurs and is represented by a transition probability W_{cr}. (Bloembergen et al, 1959). In the simplest case when the separation of two pairs of energy levels is the same, spins in the upper level of one pair exchange energy with those in the lower level of the other. The transfer of energy from one transition to another will continue throughout the spin system in an attempt to establish thermal equilibrium amongst the spin transitions involved, although the total spin system energy is always conserved. As a small amount of energy can be taken up by adjustment of the dipolar interaction of the spins (Siegman 1964) the cross-relaxation can take place over a range of energies. The analyses of Kiel (1960) and Kopvillem (1961) predict that the cross-relaxation lineshape is fairly broad and independent of concentration for very low spin concentrations. Harmomic cross-relaxation also occurs (Chang 1960) when more than one quantum is absorbed or one quantum of energy is shared by several spins. A detailed description of the effects of cross-relaxation on the rate equations has been given by Grant (1964).

In recent years attempts have been made to try and predict the effect of a non-ideal lattice on the relaxation time. As will be seen in the next chapter the theoretical predictions of the relaxation times have been made

assuming a perfect lattice. However, it is known that most materials and especially those grown at high temperatures have large dislocation densities, and so the assumptions of the theory are not justified. At present only simple modifications have been made to the existing theory to allow for the alteration of the phonon spectrum in crystals due to defects.

The majority of measurements reported in this thesis have been made on single crystals of ruby. This material has been widely used in masers and lasers and has the advantage of having a relatively simple energy level system. Several growth methods have been used in an attempt to obtain a high degree of chemical purity and crystalline perfection. Most of the rubies examined were grown by flame fusion from the vapour phase. Normally halides of aluminium and chromium are used as source vapours and are fed into an oxy-hydrogen flame. The boule grows on a carefully orientated seed crystal in a furnace at 2050^{o}C. The seed is withdrawn at such a rate that the surface of fresh material is always in the same plane of the furnace and subsidiary heating elements are used to reduce thermal gradients in the boule. The orientation of the seed crystal relative to the growth direction of the boule can be varied. The two most generally preferred growth directions are 0^{o}

and 90°, that is the growth direction is parallel and perpendicular respectively to the c-axis of the boule. The Verneuil method is similar to the above except that the starting materials are in powdered form. This has the disadvantage that the chemical purity of these materials is lower than if they were in vapour form. It is found that the chromium distribution across the boules is different for the two methods. Rubies with high chemical purity and small physical imperfection have been obtained using a Czochralski technique in which the seed crystal is placed in contact with the molten surface of the ruby starting material, and then gradually withdrawn. The boule grows on the surface of the seed and dislocation densities 100 times less than for the other methods which have been reported. A low temperature growth method using a flux has been developed working at approximately 1000°C, but until recently (Linares 1965) the size of the crystals has been small and the impurity content high.

After an outline of the experimental results in chapter 3, the results and discussion of the results will be found in the later chapters. In addition to the results on ruby one chapter has been devoted to measurements made on three or four other materials to

give an indication of the magnitude of the relaxation times at 35 Gc/s. From these some conclusions concerning the magnetic field dependence can be drawn.

Chapter 2

Theory

2.1 Introduction

The first theoretical calculations of the relaxation time τ were made by Waller in 1932. He considered a paramagnetic ion in a diamagnetic host lattice, with the spin moment and orbital moments of the ion completely decoupled, the resulting magnetism being derived entirely from the spin. If the spin and orbit are completely decoupled the only mechanism limiting the lifetime of the energy state is the spin - spin interaction - the coupling of the neighbouring spin precessions. Waller assumed that the lattice vibrations influence the spin only by modulating the spin - spin interaction. The results obtained were entirely too large to agree with experiment. Heitler and Teller incorporated the effects of the modulations of the crystalline Stark effect schematically, but their estimates were still too large by a factor of 10^2 to 10^4. In 1940 Van Vleck produced a calculation for the relaxation times of titanium and chromium in ammonium alum, based on the interaction between the spin and the modulating crystalline field. This form of interaction is

allowed as the spin is never completely decoupled from the orbit, and this is particularly applicable to the ions of the 'iron group'which occur in the periodic table from scandium to nickel. The magnitude of the results agreed quite well in the liquid air temperature range, but poor agreement was found at helium temperatures for the titanium alum. Recently Mattuck and Strandberg (1961) have modified Van Vleck's method without making any new physical assumptions but giving a clearer insight of the physical significance of the mathematical processes used. An outline of this method will now be given.

2.2 Modified Van Vleck Calculation

If the crystalline field potential is smaller than the free ion potential but greater than the spin-orbit energy, then the latter may be considered as a perturbation superimposed on the total energy, and perturbation theory can be used. The total Hamiltonian can be written in the form:

$$\mathcal{H} = \mathcal{H}_L + \mathcal{H}_o + V + 2\beta \underline{S}.\underline{H} + \lambda \underline{L}.\underline{S} + \beta \underline{L}.\underline{H}$$

β is the Bohr magneton, λ is the spin-orbit coupling

parameter, $\underline{S}$ and $\underline{L}$ are the spin and orbital angular moments of the paramagnetic ion, $\underline{H}$ is the external d.c. magnetic field, V is the energy of the ion due to the crystalline electric field, $\mathcal{H}_o$ is the energy of the free ion, and $\mathcal{H}_L$ represents the lattice energy. The lattice Hamiltonian can be written:

$$\mathcal{H}_L = \sum \hbar\omega_p \ (a_p^+ a_p + 1/2)$$

where a_p^+, a_p are the phonon creation and annihilation operators. V can be expanded as a power series of the form:

$$V = V_o + \sum_{fp} V^f A^f p_p + \sum_{ff'pq} V^{ff'} A^{fp} A^{f'q} p_p p_q + \ldots.$$

$$V^f = \frac{dV}{dQ_f} \qquad V^{ff'} = \frac{1}{2} \frac{\delta^2 V}{\delta Q_f \delta Q_{f'}} \qquad p_p = a_p + a_p^+$$

Q_f is the normal co-ordinate of the displacement of the ion nearest neighbours, A^{fp} is the ordinary displacement of the neighbours. Substituting the expansion of V in the total Hamiltonian the latter can be divided into three terms as follows:

$$\mathcal{H}_{\text{lattice}} = \sum_p \hbar\omega_p (a_p^+ a_p + 1/2)$$

$$\mathcal{H}_{\text{spin}} = \mathcal{H}_o + V_o + 2\beta \underline{S}.\underline{H} + \lambda \underline{L}.\underline{S} + \beta \underline{L}.\underline{H}$$

$$\mathcal{H}_{\text{int.}} = \sum_{fp} V^f A^{fp} p_p + \sum_{ff'pq} A^{fp} A^{fq} p_p p_q V^{ff'}$$

Alternatively, the interaction Hamiltonian can be written:

$$\mathcal{H}_{\text{int.}} = Ae + Be^2 \qquad (2.1)$$

where e is the strain and A and B are the appropriate coupling parameters. The calculation then involves using second order perturbation theory in $\mathcal{H}_{\text{spin}}$ producing the spin Hamiltonian, finding the energy levels, E_k, and the corresponding state function and then computing the appropriate matrix elements of $\mathcal{H}_{\text{int}}$ between simultaneous eigenstates of $\mathcal{H}_{\text{spin}}$ and $\mathcal{H}_{\text{lattice}}$

Two types of relaxation process must be considered. The 'direct process' in which the spin absorbs a quantum of energy from the lattice equal to the spin energy, or imparts a quantum of the same energy to the latter.

The Raman process where the spin absorbs a quantum of energy of one frequency and emits that of another, the difference in energies of the two quanta equalling the spin energy. Because the Raman process is of second order and requires a large number of phonons, it is found that the direct process dominates at low temperatures and the Raman at high temperatures. For the direct process the outlined calculation leads to a relaxation time τ of the form:

$$\frac{I}{\tau_D} = AT$$

A is a constant, T the absolute temperature. If the lowest energy levels are multiple Kramers doublets the Raman term is:

$$\frac{I}{\tau_R} = BT^7 \int_0^{\theta_o/T} \frac{x^6 e^x dx}{(e^x - I)^2} \qquad (2.2)$$

B is a constant, θ_o the Debye temperature of the lattice. For an isolated Kramers doublet, the T^7 term in equation 2.2 would be replaced by one of T^9. The function

$$J_6(X) = \int_0^X \frac{x^6 e^x dx}{(e^x - I)^2}$$

has been tabulated by Ziman (1954) and more completely by Rogers and Powell (1958). Graph 2.1 shows $J_6(X)$ plotted against X. For large X ($T << \theta_o$) $J_6(X)$ is a constant,

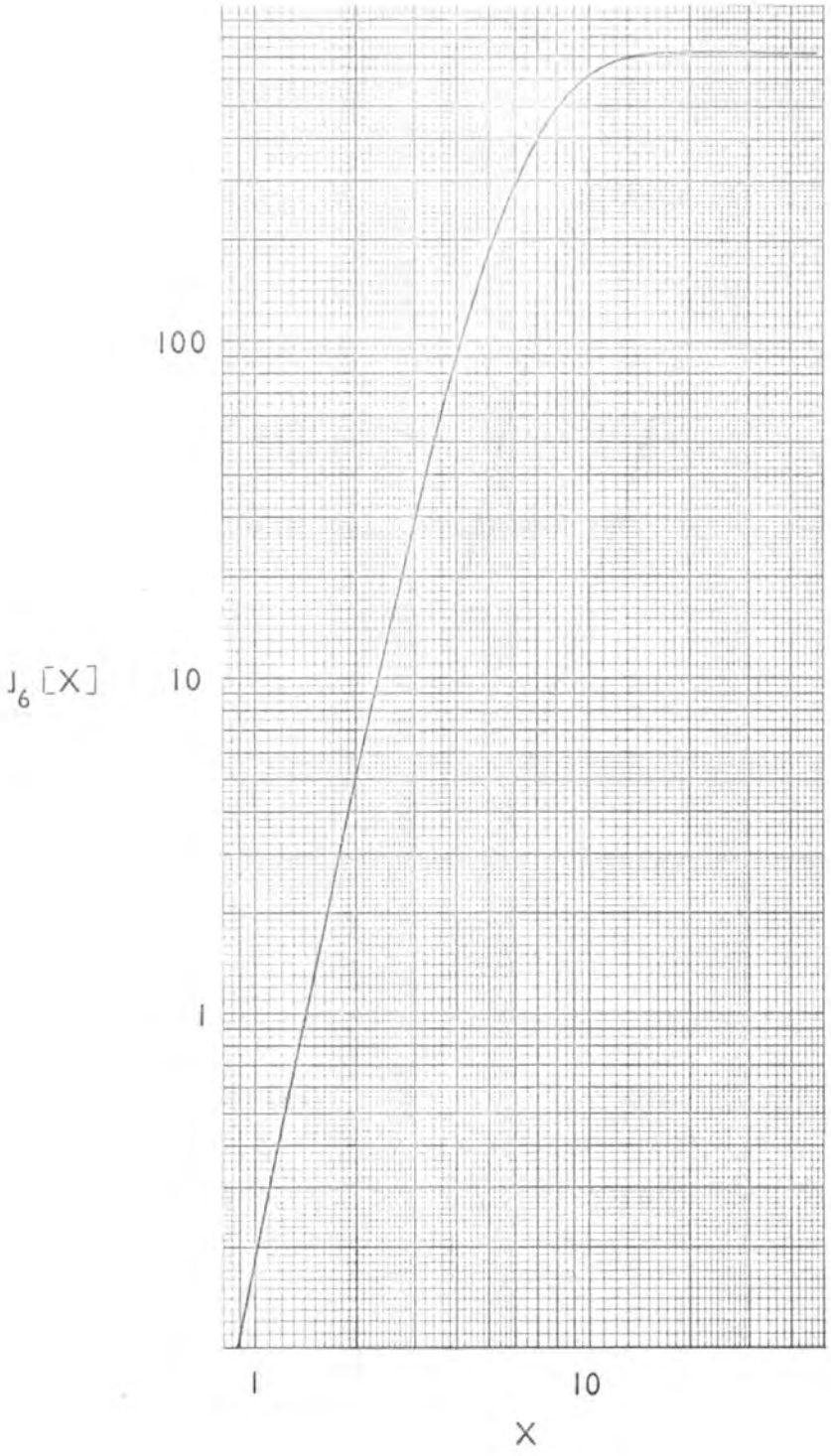

Variation of $J_6[X]$ with X

Fig. 2.1

thus :

$$\frac{I}{\tau_R} = BT^7$$

For small X ($T \geqslant \Theta_{/2}$) $J_6(X)$ varies as X^5, thus:

$$\frac{I}{\tau_R} = BT^2$$

For intermediate values of X the temperature dependence will lie between these two limits.

The general formula for the Debye temperature can be written:

$$\Theta_o = \frac{h}{k} \left(\frac{3N}{4\pi V}\right)^{1/3} \left[\sum_{i=1}^{3} \int \left\{ V_i(\Theta,\emptyset) \right\}^{-3} d\Omega \right]^{-1/3} \qquad (2.3)$$

N is the number of atoms in the solid, V the volume of the crystal and V_i $(\Theta,\emptyset)$ the velocities of the longitudinal elastic waves at 0^oK. Betts et al (1956) quote values of Θ_o using solutions of the Christoffel equations with elastic constants measured by Bhimasenacker (1950). The average value for ruby was $\Theta_o = 880^oK$, three values being obtained for the three possible solutions of the Christoffel equations. More recent values of the elastic constants have been published by Wachtman et al (1960) which have been used by Donoho for calculating the relaxation times in ruby, and these differ from previous

values quite considerably. If these constants are used a value of Θ_o is obtained equal to 1050°K. The large change in Θ_o using the two sets of elastic constants is due mainly to the magnitude of C_{14}. Bhimasenacker obtained $C_{14} = 1.01 \times 10^{18}$ dynes/cm^2 whereas Wachtman quoted $C_{14} = -2.4 \times 10^{18}$ dynes/cm^2. The large difference in the two estimations is disturbing, but the more recent results seem to be the most accurate. An alternative method for calculating the velocity of the elastic waves is possible using the values of the specific heat at constant pressure C_p, which have been measured at low temperatures. Using the values for corundum of Furukawa et al (1956) Wachtman et al (1962) have obtained the values of the Debye temperature, following the extrapolation method recommended by Barron and Morrison (1959). For temperatures below 30°K, Θ_o was found to be 1045°K, an average value using the measurements at higher temperatures was 950°K. The values of Θ_o obtained from the specific heat data are probably more accurate than those calculated from the elastic constants at room temperature, even though the vibrational anisotropy has not been considered. In table 2.1 the temperature dependences in the Raman region have been calculated using equation 2.2 for the various values of Θ_o. The conclusion from

x	Temperature Dependence	Temperature ^{o}K θ_o=850^{o}K	θ_o=950^{o}K	θ_o=1050^{o}K
≤ 2	T^{-2}	≥ 425	≥ 475	≥ 525
5	T^{-4}	170	190	210
6	$T^{-4.8}$	142	160	178
8	$T^{-5.5}$	106	119	131
10	$T^{-6.2}$	85	95	105
13	$T^{-6.8}$	66	73	80
≥ 20	T^{-7}	≤ 42	≤ 47	≤ 52

Variation of Temperature Dependence in Raman Region with θ_o

Table 2.1

these results is that the T^7 region is expected at lower temperatures and the dependence on temperature decreases as temperature increases.

For the Raman process the energies of the absorbed and scattered phonons are unimportant, their difference in energies, however, must be exactly equal to the spin energy. This means that all phonons available within the lattice can be used. In 1961 Orbach showed that another two phonon process could occur, and was particularly apparent in the rare earth salts. If, for example, the orbital levels of the ion are separated by an energy Δ and $\Delta > kT$ but $\Delta < \theta_o$ then a relaxation process will occur in which a phonon is absorbed raising a spin in an upper ground state level into the upper orbital level, when a second phonon is emitted the spin returns to the lower ground state level. The relaxation time τ_o for such a process is:

$$\frac{1}{\tau_o} = C \Delta^3 e^{-\Delta/kT}$$

For the iron group ions $\Delta > \theta_o$ and so the effect is unobservable. However, the splitting of the two Kramer's doublets may be great enough in the iron group for an Orbach process to occur across them. Previously it was noted that a multilevel Kramer's state gave a

temperature dependence of T^{-7} for τ_R, however Orbach and Blume (1962) have pointed out that in certain cases a T^{-5} dependence may be expected. Very roughly the condition for T^{-5} dominance over T^{-7} is :

$$\lambda (\lambda / \Delta) \geq kT$$

λ is the spin orbit coupling and Δ the crystalline field splitting for the orbital levels. For the Cr^{3+} ion in an octahedral environment the condition is not satisfied because of the large value of Δ . For the rare earth ions where Δ is small, a T^{-5} dependence may occur.

2.3 Donoho Calculation

In 1964 Donoho published a calculation for the relaxation times in ruby at $4.2^{o}K$ which gave the results for the different transitions across the ground levels at various polar angles θ. The basis of the calculation was to express the spin-lattice interaction Hamiltonian as a spin operator quadratic in spin and linear in strain (i.e. considering the direct process) as did Van Vleck, but to use the more general representation of Feher and Watkins namely :

$$\Sigma_{i,\ j} D_{i,j} S_i S_j$$

The tensor D is related linearly to strain as follows:

$$D_{ij} = \sum_{i,j,k,l} G_{i,j,k,l}\, e_{k,l}$$

The tensor G has many of the symmetry properties of the elastic stiffness tensor, and was known from previous measurements of Hemphill and Donoho (1963). The strain is calculated using the general expression for the displacement of an atom U(r) due to the passage of a phonon through the lattice. Then:

$$e_{i,j} = \frac{1}{2}\left(\frac{\partial U_i}{\partial x_i} + \frac{\partial U_j}{\partial x_j}\right)$$

The transition probability is given by

$$W_{i,f} = \frac{2\pi}{\hbar} |\langle i | \mathcal{H}' | f \rangle|^2 \, \mathfrak{D}_f(\epsilon_i)$$

where the interaction Hamiltonian $\mathcal{H}'$ causes transitions between states i and f, and $\mathfrak{D}_f(\epsilon_i)$ is the density of phonon states. Substituting into the equation for the transition probability the final expression is

$$W_{ij} = \frac{\omega e^{\hbar\omega/kT}}{32\pi^2 \rho \hbar (e^{\hbar\omega/kT} - 1)} \int \sum_{p=1}^{3} \left| \sum_{mnst} G_{mnst} \langle i | s_m s_n | j \rangle \right.$$

$$\left. (\epsilon_{ps} k_t + \epsilon_{pt} k_s) \right|^2 \frac{d\Omega}{v_{kp}^3}$$

v_{kp} is the phase velocity, ϵ_p the polarisation vector. W_{ij} is the transition probability per unit time for a transition in which the ion goes from state i to state j and a phonon mode of frequency $\omega = (E_i - E_j)/h$ goes from occupation number n to n + 1. Because of the vibrational anisotropy of the crystal the transition probability has to be computed as a sum over all polarisation directions and an integral part over all directions of the phonon wave vector $\underline{k}$. For a particular direction of $\underline{k}$ the Christoffel equations give three phase velocities for the three polarisation directions, in terms of the elastic constants of the material. The matrix elements of the quadratic spin operators were obtained for each direction of magnetic field, using the simplified Hamiltonian:

$$\mathcal{H}_s = g\beta\, \underline{H}.\underline{S} + D(S_z^2 - 5/4)$$

The original results were presented in the form of the relaxation times between the four levels of the ion for different directions of the applied field, θ. The three relaxation times and the associated amplitudes between any two of the levels were calculated for frequencies from 1 to 10 Gc/s. Graphs 1 to 6 in Appendix 1 show a similar set of results for a measuring frequency of 35 Gc/s communicated privately by

2.4 Modifications due to Local Strain

The previous calculations have expressed the strain e of the arrangement of atoms immediately surrounding the spin site as a superposition of strains due to normal modes of the perfect crystal (i.e. lattice waves). Klemens (1963) has pointed out that the assumption of a perfect lattice may be very wrong and that the strain at the spin site may differ appreciably because of this. Firstly, if the substitutional paramagnetic ion differs appreciably from the ion it replaces, an additional strain term arises. Secondly, the ion may be sitting at a defect site, e.g. in a distorted part of the lattice near a grain boundary, and again the strain field will be different from that in a perfect lattice.

Consider an ion at a defect site which will have one or more characteristic vibrational frequencies w_i, associated with it. If $w_i > w_D$, the Debye frequency cut off, vibrations at this frequency will be unable to propagate through the lattice but will be localised at the defect. Thus the strain is localised at the defect and a modification of the temperature dependence

of the relaxation time in the Raman region will result. Klemens (1962) calculated the dependence to be:

$$\frac{1}{\tau_{Ro}} = D' e^{-\theta_i/T}$$

Montroll and Potts (1955) showed that if the substitutional ion was at least 20% lighter than the ion it replaces then assuming the binding forces are the same, such a localised mode will occur.

If $w_i < w_D$ then the vibrations of the defect will be able to propagate through the lattice and the strain will not be localised. However, the relaxation time will be affected because the defect system undergoes forced oscillation under the influence of the lattice waves. The calculation is given in detail by Castle et al (1963), only the result will be given here :

$$\frac{1}{\tau_{R'}} = F\left\{B^2\left(\frac{T}{\theta_o}\right)^7 J_6\left(\frac{\theta_o}{T}\right) + \alpha^2 B'^2\left[\left(\frac{T}{\theta_o}\right)^3 J_2\left(\frac{\theta_o}{T}\right) - \left(\frac{T}{\theta_o}\right)^3 J_2\left(\frac{\theta_i}{T}\right) + \frac{T^{11}}{\theta_i^8\,\theta_o^3} J_{10}\left(\frac{\theta_i}{T}\right)\right]\right\}$$

F,B,α, and B' are constants and the integral $J_2(\theta_o/T)$ is of the same form as $J_6(\theta_o/T)$ except x is squared and not to the power 6. It can be shown that the fourth term in this equation will always be less than the third. This equation represents a simplified situation because two distinct strains were considered, one for $w < w_i$, and the other for $w > w_i$. We must now consider two further cases (i) w_i not very much below w_D (ii) w_i very much below w_D. The first case has been discussed by Castle et al (1961) for Cr^{3+} in MgO, where the heavier chromium ion causes a defect site which may have a frequency of the order of $w_i = m^{-1/2} w_D$, m is the ratio of the masses of chromium and magnesium ions. For lattice waves of higher frequencies the strain is enhanced and the spin-lattice relaxation time varies more rapidly than the Raman prediction for perfect material. If w_i is very much below w_D then there is a wide range of temperature for which $\theta_i < T < \theta_o$ and the temperature variation of τ_R. will be T^{-3}.

The spin may be coupled to the strain e as in equation 2.1, and it may also be coupled to the imperfect strain e' through a relation analagous to 2.1 with coupling parameters A' and B'. The effect of an imperfect lattice on the direct process will be dependent

on the symmetry of the spin site. For a site with a high symmetry the coupling coefficient A' will be zero, although for the Raman process it is non-zero because of the non-linearity of the effect of the strain on the electronic states (Castle 1963). If the coupling coefficient is non-zero for the direct process the temperature dependence will be unaffected but the magnetic field dependence will be altered.

2.5 Methods for the measurement of the Relaxation Time

The six methods outlined below are the ways in which the relaxation times in paramagnetic materials have been measured to date.

(1) Non-resonant Technique This method was originally developed in Leiden in the 1930's by Gorter and has subsequently been used to investigate a considerable number of paramagnetic materials. As a paramagnetic ion has an unpaired spin there is a resultant dipole moment present. If an oscillating magnetic field is applied to the paramagnet it is found that as frequency of the oscillation is raised there is developed a component of magnetisation out of phase with the oscillation. In terms of the differential susceptibility $\chi = dM/dH$

$$\chi = \chi' - i\chi''$$

Casimir and du Pre (1938) using thermodynamic relationships expressed χ' and χ'' in terms of isothermal and adiabatic susceptibilities, the frequency of oscillation and the relaxation time τ. This method gives a value of τ averaged over a number of levels, but it can be used for obtaining τ for various values of d.c. magnetic field.

(2) C.W. Saturation In 1953 Eschenfelder showed that the relaxation time could be deduced by measuring the power absorbed when spins are raised from a lower to an upper level. The power absorbed P_a is given by

$$P_a = \frac{N(h\nu)^2 W_i}{(2S+1)kT(1+W_i/W_s)}$$

N is the number of spins in the sample, W_i the stimulated transition probability and W_s the relaxation transition probability.

$$\frac{W_i}{W_s} = \frac{1}{2}\gamma^2 H_i^2 g(\nu)_m \tau \ (S+M)(S-M+1)$$

H_i is the r.f. magnetic field, $g(\nu)_m$ the lineshape factor and γ the gyromagnetic ratio.

The difficulty of the method is in determining accurately the term $H_i^2 g(\nu)_m$, and it has the limitation of giving only one average relaxation time between the

levels being investigated.

(3) Pulse Saturation Technique This method originally developed by Davis et al in 1958 is useful because of the possibility of observing a multiplicity of relaxation times. The populations of the spin levels are equated by a pulse of microwave power and then a low power signal is used to monitor the absorption of the sample, which is usually found to recover exponentially. The assumption of a uniformly saturated absorption line may cause complications if the line is inhomogeneously broadened.

(4) Inversion Recovery This method due to Castle et al (1960) uses the fact that the populations of two levels can be inverted by applying a power pulse as the magnetic field is swept rapidly through the line. By observing the recovery of the system from a negative spin temperature through saturation to positive spin temperature it is possible to detect phonon imprisonment. If this is present the slope of the recovery curve is increased above saturation and retarded below it. Inhomogeneous broadening can be detected by 'hole burning', but does not affect the result as the whole of the line is observed.

(5) Microwave Acoustic Measurements Dobrov et al. (1962) measured the relaxation time in ruby by monitoring the absorption of acoustic waves passing through the crystal. The values obtained were in general higher than those obtained by the pulse saturation technique.

(6) D.C. Magnetisation Technique In 1962 Feng and Bloembergen reported relaxation times measured by detecting the voltage induced in a pick-up coil as the spins in the paramagnet returned to equilibrium after a saturating pulse. Although difficulties arise because of the small signal/noise ratio of the system the spins can be monitored during the pulse and cross-relaxation effects can be seen.

Chapter 3

Experimental

3.1 Introduction

Of the various methods available for the measurement of relaxation times discussed previously, the pulse saturation technique was adopted because of the ease with which the existing spectrometer could be adapted to it, the possibility of detecting more than one exponential within the recovery signal, and its general use by other workers allowed a direct comparison of results.

In order to obtain results at frequencies around 35 Gc/s magnetic fields of the order of 15,000 oersteds are required. The limitations imposed by the magnet pole gap to obtain such fields, made the use of a Q-band cavity impossible with the existing glass dewar system. Instead, the samples were placed at the end of a shorted piece of waveguide which effectively acted as a low Q cavity. As sensitivity considerations were not of prime importance this limitation was acceptable.

3.2 Apparatus

Figure 3.1 shows a block diagram of the microwave apparatus. It can be considered as a low power spectrometer, such as is used for linewidth measurements with superheterodyne detection, to which is added a high power valve suitably modulated to produce saturating pulses.

The usual operation of aspectrometer with superheterodyne detection necessitates the use of a second low power klystron to provide the local oscillator frequency for the balanced mixer. This frequency is such that the difference in klystron frequencies is equal to the intermediate frequency of the amplifier, which is of the order of 50 Mc/s. At frequencies near 35 Gc/s it is impossible to separate two such frequencies on a wavemeter, and furthermore thermal drift makes it very difficult to keep any such separation constant. To overcome this, a modification was built which allowed the local oscillator frequency to be derived from the monitor klystron. A transmission crystal modulator which contained a detector diode was placed across the waveguide adjacent to the klystron and a 45 Mc/s signal was applied to the diode from an R.F. generator. The resulting waveguide frequencies were the monitor klystron frequency, and two further frequencies separated from it by 45 Mc/s. This modification is described in Appendix 2, which is a Research Note published

in the Journal of Scientific Instruments, 1965, 42, 648-9, jointly with G. Brown and J. S. Thorp. The advantage of such a modification is that by adjusting the frequency output of the R.F. generator the amplifier can always be operated at its optimum working condition, even though the monitor klystron frequency may be changed. The broadening of the absorption line due to a spread of frequencies reaching the sample was not detectable, and this would not be expected as the power level in the sidebands was only approximately 10 μW. An operational disadvantage of the system is that the balance of the bridge is affected by adjustments in the power level in the local oscillator arm of the bridge, unless a large number of isolators are used.

The monitor klystron, an E.M.I. valve type R.5146, produced about 20 mW in the frequency range 34.0 - 35.5 Gc/s. The best method of cooling giving the greatest frequency stability was obtained by mounting the klystron in an oil bath, and the noise level in the klystron output was further reduced by driving the heaters from a battery supply. The transmission crystal modulator was placed as near the klystron as possible to give the most powerful sidebands. The local oscillator power was then tapped off the main waveguide run by a 3 db. coupler to the balanced mixer through a variable attenuator. The operating frequency was monitored on

a combined transmission/absorption wavemeter, Mid-Century type M C 22/2A. The sample was placed at the end of a shorted length of internally silver plated copper-nickel waveguide connected directly to the magic 'T'. The opposite arm of the 'T' held the E - H tuner, Mid-Century type MC 22/13D, and a matched load. The signal from the sample was fed into the balanced mixer which contained two crystal diodes of opposite polarity, G.E.C. type VX3171 and SIM 8. These were connected in parallel, which had the effect of eliminating the klystron noise present in the local oscillator signal. The resulting intermediate frequency (i.f.) of 45 Mc/s was amplified in a 12 stage stagger tuned amplifier, detected and displayed on a cathode ray oscilloscope. The i.f. could be varied by adjusting the frequency of the R.F. generator feeding the transmission crystal modulator. The optimum i.f. was determined by applying the 400 c/s internal sinusoidal modulation of the generator, and obtaining the largest and least distorted signal of the oscilloscope. The nominal 10 Mc/s bandwidth of the i.f. amplifier which was necessary when using a separate local oscillator source, was reduced to 3 Mc/s to give an increase in gain. Further reductions in the bandwidth led to parasitic oscillations within the amplifier.

The high power klystron was a water cooled Elliott

valve type 8TFK2 giving up to 20 watts at frequencies near 35 Gc/s. The Elliott Power Unit type PKU1 was modified by an Elliott Modulator Unit type 668 which supplied a modulated voltage to the cathode of the valve. The pulse length was variable from 30 μs to 600 ms with a p.r.f. ranging from 1 Kc/s to .15 c/s. The fall time of the power pulse obtained from the klystron was better than 3 μs. The detector diode on the absorption component of the combined transmission/absorption wavemeter was connected to an oscilloscope. When the monitor klystron frequency had been suitably adjusted the wavemeter was tuned using the transmission component. The frequency of the pulsed klystron was then adjusted until a pulsed output was obtained from the absorption component. The frequencies were then identical and any variation could be seen immediately. The pulse train displayed on the oscilloscope was of constant height, except for a slight 50 c/s ripple which was due to the A.C. heaters. This indicated that the klystron was operating at the same part of its mode on each pulse.

The absence of a cavity to contain the sample made it very difficult to determine a method for the systematic balance and adjustment of the spectrometer. The klystron frequency was varied until a strong guide or sample

resonance occurred. Some preliminary measurements to obtain the frequency of a sample resonance were made using a simple transmission experiment. However, when the absorption line was displayed and gave a large signal with the least noise, this was at a different frequency from the strong absorption in the transmission experiment. Thus there was some doubt as to which resonance was being used. The signal contained both dispersive and absorptive components of the susceptibility. The E - H tuner was adjusted to remove the dispersive component, so that as the magnetic field was swept through the line, only the absorption signal was detected. Removing the 50 c/s modulation and displaying on the D.C. range of the oscilloscope, the field was again swept through the line. The absence of any overshoot on the baseline only occurred when a true absorption signal was present.

The modulation coils, which were wound concentrically around the pole pieces of the Newport 8 inch Electromagnet type D, were driven from the mains supply. The magnet could produce 16,000 oersteds over a 4.5 cm. gap, and was calibrated by a combined proton/lithium resonance magnetometer. The ability to detect the lithium resonance indicated that the homogeneity was at least 1 part in 5,000 over a volume of 4 cc.

Measurements were made in the liquid helium, liquid

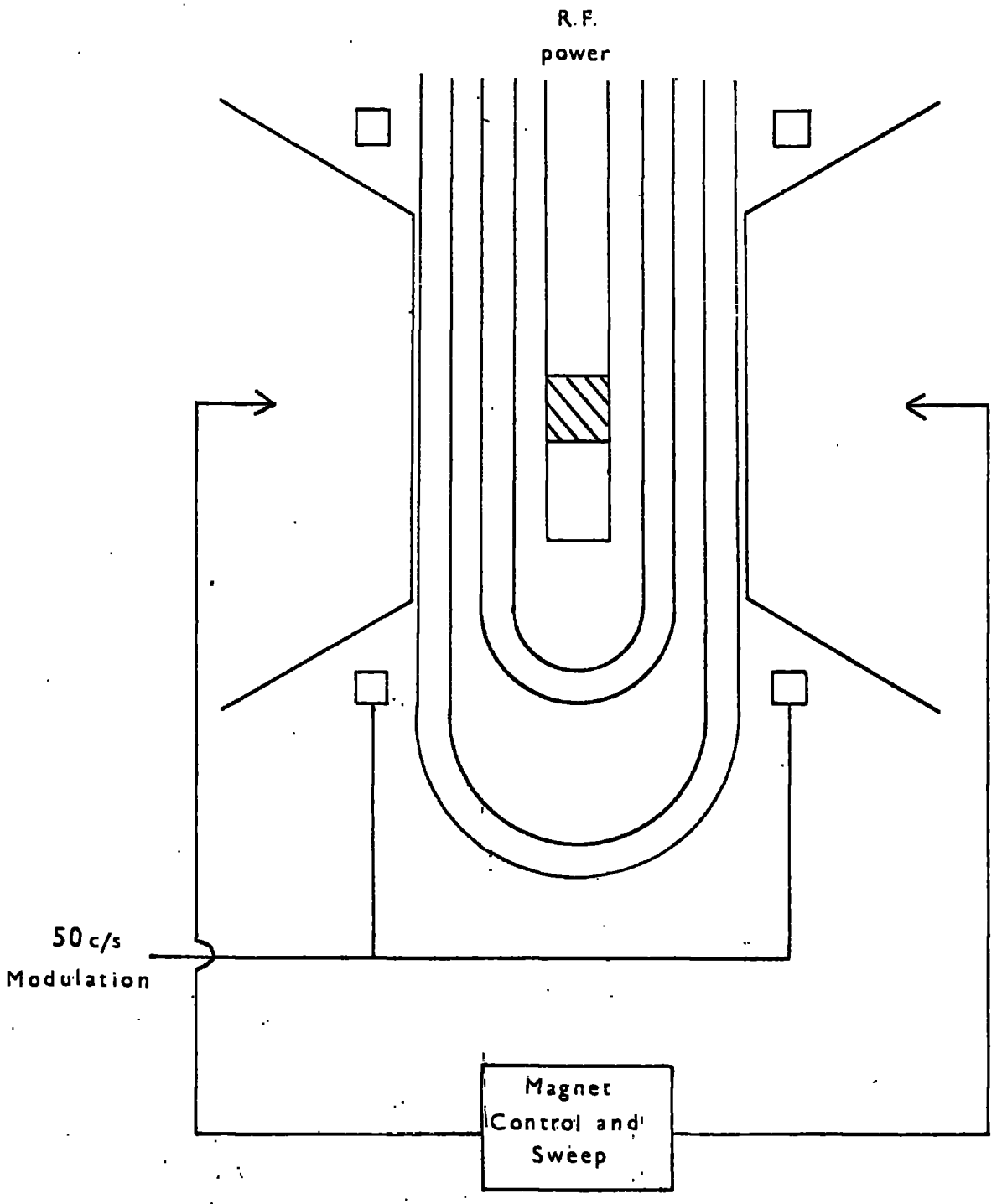

Location of Sample in the Magnet

Fig. 3.2

neon and liquid nitrogen ranges. As no previous measurements at liquid helium and liquid neon temperatures had been made in the Department, the techniques that have been developed will be described. Figure 3.2 shows diagramatically the dewar system used, and the relative positions of sample, modulation coils and magnet pole pieces. The two tail dewars, made of Pyrex glass, were double walled and completely silvered except for two sighting lines. The outer dewar which held the liquid nitrogen was permanently evacuated, whilst the inner dewar had an interspace which could be evacuated and was sealed by a ground glass tap. Due to limitations on the height of the spectrometer imposed by the ceiling of the laboratory, the overall length of the inner dewar was restricted to 87 cm. This meant that the greatest possible head of nitrogen above the level of the helium during an experiment was only 20 cm. The subsequently high boil off rate of the helium was reduced by placing two polished aluminium heat shields above the helium level. The copper - nickel waveguide had only a 0.005 inch wall and very little heat conduction along it resulted. The waveguide was terminated with a brass plunger and sealed in position with Woods' metal. A few small holes were made in the waveguide above the possible level of the helium to allow the waveguide to be evacuated. A piece of mica

placed across the waveguide where it left the dewar system allowed the inner dewar to be sealed off from the atmosphere. A copper - constantan thermocouple was strapped to the guide by the sample, and a carbon resistor was used as a depth gauge. Preliminary cooling of the sample took 2 to 4 hours with liquid nitrogen in the outer dewar, and helium gas as the exchange gas in the inner. The interspace of the inner dewar had previously been evacuated by an Edwards two stage backing pump.

Liquid helium was transferred either by glass or stainless steel siphon from a travelling dewar. About 1 litre of helium was transferred in 10 minutes. Helium temperatures were maintained for up to 4 hours after the transfer, and this was quite long enough for normal experiments. The escaping helium gas was collected in balloons and a compressor was available if the gas was required. Temperatures below 4.2^{o}K were obtained by pumping the inner dewar with an Edwards backing pump. The temperature was estimated from the pressure above the helium which was measured on a McLeod gauge. The lowest attainable temperature, limited by the overall pumping speed of the system, was 1.4^{o}K. As the microwave system had a very low Q it was possible to measure τ as the sample warmed up from helium temperatures. The

particular range of interest was from 20°K to 50°K and although the sensitivity of the copper-constantan thermocouple was low at these temperatures, the temperature could be estimated to 1/2°K using the calibration of Powell and Bunch (1959). The main difficulty encountered was that there was a difference in temperature between the sample and the thermocouple even though the latter was strapped to the outside of the waveguide immediately opposite the sample. To overcome this difficulty and to check the accuracy of the thermocouple liquid neon was used. One litre was sufficient to allow four separate transfers and by reducing the pressure of the gas above the liquid a minimum temperature of 18°K was obtained. The temperature was estimated using the vapour pressure values of neon obtained by Grilly (1962). The thermocouple was found to have an error well within that quoted above.

Temperatures up to 120°K were produced by passing a current of a few milliamps through a small heating coil wound around the outside of the waveguide. The sample was initially cooled to 77°K with liquid nitrogen placed in the outer dewar. The inner dewar was then evacuated and measurements were made when stable temperatures were obtained.

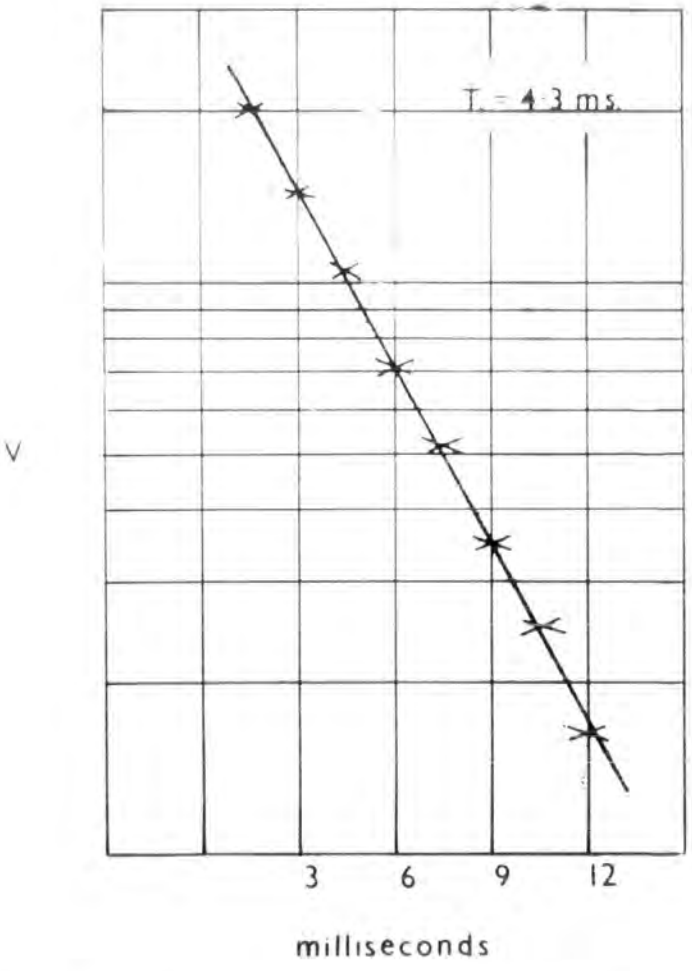

Display and Evaluation of Relaxation Curve

Fig. 3.3

3.3 Recording of Data

When the bridge had been adjusted to obtain the absorption signal and the frequency of the high power klystron adjusted to that of the monitor klystron, the modulation field was removed. The output from the receiver was of the form shown in figure 3.3 as the magnetic field was set at the centre of the absorption line. The monitor klystron power was reduced to check for saturation effects, although these were not usually present because of the low Q if the system. The receiver was not switched off during the time the power pulse was applied as no saturation effects were detected. This was verified by applying a 100 Kc/s external modulation to the R.F. generator driving the transmission crystal modulator. The output during the power pulse is shown in figure 3.4. The interruption in the wave train at the end of the pulse was about 5 μs, and no further distortion was present. The actual shape of the waveform was distorted as the source providing the modulation was being driven near its limit of performance.

Three methods of obtaining the time constant of an exponential decay from the curve were considered.

(a) Recording the curve by photography, measuring co-ordinates from the photograph and plotting them on semi-logarithmic graph paper, then obtaining the gradient of the resulting straight line.

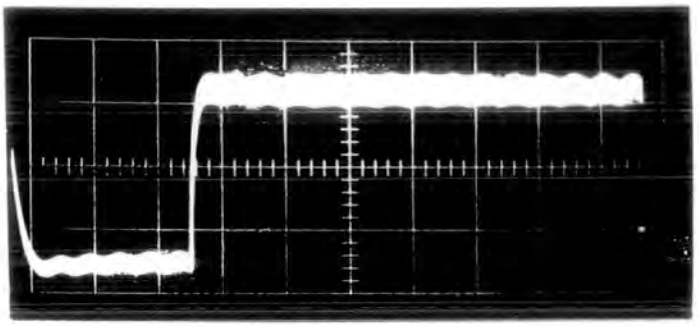

Superhet. Reciever Output

During and After Power Pulse

Time base 20 μs/div.

Modulation frequency 100 Kc/s

Fig. 3.4

(b) Comparison of the exponential with one of known and variable time constant produced by an exponential generator.

(c) The use of an exponential time base with a variable time constant, or a logarithmic amplifier. These would change the form of the displayed curve to a straight line with a gradient which could be simply calculated.

An exponential generator was built but discarded at an early stage when it was found that a change of 5% in the time constant could not be readily detected, and the possibility of accurate comparison measurements seemed small. Similar arguments applied to the exponential time base, although it should have been easier in this case as the final curve had to be a straight line. The methods using photography and a logarithmic amplifier are identical except the straight line obtained by the former method necessitates plotting the curve by hand.

The photographic method was chosen; initially 35 mm film was used, but later Polaroid film was adopted so that the quality of the photograph could be known immediately. Figure 3.3 shows the result of an exponential decay, when plotted on semi-logarithmic graph paper. The points lie clearly on a straight line. It

was sometimes found that the line obtained on a semi-logarithmic plot was curved. This can arise from two exponentials of different time constants c.f. 3.4. In such a situation the last part of the curve was used to obtain a value for the relaxation time. This method assumes a linear time base, and care was taken in choosing a suitable oscilloscope. A Tektronix 545 A or a Solartron CD 532/S2 was used, as these had a maximum error of 5% on the time base linearity.

3.4 Interpretation

The exponential form of the decay is verified by the straight line on a semi-logarithmic plot. However, the immediate interpretation of the gradient as the relaxation time may not be justified. If there are more than two energy levels, p say, then the rate of change of population of level i, represented by $\dot{n}_i$ is

$$\dot{n}_i = \sum_{j=1}^{p} (W_{ji} n_j - W_{ij} n_i) \qquad i = 1,2,\ldots,p$$

where W_{ji} is the transition probability between levels j and i. These equations will, in general, yield p - 1 independent relaxation times, and the approach of the system to equilibrium after the saturation of one pair

of levels will generally depend on all p - 1 relaxation times. If the same pair of levels are saturated and observed after the saturation pulse then the normalised population difference will have the form

$$S = \frac{n_i - n_j}{n_{io} - n_{jo}} = 1 + A_1 e^{-t/\tau_1} + A_2 e^{-t/\tau_2} + A_3 e^{-t/\tau_3} + \ldots$$

where n_i and n_j are the instantaneous populations of levels i and j, and n_{io} and n_{jo} are their respective equilibrium values. S is proportional to the signal observed from the superhet. In the theoretical predictions of Donoho for ruby at 35 Gc/s, discussed in Chapter 2, one of the three amplitudes A is very small. Then if the equations are considered with only two amplitudes A_1 and A_2, and related relaxation times τ_1 and τ_2, three cases need to be examined.

$A_1 >> A_2$ The exponential decay will be predominantly composed of A_1 and will have a time constant τ_1.

$A_1 \simeq A_2$ Then if the relaxation times τ_1 and τ_2 are similar the time constant obtained will be an intermediate ~~average~~ value. If the relaxation times are considerably different, then they will each be determined.

$A_2 >> A_1$ This is similar to the case of $A_1 >> A_2$ except τ_2 will be determined.

The estimation of error in measurements of this kind is very difficult. The error arises firstly from the fact that the exponential displayed on the oscilloscope may not be the correct one, and secondly from measurements off the photographs of this. The time constant of the displayed exponential depends on the balance of the bridge, and this is dependent on the frequency drift of the klystrons. To determine the magnitude of the effect of misbalance of the bridge, the relaxation time was measured when the bridge was adjusted for absorption only, and then for dispersion only. The error in the relaxation time of the dispersion signal was approximately 25%. The error in taking measurements from the film was less than 5%. An estimate of the total error obtained from repeating measurements on the same sample, which includes both sources of error, was between 10 and 15%, the main error resulting from misbalance of the bridge.

Chapter 4

Influence of Texture in Vapour Phase Ruby

4.1 Introduction

In order to make a detailed study of the relaxation times in ruby, it has been necessary to determine and regulate certain parameters that may affect the value of τ within a particular sample. The parameters regarded as particularly important are (a) growth method, (b) chemical purity, (c) concentration of paramagnetic centres, (d) physical texture of the sample. By choosing samples of one particular growth method it has been found that parameters (a) and (b) have been kept constant. The chemical impurity was found to be small if vapour phase rubies were used; the actual level of these impurities will be discussed in Chapter 5. As the concentration of the Cr^{3+} ions could be determined and a range of concentrations was available, the greatest attention has been given to the influence of texture and the way in which it has been estimated will now be described.

4.2 Estimation of Texture

The physical imperfections present within ruby single crystals arise mainly from the high growth temperature. Vapour phase rubies grown at 2050°C contain a large number of dislocations, fairly perfect but slightly misorientated crystallites and a certain amount of strain due to the thermal gradients within the growing boule and furnace.

(1) Dislocations The dislocation density was estimated by counting the etch pits produced on the (0001) face by etching the sample at 320°C with ortho-phosphoric acid (Scheuplein and Gibbs 1960). Spurious 'pits' were formed along scratches on the surface, and care was taken to ensure that the surface was highly polished. The etch pits due to the presence of a dislocation were triangular, reflecting the underlying crystal symmetry. An extensive discussion of the validity in assuming a 1:1 correspondence of dislocation to etch pit has been given by Scheuplein and Gibbs. A photograph of a surface is shown in Appendix 3, which is a letter to the Editor of the British Journal of Applied Physics 1964, Volume 15, 775-6, written in conjunction with J. S. Thorp and D. A. Curtis, giving a brief summary of some of the measurements reported here. The range of

dislocation densities measured was from 0.6 to 2.8 $10^5/cm^2$. with an error of 25%, arising mainly from the difficulty in estimating the number of pits lying along the grain boundaries.

(2) Mosaic Structure. An x-ray examination of the samples using the Laue back reflection technique has been undertaken. The method and necessary modifications of the equipment have been described by Curtis (1964) and no further mention of them will be made here. The photographs resulting from such an examination are shown in Appendix 3. A fine beam of x-rays is reflected from planes of atoms near the surface of the sample and recorded on a photographic plate. If the material under the x-ray beam is perfect a pattern of diffraction spots is obtained on the film, the size of the spots depending on the geometry of the apparatus. In some cases there is a distinct splitting of the spots because there is mosaic structure in the sample. Mosaic structure is a term used to describe the existence of adjacent regions of nearly perfect material which are slightly misorientated. The splitting of the spots is proportional to the extent of the misorientation, and this can be as much as 3^o. The size of the crystallites is comparable to the grain size as seen on the etched surface of the samples (Thorp et al 1964).

(3) C-axis Misorientation. If a Laue photograph is taken with the impinging x-ray beam almost parallel to the c-axis of the sample a regular pattern of spots is produced from which the position of the c-axis can be determined. Curtis (1964) described how the c-axis position at several points on the sample surface can be recorded on the same film using a sectored disc for blanking off part of the film during various exposures. It is found that the c-axis in the material does vary from one part of the crystal to another. This misorientation has a continuous distribution and it has been found that the misorientation between points taken at random on the crystal can be as much as 3.5^{o}. This slight bending of the lattice indicates the presence of strain.

The x-ray data shows that there is a wide range of both mosaic and c-axis misorientation, up to a limiting maximum, within a single sample. The analysis technique of measuring displacements directly from the film, is only accurate to $\pm$ 15' of arc and so measured misorientations of 45' or less may be very inaccurate. Due to the amount of work involved only about 10 values of misorientation for each sample could be reasonably measured. To take a simple mean of the figures with such a large error for

the low values may lead to a mean with an error of the order of 50%.

If the distribution of c-axis directions about the preferred c-axis direction in the crystal is assumed to be Gaussian, then the probability of finding two misorientations x_1 and x_2 together where $x_1 - x_2 = a$ can be represented as :

$$Y(x_1, x_2) = \int_{-\infty}^{\infty} A^2 e^{-Bx_1^2} \; e^{-B(x_1 + a)^2} \; dx$$

where

$$A = \frac{1}{\sqrt{2\pi}\ \sigma}, \quad B = \frac{1}{2\sigma^2}$$

σ is the standard deviation of the underlying distribution. The result of the integration is

$$Y = \frac{1}{\sqrt{\pi}\ \sigma} \; e^{-a^2/2} \qquad (4.1)$$

Thus the distribution of misorientation, taken at pairs of random points, is Gaussian with the same standard deviation as the underlying distribution. As the measurements from the x-ray films cannot distinguish between positive and negative values of misorientation, the resulting distribution of misorientation will be expected to lie in the positive x - y quadrant. The above calculation was performed jointly with C.J. Kirkby who has shown by taking a large number of photographs

of one sample, that the measured distribution of misorientation is Gaussian.

From equation (4.1) it is found that the mean of the distribution $\bar{x}$ is equal to 0.8σ, and there is a 15% probability of an observed value lying between $a = 1.3$ and 2σ. As 95.5% of the distribution lies below the value $a = 2\sigma$, the mean of 6 - 10 values of misorientation can be estimated to 15% halving the maximum value observed. As the % accuracy of the measures values increases the larger the misorientation, the overall mean can be estimated using this method with an error of 35%.

Apart from an estimate of the chromium concentration in selected samples using spectrographic analysis, a spectrophotometric method reported by Dodd et al (1964) has been employed. The Beer-Lambert Law states that the ratio of the intensity of transmitted light at any one frequency with and without an absorbing sample present is

$$\frac{I_o}{I} = e^{\mu cd}$$

μ is the absorption coefficient, c the concentration of the light absorbing centres and d the length of the light path in the material. The effect of surface scattering for ruby can be corrected for by measuring the transmitted

Concentration %wtCr: Al_2O_3	Impurities	Dislocation Density /cm^2	Mean Mosaic Misorient^n.	Mean C-axis Misorient^n.	T_1 $\theta^1 = 0^o$ $T = 4.2^oK$ millisecs	T_1 $\theta^1 = 90^o$ $T = 4.2^oK$ millisecs
0.002			44'	65'	17.0	17.0
0.013	Cr^{4+} 0.003%Fe		43'	55'	17.2	15.5
0.015			8'	85'	11.0	12.4
0.032		$2.6x10^5$	28'	43'	14.8	22.0
0.032	Cr^{4+}		115'	74'	10.1	11.0
0.037		$1.0x10^5$	18'	48'	18.6	19.9
0.041			37'	71'	18.0	14.3
0.052			15'	36'	21.9	24.0
0.052		$2.5x10^5$	20'	55'		12.5
0.081	0.003%Fe		0'	51'	27.7	23.0
0.20		$0.87x10^5$	20'	72'	4.4	4.0

Vapour Phase Rubies, + 1/2 to -1/2 transition

Table 4.1

intensity relative to a baseline at 6,700 Å, where absorption due to chromium centres is zero. Thus no special preparation of the samples is necessary, and the method has the advantage that, being non-destructive, it can be applied to samples actually used for the relaxation time measurements. Using the values of the absorption coefficients reported by Dodd the chromium concentrations were estimated to 5% of the spectrographically determined values.

4.3 Results

(1) Concentration Dependence Rubies with a chromium concentration range of 0.002% (weight % $Cr:Al_2O_3$) to 0.2% have been investigated. The relaxation times τ measured for the 1/2 to -1/2 transition at 4.2°K are shown in table 4.1, for $\theta = 0^\circ$ and 90°. Although there are differences in τ for samples with a similar chemical concentration, there is no apparent dependence of τ on concentration up to 0.08%. The reduction in the value of τ for the 0.2% sample is marked. Over a similar concentration range in vapour phase rubies Standley and Vaughan (1965) obtained similar results at a frequency of 9.3 Gc/s, although the concentration independence region extended to 0.2%.

Using the technique of electron probe micro-analysis Dils et al. (1962) have shown that appreciable variations of chromium concentration can occur over small distances within rubies. Thorp et al (1964) (Appendix 3), have shown that high concentration regions in ruby boules coincided with regions of high dislocation density. Thus it may be that the actual chromium concentration in ruby is greater than the chemical determination in some regions of the sample. Because of the nature of the disrupted lattice around a grain boundary it may be energetically preferable for chromium ions to occupy such imperfect sites. If this was the case, at very low chemically determined concentrations the effective concentration would be greater because of this clustering effect. If this mechanism was operative τ would be expected to be independent of the chemically determined concentration, until the number of ions was large enough for exchange interaction to limit τ. Kirkby (private communication) has found that the linewidth of the 1/2 to -1/2 transitions at $\theta = 0^{o}$ in the same samples as have been used in this work, were greater than the predicted values of Grant and Strandberg (1964) for the chemically determined concentrations. These results may be explained on the

basis of chromium clustering in certain regions of the crystal.

Kochelaev (1960) has shown that a concentration dependence is to be expected even if the paramagnetic ions are regularly spaced in perfect lattice sites, and no exchange interactions occur. As the chromium ions replace diamagnetic ions of a different mass in the lattice, they are in fact defects. Lattice waves scattered by such defects can produce a large change in the relative displacements of adjacent atoms and so effect τ. The dependence of τ on the concentration c becomes

$$\tau \quad \alpha \quad c^{-4/3}$$

If a value of τ = 20 ms. is supposed for a concentration of 0.02% the above formula predicts a value of τ = 7 ms. at 0.08%.

(2) Texture Dependence. The results of the examination of the texture of the samples used are shown in table 4.1. The author is indebted to C.J.Kirkby for a majority of the x-ray results. In all of the samples measured the dislocation density was high and over the very limited range of densities observed no correlation with τ could be seen. The mean values of

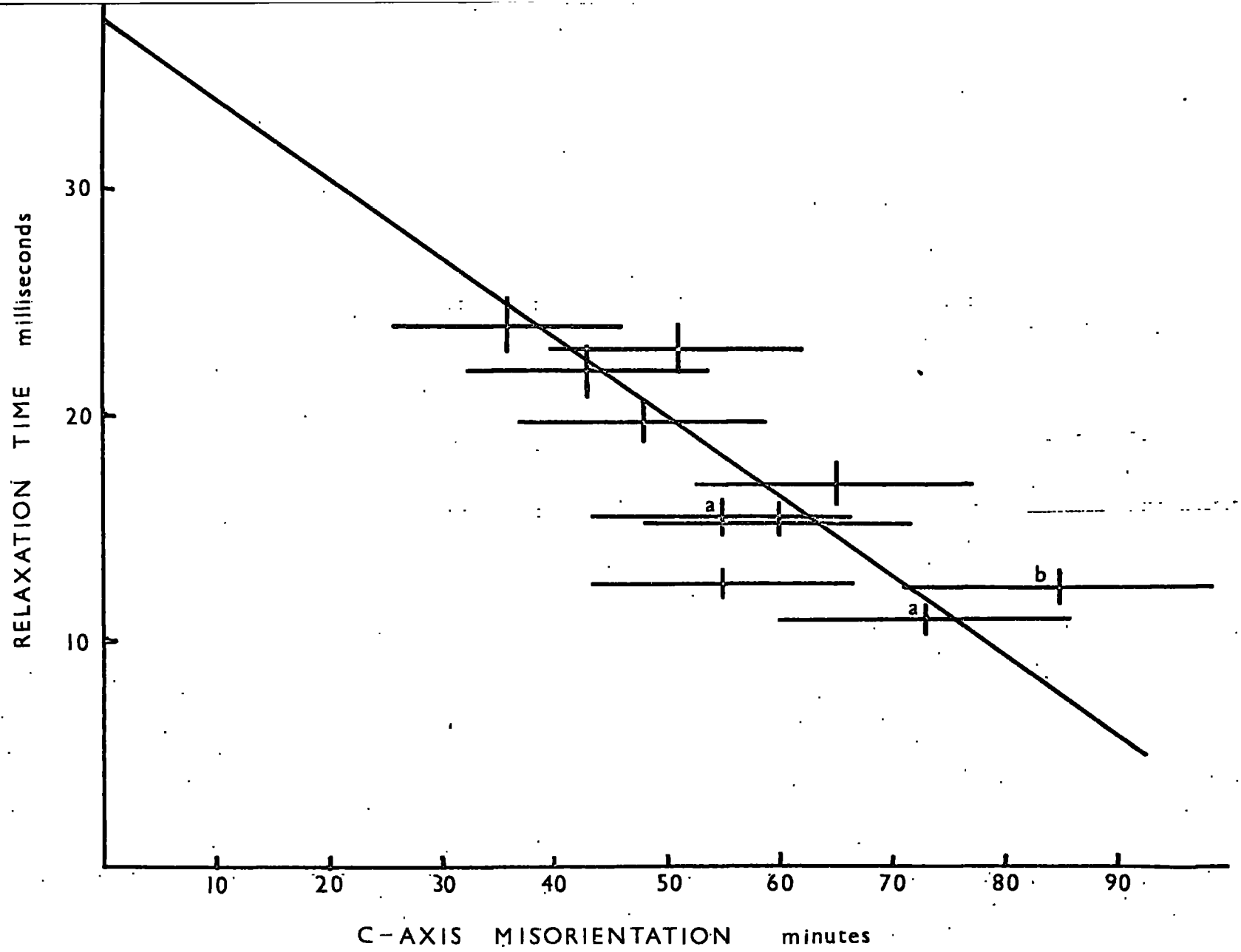
RELAXATION TIME milliseconds
30
20
10
a
b
a
10
20
30
40
50
60
70
80
90
C-AXIS MISORIENTATION minutes

Fig. 4.1

mosaic and c-axis misorientation show that although an occasional sample had a low value of mosaic misorientation, the c-axis value was always quite large. Figure 4.1 is the mean c-axis misorientation plotted against the value of τ at 4.2°K, for the 1/2 to -1/2 transition at $\Theta = 90^{\circ}$. The straight line through the points was fitted by the method of least squares (Topping 1960), the errors on the individual points are indicated by the bars. Although the mosaic values for the different samples vary as shown in table 4.1 there is no correlation between them and τ. The points marked (a) are values from samples containing Cr^{4+} which have an orange appearance. The point (b) is a value from a sample grown at 90°, the other points are for samples grown at 0°. A similar dependence of τ on texture was obtained for other transitions. It is concluded for this transition that for samples with a dislocation density of approximately $10^5/cm^2$ and no c-axis misorientation, the relaxation time would be near 38 ms. This must be compared with the Donoho prediction of 120 ms.

(3) Temperature Dependence. Figure 4.2 shows the temperature dependence of a representative selection of the samples from 1.4°K to 120°K. Consider first

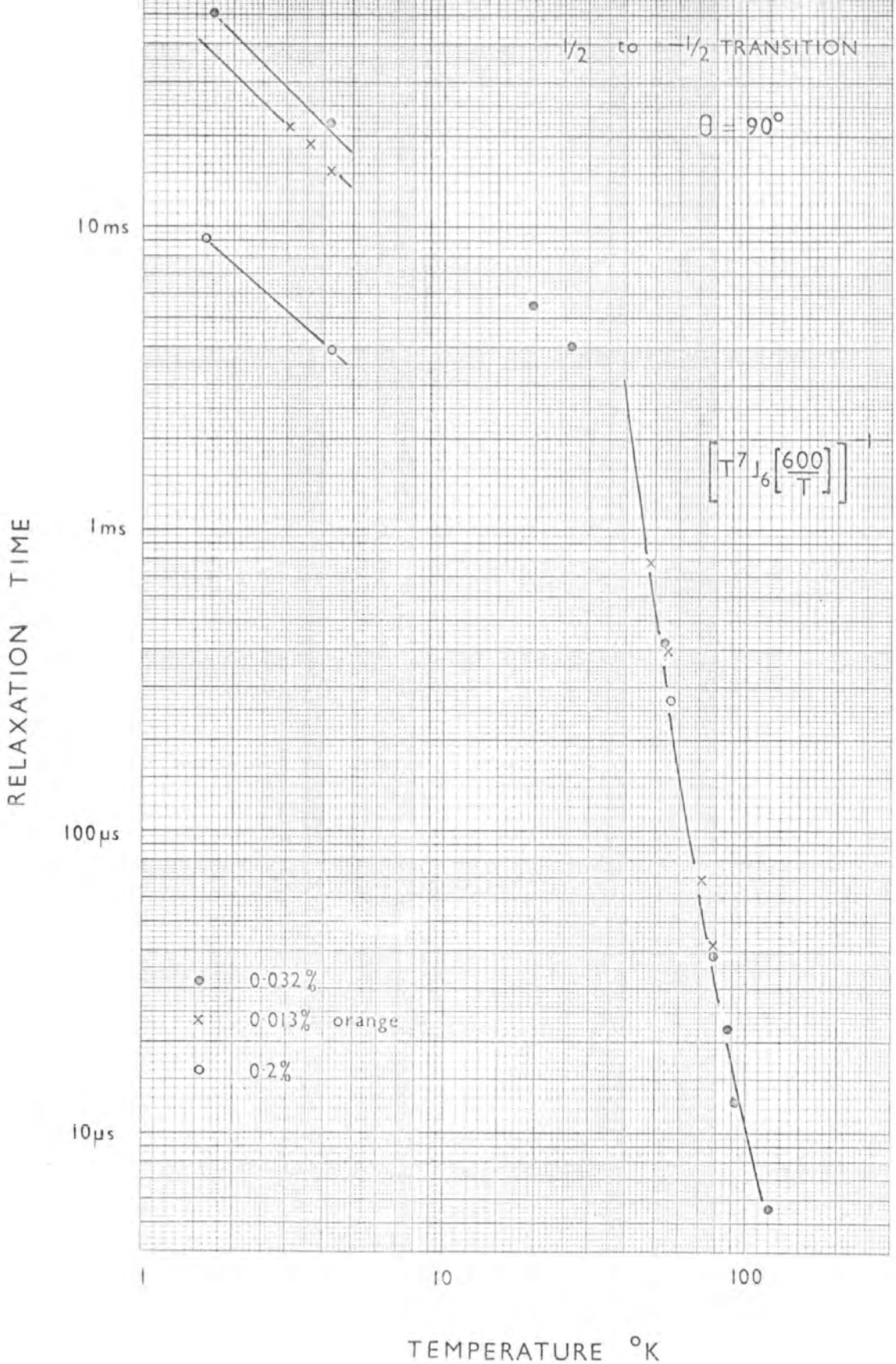
1/2 to −1/2 TRANSITION
θ = 90°
10 ms
1 ms
100 μs
10 μs
RELAXATION TIME
$\left[T^7 J_6\left[\frac{600}{T}\right]\right]^{-1}$
0·032%
0·013% orange
0·2%
1
10
100
TEMPERATURE °K

Fig. 4.2

temperatures $> 40^{o}K$. All samples measured had the same values of τ within experimental error. The relaxation process at these temperatures is Raman and all the phonons within the lattice are used. The temperature dependence can be fitted to the relationship $T^{-7}J_6(\Theta_o/T)^{-1}$, when a value of Θ_o is chosen as $600^{o}K$. Although there is some difficulty in fitting the results to the shallow curve the value of Θ_o is accurate to $\mp 100^{o}K$. Hence the results follow a temperature dependence for a perfect material when a value of Θ_o is chosen which is appreciably smaller than that calculated by any other method. This form of dependence is in qualitative agreement with previous workers using the pulse saturation technique, but in complete disagreement with Michel (1960) who used a c.w. method and found the Raman process dominant for temperatures $> 150^{o}K$.

At lower temperatures all the samples measured obeyed a T^{-1} relationship including the 0.2% sample. Standley and Vaughan (1965) found that a 0.2% sample had a stronger temperature dependence than those of lower concentration although the value of τ at $1.4^{o}K$ was of a similar magnitude. If exchange interaction is limiting the value of τ for the higher concentrations a stronger temperature dependence may be expected.

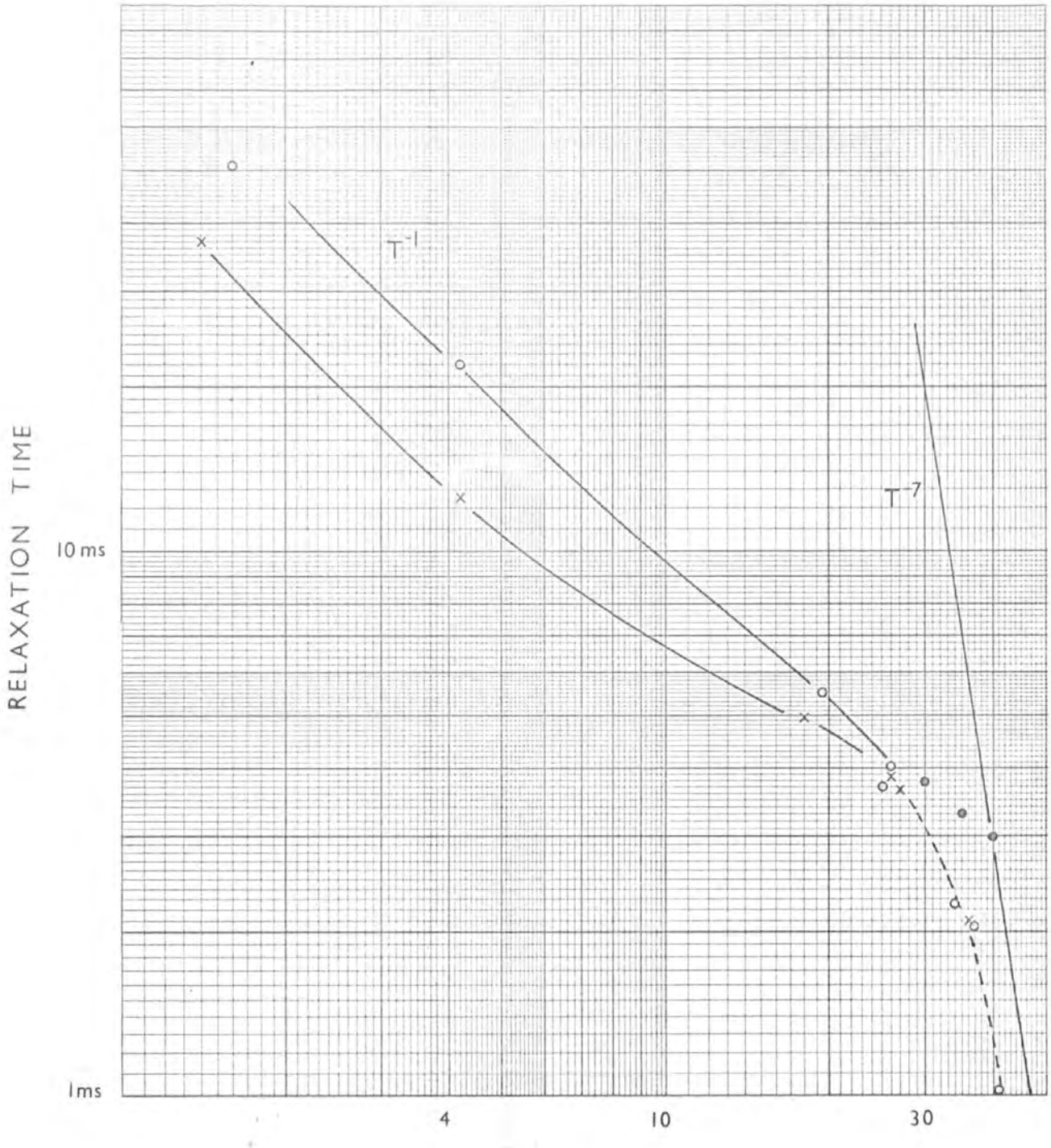

Fig. 4.3

The ratios of the values of τ at $4.2^{o}K$ is seen to hold at lower temperatures.

Figure 4.3 shows the temperature dependence for two samples for $T < 40^{o}K$ in more detail. Temperatures in the region $18^{o}K$ to $27^{o}K$ were obtained using liquid neon, measurements were made at temperatures greater than $27^{o}K$ as the sample warmed up to nitrogen temperatures. Although the difference in the values of τ at $4.2^{o}K$ is large, and can be attributed to the difference in c-axis misorientation, at $27^{o}K$ the values of τ are very similar. If values for the direct process are calculated from the equation

$$\frac{1}{\tau} = \frac{1}{\tau_D} + \frac{1}{\tau_R}$$

where τ_R is the Raman term obtained from an extrapolation of the curve at higher temperatures, and τ is the observed relaxation time, the values of τ_D are seen to lie on a line of gradient -1 passing through the common $27^{o}K$ point. Thus for the temperatures $> 27^{o}K$ the curvature in the temperature dependence is explainable solely in terms of the direct and Raman processes. It appears that the values of τ for the two samples are attributable to the direct process for $T < 30^{o}K$ and the effects of c-axis misorientation are

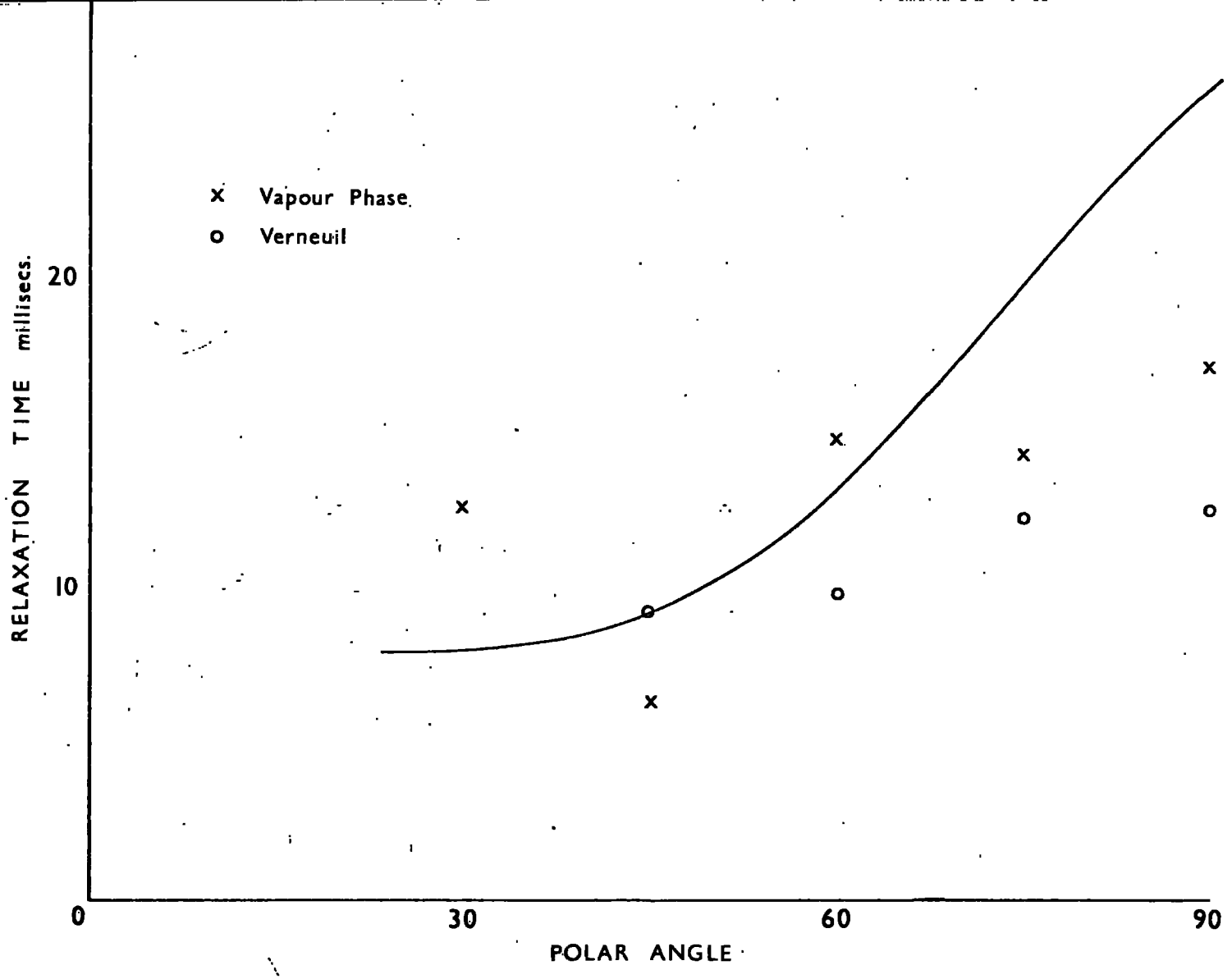

ANGULAR VARIATION OF 1/2 to 3/2 TRANSITION

Fig. 4.4

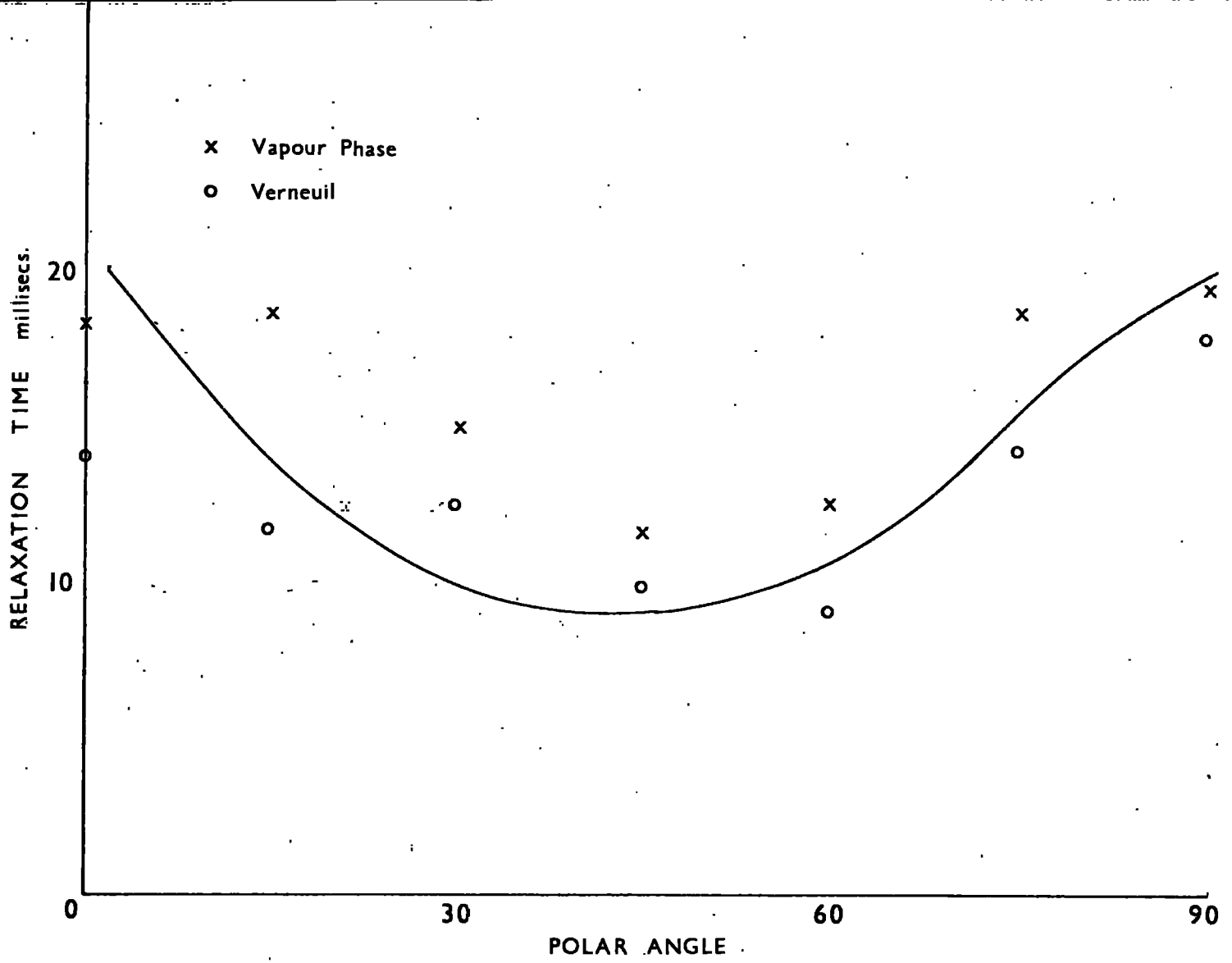

ANGULAR VARIATION OF 1/2 to −1/2 TRANSITION

Fig. 4.5

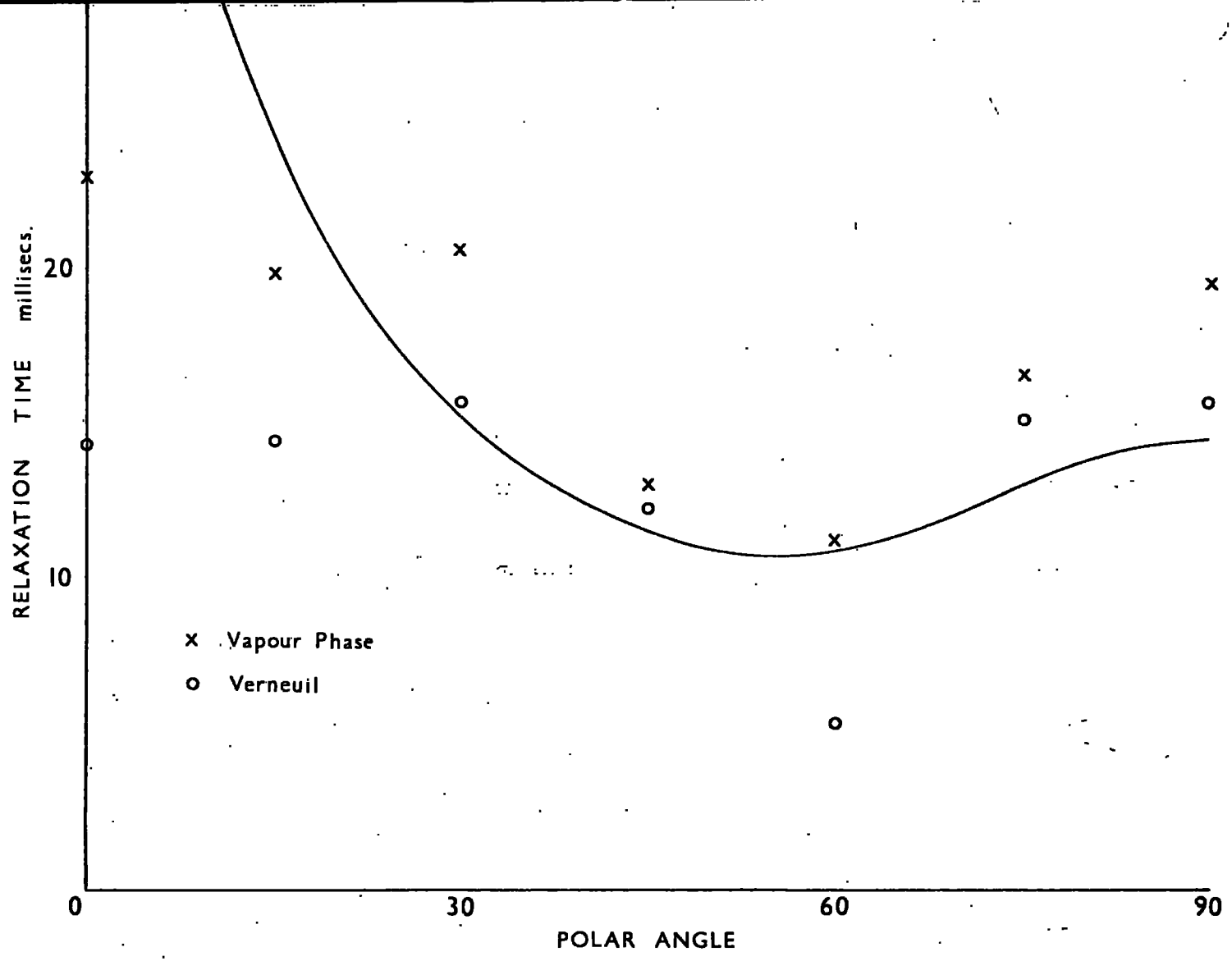

ANGULAR VARIATION OF $-1/2$ to $-3/2$ TRANSITION

Fig. 4.6

temperature dependent.

Klemens (1962) has shown that for a perfect material the temperature at which the relaxation times due to the direct and Raman processes become equivalent is approximately

$$T_c \simeq \frac{1}{2} \theta_o^{2/3} (E/k)^{1/3}$$

E is the energy of the incident radiation. From figure 4.3 $T_c = 40^oK$, which leads to a value of $\theta_o = 550^oK$.

(4) Angular Dependence The angular dependence of the three $\Delta m = 1$ transitions has been examined, and is shown in figures, 4.4, 4.5 and 4.6. Measurements were restricted to $\theta > 30^o$ for the 1/2 to 3/2 transition because of magnetic field considerations. From the graphs in Appendix 1, it can be seen that only an appreciable second amplitude in the recovery signal would be expected between $\theta = 30^o$ and 60^o for the 1/2 to 3/2 transition. This second relaxation time was not observed. The points shown are averages of the results from various samples at 4.2^oK, and the theoretical curve has been reduced by a factor of 6. The 1/2 to -1/2 transition gives fair agreement with the predicted angular variation although the magnitude of τ is 6 times too small. Because of the

high magnetic fields required for these measurements cross-relaxation with other transitions is possible at many angles. In particular at 45^{o} and 60^{o} there are 1:1 cross-relaxation points, and near $\theta = 0^{o}$ the harmonic 4:3 transition is very close to the 1/2 to -1/2 transition. The effect of the 1:1 cross-relaxation points has been measured and is found to have an appreciable shortening effect on the relaxation time over several degrees. It is possible that the reduction of τ between 40^{o} and 60^{o} is due to this cause and the agreement with theory is purely fortuitous. This becomes more apparent when the lack of agreement between theory and experiment is seen for the other transitions. The 1/2 to 3/2 transition has a 3:2 cross-relaxation point at $\theta = 90^{o}$ and a 5:3 one near 75^{o}. This may account for the points lying below the theoretical curve. A similar argument may be used when considering the -1/2 to -3/2 transition near $\theta = 0^{o}$, where an harmonic 2:3 point occurs. For all three transitions a direct cross-relaxation point occurs near 45^{o} or 60^{o} or at both angles. The conclusion from these measurements is that at all angles the value of τ is approximately 6 times smaller than the predicted value, and no definite statement can be made as to the agreement of the angular variation of τ with the theory. The

effect of c-axis misorientation at different angles was generally similar to that at 0^{o} and 90^{o}, although the dependence shown in figure 4.2 was not always followed. This was probably due to spurious cross-relaxation effects. However, the 1/2 to -1/2 transition at $\theta = 90^{o}$ should give results free from such effects, and so this was the transition that was generally measured.

4.4. Discussion

The dislocation density in all of the samples was of the order of $10^{5}/cm^{2}$. Brice (1965) reports that the number of dislocations per cm^{2}. N_{d}, has been estimated for samples of germanium using the formula:

$$N_{d} = \frac{\alpha}{b} \cdot \frac{dT}{dr} \qquad \ldots(4.2)$$

α is the coefficient of linear expansion of the material, b the Burgers vector and dT/dr the radial temperature gradient in the growing crystal. In the growth of rubies from the vapour phase the boule is moved from side to side across the flame so that a regular deposit of material is made on the molten surface. The usual temperature gradients across the furnace are of the order of $100^{o}C/cm$. but the gradients near the liquid molten interface of the boule may be

higher. Substituting the values of α, b and dT/dr for ruby into equation (4.2) N_d is of the order of $10^4/cm.^2$, but as we have no accurate knowledge of the temperature gradient this figure may well be an underestimate. Thus the dislocation densities found in vapour phase rubies can be attributed to the thermal gradients present in the boule and furnace during growth.

Figure 4.2. shows that the temperature dependence in the Raman region can be fitted to the theory for a perfect crystal if a Debye temperature of 600^oK is chosen. This is 2/3 of the value predicted by low temperature specific heat measurements, which should give the most accurate value for the temperature range in question. The crystallographic study of the samples has shown that the lattice is badly disrupted, and even if the possibility of clustering of chromium near the dislocation is ignored, there will be an appreciable number of chromium ions in the disturbed part of the lattice. In this case chromium ions will be sitting at sites around which the local strain could be very different from a perfect lattice site, due to the presence of neighbouring interstitials, vacancies and disordered lattice. Rosenstock (1962) has discussed a similar situation with regard to specific heat measurements in disordered solids. The chromium ion in such

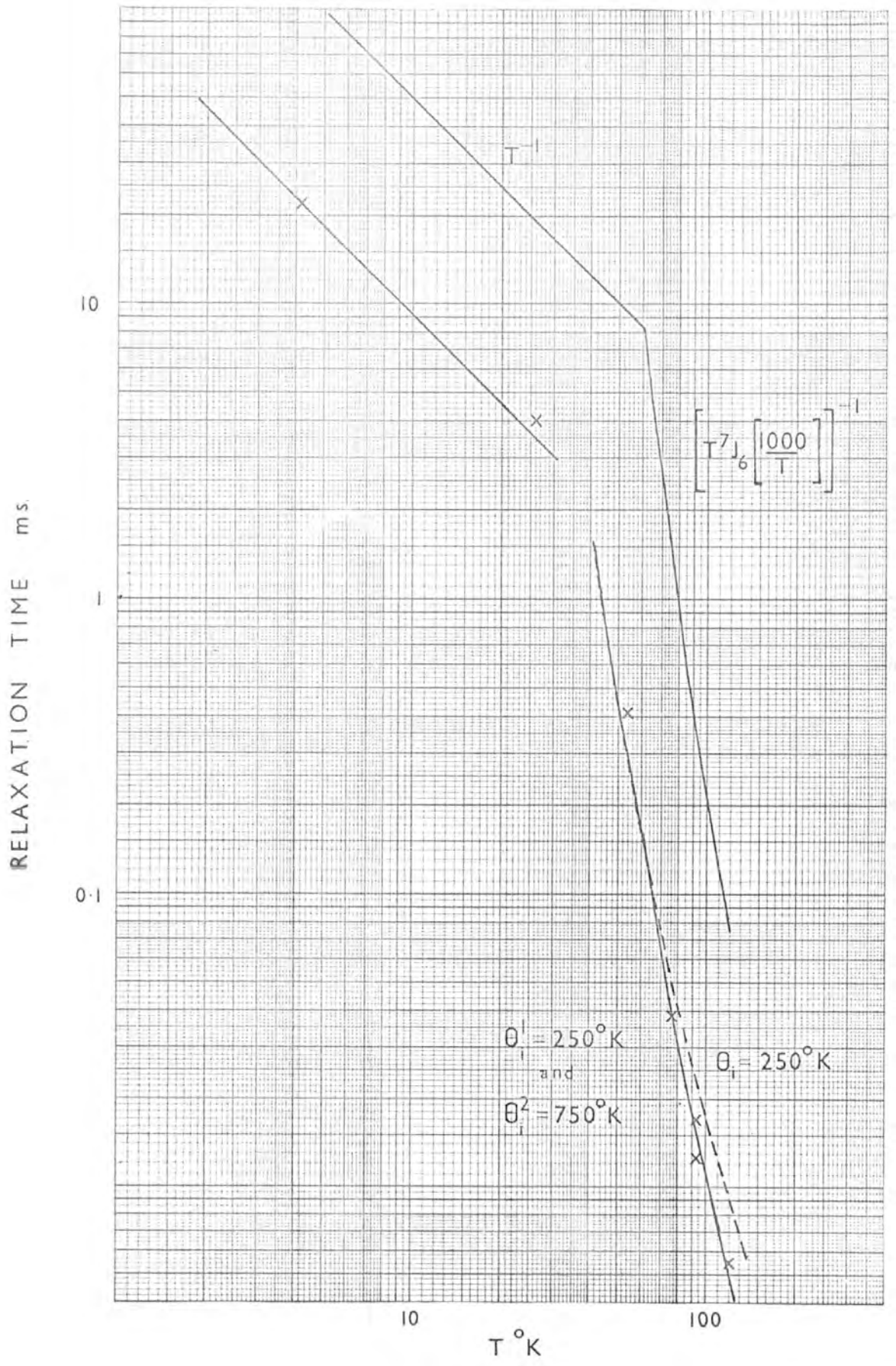
RELAXATION TIME ms.
10
1
0·1
T^{-1}
$\left[T^7 J_6\left[\frac{1000}{T}\right]\right]^{-1}$
$\theta_i^1 = 250°K$
and
$\theta_i^2 = 750°K$
$\theta_i = 250°K$
10
100
T °K

Fig. 4.7

circumstances may have a characteristic frequency w_i which is very different from the normal mode frequency w_D of a perfect lattice. If a number of ions are so situated the relaxation of the whole sample will be determined by their relaxation time. In figure 4.7 an 'ideal' situation is envisaged in the upper solid curve with the value at 4.2°K being that of Donoho, and the direct process is assumed to apply up to 60°K, which is the value of T_c given by equation (4.1). For temperatures greater than 60°K the Raman temperature is plotted with Θ_o = 1000°K. The experimental points lie well below this solid curve, and applying formula (2.4) for the modified Raman dependence due to local strain the dotted curve has been drawn. The value of Θ_o = 1000°K has been used and an equivalent impurity temperature of $\Theta_i^{\frac{1}{7}}$ = 250°K. The experimental results are seen to lie below this curve for temperatures greater than 80°K. However, Castle et al. have shown that for MgO the mass difference between the substituted chromium ion and the magnesium ion is such that the chromium ion is an impurity centre with a characteristic frequency $w_i = m^{-1/2} w_D$, where m is the ratio of the masses of the chromium and magnesium ions. An enhancement of the relaxation times can thus be expected for

temperatures greater than $\theta_D/10\ (m)^{-1/2}$ i.e. 75°K in ruby. Using the same value of θ_o as previously θ_i^2 is 750°K for the chromium ions replacing the aluminium ions in ruby. The temperature dependence combining the two defect temperatures has been plotted in figure 4.7 (lower solid line) using an equation of the form:

$$\frac{1}{\tau_R} = A\left[\left(\frac{T}{\theta_o}\right)^3\left\{J_2\left(\frac{\theta_o}{T}\right) - J_2\left(\frac{\theta_i^1}{T}\right)\right\} + \frac{T^{11}}{(\theta_i^1)^8\theta_o^3}\,J_{10}\left(\frac{\theta_i^1}{T}\right)\right] +$$

$$B\left[\left(\frac{T}{\theta_o}\right)^3\left\{J_2\left(\frac{\theta_o}{T}\right) - J_2\left(\frac{\theta_i^2}{T}\right)\right\} + \frac{T^{11}}{(\theta_i^2)^8\theta_o^3}\,J_{10}\left(\frac{\theta_i^2}{T}\right)\right]$$

Omit line 10. Replace by " ... 1 and 14 respectively. Thus the temperature ... "

to the experimental results by considering two chromium defect sites with equivalent temperatures of 250°K and 750°K. The latter arises directly from the substitution of chromium for aluminium in perfect lattice sites, and the former due to the lattice site being in a distorted part of the crystal. $\theta_i^1 = 250^oK$ is equivalent to placing an ion of mass 8 times that of chromium in a perfect lattice site, or a chromium ion at a site where

the interatomic coupling forces are reduced by a factor of 8. Although $w_i < w_D$, Brout and Visscher (1962) have shown that if the mass difference is large then the effect will be mainly localised near

Omit lines 5 to 8

Replace by :

... the defect. This may account for the fact that the contribution from all of the higher temperature defects is not as large as one would expect considering the relatively large number of chromium ions in the higher temperature sites. The volume of distorted material around the grain boundaries estimated from the etch pit photographs is 1% of the total volume, compared with the 7% effect of the low temperature sites on the relaxation behaviour.

probabilities may not be meaningful, whereas the phenomenological approach of Castle et al. used here predicts changes of temperature dependence which are far more easily verified than absolute magnitudes.

The types of imperfection considered above may account in part for the difference between the experimental and theory at 35 Gc/s of 6 times and a difference

at 9.3 Gc/s of 2 times reported by Standley et al (1965), as Castle et al has shown that the coupling constant for the direct process is frequency dependent. The displacement of atoms represented by a c-axis misorientation of 1^{o} is equivalent to a strain of 10^{-2} or less, and such a slight environmental change of the chromium ions would not be expected to effect the relaxation times in the direct region to any great extent. The equation for the transition probabilities used by Donoho contains a cube power of the velocity of the lattice waves. The velocity of propagation will depend on the interatomic distances as these determine the elastic constants in a volume of the crystal. If a region of compression or dilation is present, there will be a chenge in the velocity of propagation and an effect similar to Rayleigh scattering will occur (Ziman 1959). As the temperature increases the effect of the strained regions will diminish as the thermal vibrations of the ions increase. The effect on the quadratic spin operators in the Donoho equation of a 1% change in the D term of the spin Hamiltonian has been calculated using an Elliott 803 computer and the Elliott L.M.22 programme. The change in the operators is only .1% for a 1% change in 2D.

The presence of a fast relaxing centre within the lattice may give a modified temperature dependence of

the relaxation of the chromium ions in the direct region as shown in figure 4.3. However this would not explain the dependence of τ on the c-axis misorientation at 4.2^{o}K.

Chapter 5

Effects of Growth Methods and Impurities

5.1 Introduction

In the previous chapter the examination of the relaxation of the Cr^{3+} ion has been described for rubies grown from the vapour phase. Specimens grown by the Verneuil and Czochralski methods have also been investigated, and the results will be presented here. An important difference in rubies grown by the different methods is the level of impurities within the samples. In a later part of the chapter the results of an examination of a sample in which one impurity had been purposely increased will be presented.

5.2 Comparison of Czochralski, Verneuil and Vapour Phase Rubies

Only one sample grown by the Czochralski method was available during the present work, and so the results quoted cannot be claimed to be any more representative of this method than one sample taken at random from a growth batch is representative of that growth. Several Verneuil grown samples were examined with concentrations

Growth	Elements (%)						
	Cr	Fe	B	Mn	Ni	Mg	Ti
Czochralski	0.042	< 0.002	trace < 0.002	n.d. < 0.0005	n.d. < 0.002	n.d. < 0.001	n.d. < 0.005
Vapour Phase	0.013	0.003	trace < 0.002	n.d. < 0.0005	n.d. < 0.002	trace < 0.001	n.d. < 0.005
Verneuil	0.052	0.006	≃ 0.002	trace < 0.0005	trace < 0.002	n.d. < 0.001	n.d. < 0.005

Results of Spectrographic Analysis

Table 5.1

n.d.
none detectable

near 0.05% but no extensive range of concentrations was available. Table 5.1 contains the results of a spectrographic analysis of three samples grown by the different methods, which was kindly performed by R. A. Mostyn. This method of analysis limits the minimum detectable level of elemental impurities to approximately 0.001% i.e. 10 parts per million. The results show that the basic difference between the samples is the iron content, in the Czochralski sample the iron level was below the limit of detection, the vapour phase samples had a concentration near 0.003% whereas the Verneuil samples contained two or three times this amount of iron. The presence of iron in the microwave spectrum was only seen in the Verneuil samples, where it was observed as Fe^{3+}. The amount of other impurities in the samples was only small, although the Verneuil samples again contained more than the others.

The temperature dependence of the three types of sample is shown in table 5.2. For temperatures greater than $40^{o}K$ the values measured in all samples were the same to within experimental error, at any particular temperature. Below $40^{o}K$, there were differences in the relaxation times, but none that could not be explained in terms of the c-axis misorientation effect discussed in the previous chapter. The Czochralski sample did not have the

	Dislocation Density /cm^2	Concentration at%Cr:Al_2O_3	Relaxation Times 1.7°K*	4.2°K	60°K*	77°K	100°K*
Vapour Phase	2.6×10^5	0.032%	50 ms	22 ms	190 μs	40 μs	11 μs
Vapour Phase +		0.013%	41 ms	15.5 ms	190 μs	41 μs	
Verneuil		0.052%	41 ms	17.5 ms	170 μs	38 μs	
Czochralski	$5 \cdot 7 \times 10^4$	0.042%	41 ms	17.5 ms	165 μs	40 μs	11 μs

Temperature Dependence of +1/2 to -1/2 transition at $\theta = 90^\circ$

* interpolations where necessary from temperature plots

+ "orange" ruby

Table 5.2

markedly reduced dislocation density that has been claimed for this particular growth method, and so all of the samples measured had very similar textural properties.

The level of the iron impurity in the samples did not have any noticeable effect on the relaxation times. The angular variations of the three $\Delta m = 1$ transitions in a Verneuil sample are shown in figures 4.4, 4.5 and 4.6. The results are very similar to those obtained from vapour phase rubies, as were also the results from the Czochralski sample. The similarity of the results for Verneuil and vapour phase samples is contrary to those obtained at 9.3 Gc/s by Standley et al (1965), in which the magnitude and angular variation was smaller in the Verneuil samples. As the ratio of the relaxation times of chromic and ferric ions at 9 Gc/s and 35 Gc/s is approximately the same, the difference must arise from the presence of differing amounts of other impurities within samples grown by the same method.

5.3 The Effect of Fe^{3+}

The ground state energy levels of Fe^{3+} in Al_2O_3 are well known (Bogle and Symmons 1959), consisting of three Kramer's doublets arising from a spin of 5/2, with an overall zero field splitting of 31.3 Gc/s. The ferric ions occupy two inequivalent sites in the lattice, but

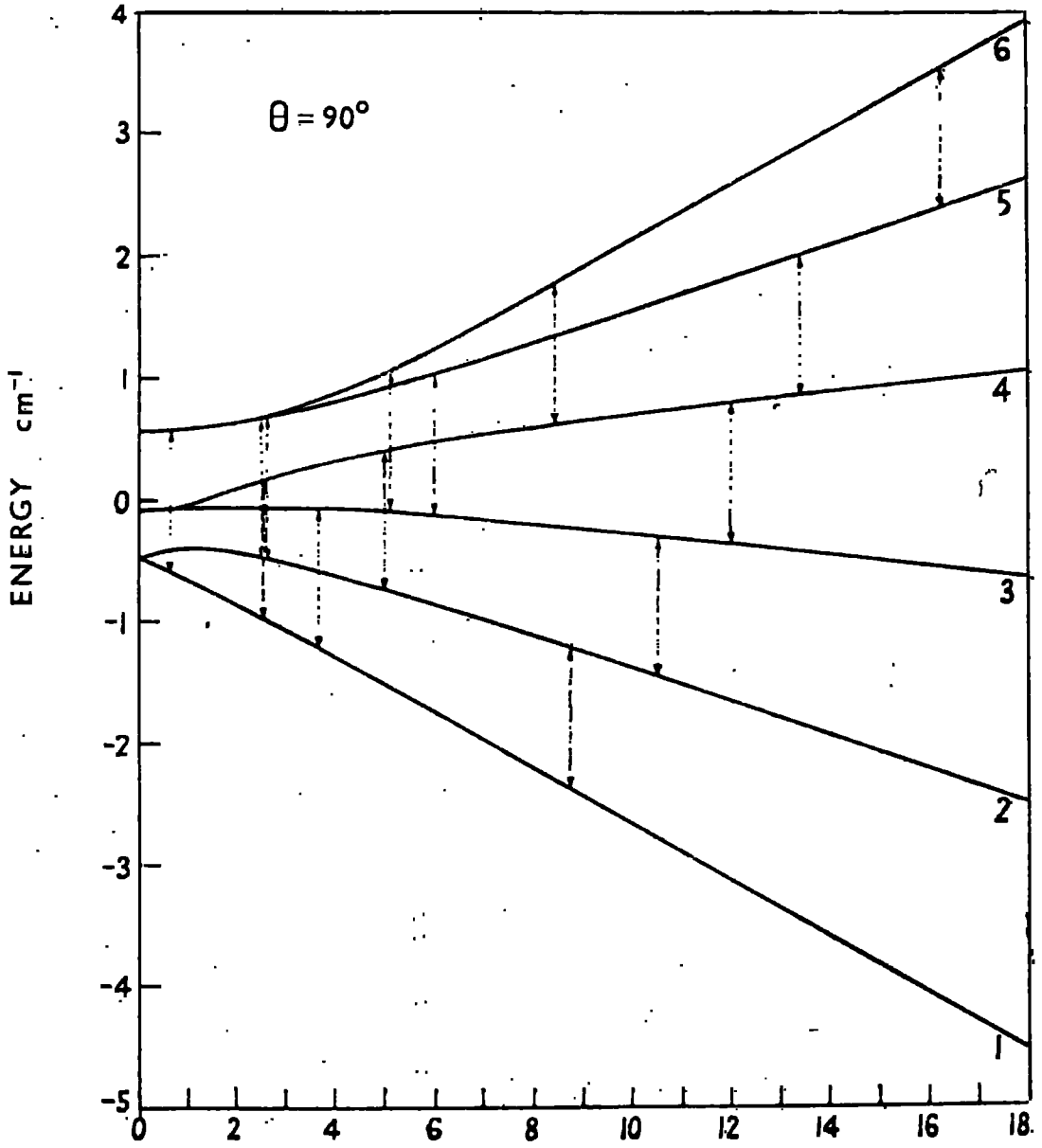

Ground Levels of Fe^{3+} ion in Al_2O_3

Fig. 5.1

	Cr	Fe	Cr and Fe	Cr	Fe	
			2 - 3			
	+1/2 to -1/2	3 - 4	+1/2 to +3/2	-1/2 to -3/2	4 - 5	Transition
	11,900	11,600	10,020	14,300	13,150	Magnetic Field (oerste
Temperature						
77°K	34.3 μs	3 μs	4.4 μs	29.5 μs	3 μs	
50°K	184 μs	30 μs	41 μs	206 μs	19.5 μs	
4.2°K	5 ms	.95 ms	3.8 ms	9 ms	1.1 ms	

Relaxation Times in Verneuil Sample,
Cr: 0.037% Fe: 0.02%. $\theta = 90^{o}$

Table 5.3

at certain orientations of the magnetic field relative to the c-axis these sites become magnetically equivalent. One of these positions is $\theta = 90^{o}$, when the energy levels are as shown in figure 5.1 with the approximate magnetic fields for the 35 Gc/s transitions marked. In a sample containing both chromium and iron the $\theta = 90^{o}$ position is particularly important, because the iron 2 - 3 transition lies within 20 oersteds of the 1/2 to 3/2 transition of chromium at 35 Gc/s, and the 3 - 4 transition is separated from the 1/2 to -1/2 transition by 300 oersteds. Thus it is possible to study cross-relaxation effects between transitions of the two ions, which will be particularly important as the Fe^{3+} ion has a relaxation time 10 times shorter than the Cr^{3+} ion.

Measurements have been made on a Verneuil grown sample containing 0.037% chromium and 0.02% iron. The values of τ for the different observed $\Delta m = 1$ transitions are shown in table 5.3 at temperatures between $4.2^{o}K$ and $77^{o}K$. The coincidence in magnetic field of the 2 - 3 and 1/2 to 3/2 transitions is exact at $77^{o}K$, but at room temperature and $4.2^{o}K$ the two lines are just distinguishable. This indicates a temperature dependence of the zero field splitting either in the Cr^{3+} or Fe^{3+} ions, or in both. The -1/2 to -3/2 transition has a generally larger value of τ than the other transitions and as can be seen from table 5.3 the field separation

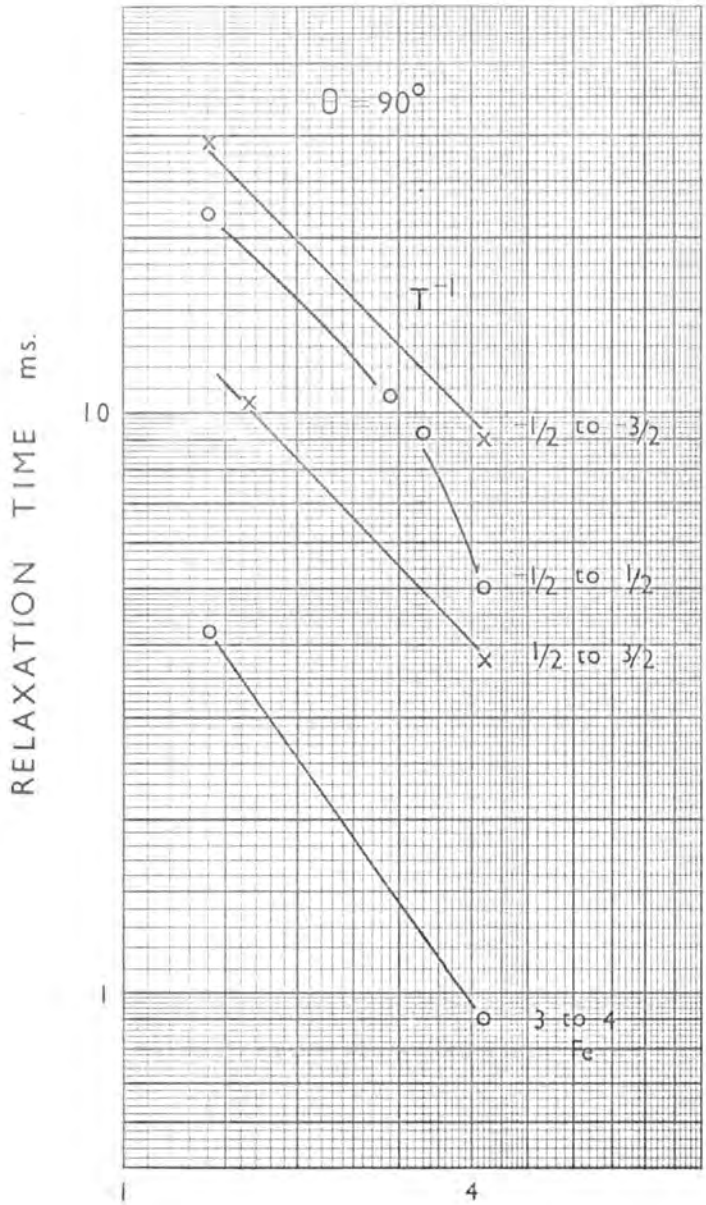
θ = 90°
T⁻¹
1/2 to 3/2
1/2 to 1/2
1/2 to 3/2
3 to 4
Fe
RELAXATION TIME ms.
10
1
1
4
TEMPERATURE °K

Fig. 5.2

from the nearest ion line is 1,150 oersteds. The temperature dependences of the different transitions below 4.2°K is shown in figure 5.2. The 1/2 to 3/2 and -1/2 to -3/2 transitions show a T^{-1} dependence, but the 1/2 to -1/2 and the neighbouring 3 - 4 transitions have a stronger temperature dependence.

Mills (1965) has shown that the presence of a second paramagnetic species in a lattice can affect the relaxation of the existing ions by disturbing the phonon spectrum. However, the number of secondary ions required to cause this effect has to be greater than 10^{19}/cc. In the present example it appears that the reduction of the relaxation time is due to cross-relaxation of the form discussed by Bloembergen et al. (1959) where the energy difference between the spins is taken up by the dipolar interaction. This means that the cross-relaxation time increases rapidly with energy separation of the spins. Nisada (1965) using the method of Schumacher (1958) has calculated the effect of N_b ions with a value of $\tau = T_B$ on N_A ions with $\tau = T_A$. Assuming a simple two level system for each ion, and that $T_B \ll T_A$, the equation for the effective relaxation time T of ions A is :

$$\frac{1}{T} = \frac{1}{T_A} + \frac{1}{(1 + \mu)T_B + T_{AB}} \qquad (5.1)$$

$\mu = N_A/N_B$ and T_{AB} is the cross-relaxation time. If we allow for the fact that the chromium ion has four levels and the iron, six, and assume for the sample being investigated that $T_{AB} = 0$ for the 2 - 3 and 1/2 to 3/2 transitions, and at 4.2°K T_A and T_B have values 15 and 1.25 ms. respectively, T is found to be 3.6 ms. as compared with a measured value of 3.8 ms. The agreement is good, and if a T^{-1} dependence is assumed for T_A and T_B, it is as good at lower temperatures.

The effect of iron on the value of τ for the 1/2 to -1/2 transition would be expected to be less because the iron line is 300 oersteds away, and the cross-relaxation time will be appreciable. Using (5.1) T_{AB} can be estimated at 4.2°K to be approximately 4 ms. Thus in measuring τ for the 1/2 to -1/2 transition, the cross-relaxation time between the transition and the 3 - 4 transition is being recorded. With this value and the measured value of T_B (5.1) underestimates the value of τ for the 1/2 to -1/2 transition by a factor of 2 at 1.4°K. The temperature dependence of this transition is seen to be particularly strong and it seems as if there is another mechanism that is affecting τ. The -1/2 to -3/2 transition seems to be unaffected by the presence of iron as would be expected, the mean c-axis misorientation for the sample was 80'

τ^-/τ^+	Fe%	Cr%	Z
2.4	0.02	0.037	32.5
1.24	0.009	0.044	92.2
1.0	0.007	0.016	100
1.0	0.003	0.08	320
0.87	-	Theory	

τ^- : -1/2 to -3/2

τ^+ : +1/2 to +3/2

$$Z = \frac{Cr\%}{Fe\%} \quad \frac{1}{(Fe+Cr)\%}$$

Effect of Iron Content on Relaxation Times of Chromium Ion

Table 5.4

and this accounts for the rather low value of τ for this transition. To eliminate the effects of sample imperfection the ratios of the relaxation times of the -1/2 to -3/2 and 1/2 to 3/2 transitions can be used, the larger the ratio indicating the greater the effect of the iron. The value of this ratio for most samples was near 1, the values of Donoho give a ratio of 0.87. Thus it appears that the smaller amounts of iron are not affecting the 1/2 to 3/2 transition. The ratio of the number of chromium to iron ions is not the only important factor, but the total number of ions must also be considered, as this determines the probability of chromium and iron ions occupying adjacent sites. Let us define a number Z given by :

$$Z = \frac{N_A}{N_B}\left[\frac{1}{N_A + N_B}\right]$$

N_A is the number (or concentration) of chromium ions, and N_B a similar term for iron. Table 5.4 shows the ratio of the -1/2 to -3/2 and 1/2 to 3/2 relaxation times for a number of samples grown by the vapour phase and Verneuil methods, and its dependence on Z. From this table the empirical result can be concluded that for $Z < 80$ the effect of iron on the relaxation of the 1/2 to 3/2 transition at $\theta = 90^{\circ}$ will be appreciable.

The relaxation times of transitions in the Fe^{3+} ion in Al_2O_3 (sapphire) have been measured at X-band by

Concentration	Transition 1 - 2	2 - 3	3 - 4	4 - 5
0.001%	2.45 ms	2.07 ms	1.95 ms	1.85 ms
0.006%	1.85 ms	-	0.85 ms	-
0.009%	-	-	0.92 ms	0.85 ms
0.02%	2.3 ms	-	0.95 ms	1.1 ms

$T = 4.2^{o}K \quad \theta = 90^{o}$

Relaxation Times for Fe^{3+} ion

Table 5.5

Kask et al (1961), and at Q-band by Pace et al. (1961). The former authors found a strong concentration dependence of τ in the range 0.02% to 0.05% iron, τ decreasing from 10 ms to 1.5 ms. at 4.2°K. At the same temperature Pace et al found that the values for the $3\Delta m = 1$ transitions in a sample with a concentration of 0.3% lay between 1.5 and 2.0 ms. Measurements have been made on a single sample of Verneuil grown sapphire with a concentration of 0.001% iron, and a chromium concentration of less than 5 times this figure. The results are in general agreement with those of Pace et al., lying between 1.7 and 2.5 ms. at 4.2°K and following a T^{-1} dependence at lower temperatures. Table 5.5 contains values of the relaxation times for various iron transitions and concentrations. Apart from the 0.001% values, the iron transitions have been measured in rubies. The values for sapphire are greater than for similar transitions in other samples, but no strong concentration dependence is apparent up to 0.02%.

5.4 Conclusion

The relaxation times for rubies grown by the different methods are very similar, unless the iron content is increased purposely. As the values of τ for most of the transitions within the Fe^{3+} ion are only 10 times shorter than those of the Cr^{3+} ion, the

effects of cross-relaxation are not very great and are limited to quite small energy ranges. If a fast relaxing impurity is responsible for the generally rather low experimental results then it would be expected that a value of $\tau < 10^{-6}$ second would be necessary to compensate for the small number of ions that must be present, unless it is another valence state of chromium or iron. A very short relaxation time would also lead to a broad absorption line or lines, and this would increase the probability of cross-relaxation over a greater range of energies.

Chapter 6

Properties of Natural and X-irradiated Ruby

6.1 Introduction

Recently Hoskins and Soffer (1964) reported that ruby boules had been grown using a method of nitride substitution allowed doping with Cr^{3+} and Cr^{4+} ions. The subsequent appearance of the specimens was orange as opposed to the usual pink coloured ruby containing only Cr^{3+}. Orange ruby had also been grown from the vapour phase apparently during normal growth conditions, but its occurrence was unexplained. Jolley and McLaughlan (1963) found that the inversion ratio of this latter natural orange ruby at the double pumping position was three times greater than that of pink ruby.

The colouring of pink ruby by exposure to x-rays had also been observed, but as undoped Al_2O_3 had turned straw-coloured on exposure to x-rays, it appeared that this was a similar effect. Other sources of high energy radiation have been used for colouring ruby specimens, a Xenon flash tube (Schultz, 1964), and γ-rays (Maruyama et al. 1964), and Vereschagin et al. 1965). In our experiments we have used 40 K.V. x-rays from a tungsten target as a

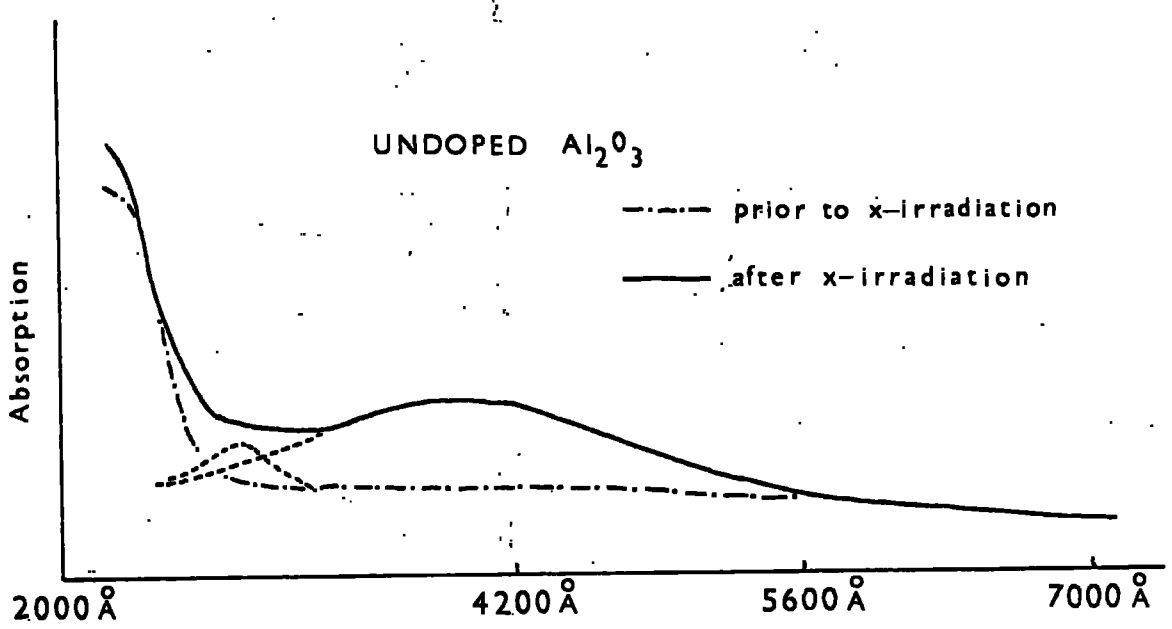

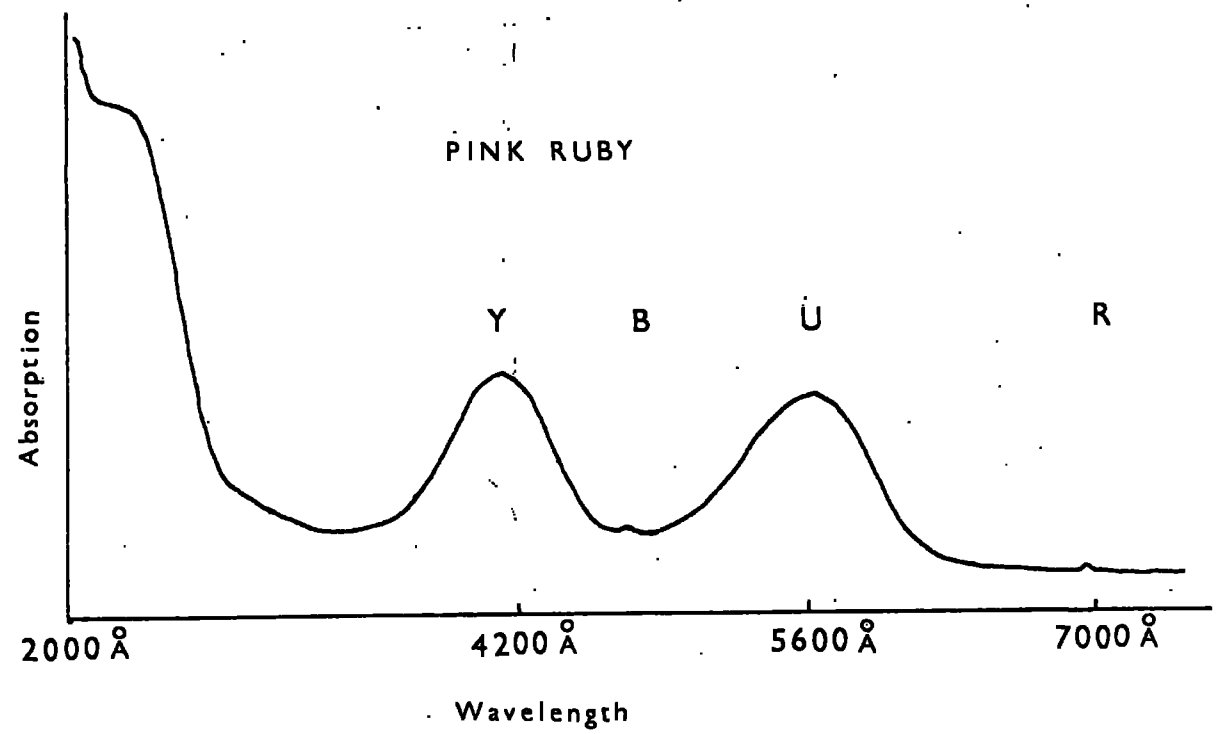

OPTICAL SPECTRA

Fig. 6.1

convenient source of high energy radiation.

6.2 Optical Properties

The absorption of radiation with a wavelength between 2,000 Å and 7,000 Å by various samples of ruby and undoped Al_2O_3 was measured on an Optica Spectrometer type CF4DR. The samples were cut and optically polished such that the light passed through them parallel to the c-axis. This arrangement meant that the E vector of the electromagnetic wave was always perpendicular to the c-axis, and no parallel component was present. A double beam arrangement was used to obtain the absorption spectrum, two identical sample holders were made so that a blank one could be placed in the reference beam as this gave enhanced sensitivity. The samples were irradiated for about 18 hours, as it was known from previous experience that colouration effects had saturated by this time.

Figures 6.1 and 6.2 show the results obtained at room temperature. The absorption spectrum of the pink ruby agrees well with that obtained by Maiman et al (1961), and the visible part of the spectrum is distinguished by the two absorption peaks of equal magnitude which reach a maximum at 4,200 Å and 5,600 Å. The nomenclature used for identifying the peaks is that used by Sugano and

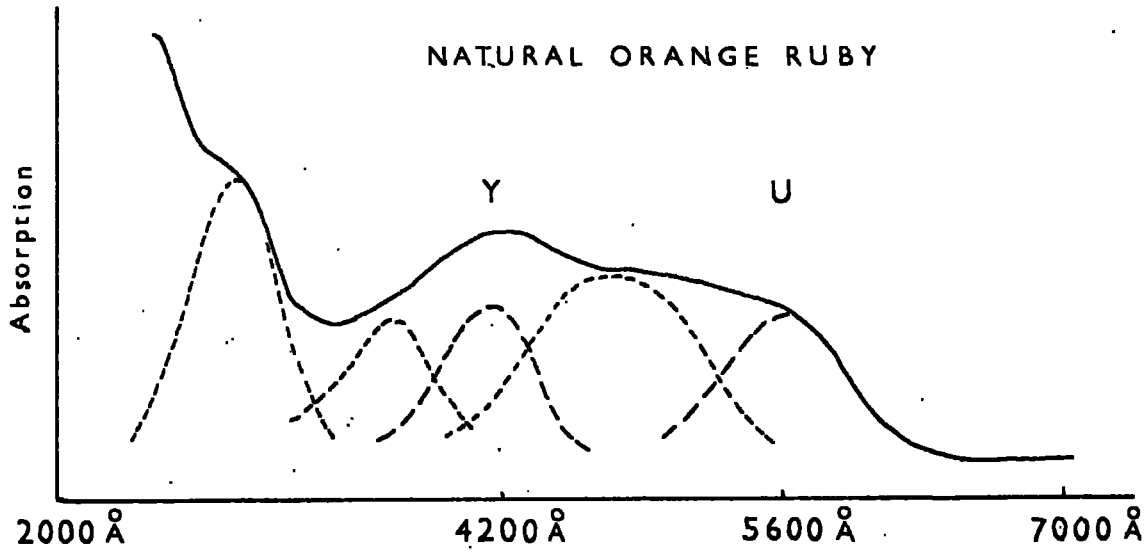

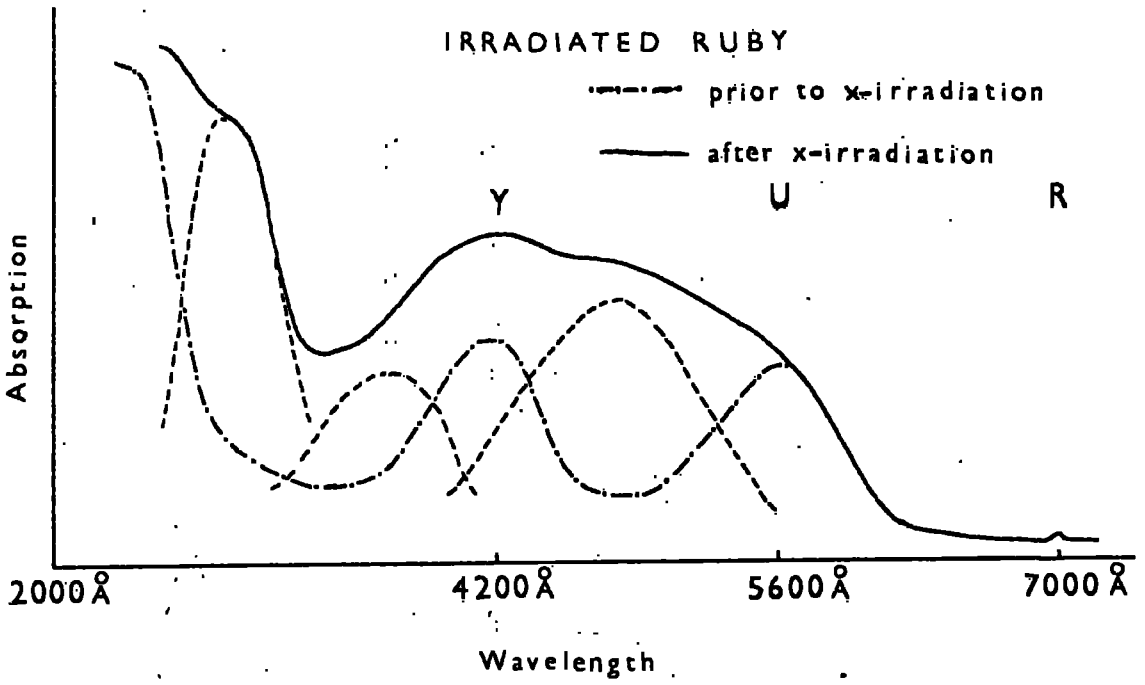

OPTICAL SPECTRA

Fig.6.2

Tanabe (1958). The spectrum of undoped Al_2O_3 has been closely investigated by several authors (e.g. Levy 1961, Lehman 1964). The absorption peak centred at 2,200 Å is thought to be due to a defect centre. After x-irradiation the sample appears straw coloured, a broad absorption band occurring in the blue part of the spectrum. This was first reported by Hunt and Schulpein (1951). If this band is assumed to be symmetrical then the absorption of the sample can be shown to consist of a broad band centred at 4,100 Å and a smaller narrower band at 2,800 Å. These figures are in approximate agreement with the results Levy (1961) obtained after γ-irradiation of Al_2O_3.

Figure 6.2 shows the absorption of a sample of natural orange ruby grown from the vapour phase with no special charge compensation. If allowance is made for the Y and U bands which originate in the Cr^{3+} ion, three distinct extra bands can be seen. The analysis of the spectrum into bands assuming a Gaussian distribution has been applied by Levy, Maruyama and others. The application of this analysis to the remaining absorption spectrum gives three bands peaking at 4,700 Å, 3,600 Å and 2,800 Å respectively. The first two peaks compare with those found by Hoskins and Soffer in the charge compensated ruby which occurred at 4,700 Å and 3,700 Å.

Published results are not available for wavelengths below 3,000 Å. The x-irradiated pink ruby has a very similar absorption spectrum with peaks occurring at 4,800 Å, 3,650 Å and 2,800 Å. These figures agree very well with the results of Maruyama and Matsuda from γ-irradiated ruby, which show peaks at similar wavelengths and an additional one at 2,200 Å. The thickness of the samples used in the present experiments did not permit the peak occurring near 2,200 Å to be resolved. Comparison of the x-irradiated ruby and undoped Al_2O_3 shows that the magnitude of the band occurring at 2,800 Å is greater in the chromium doped sample. In Al_2O_3 this band was attributed to defects within the lattice so that it appears that the introduction of chromium into the lattice increases the number of defects.

6.3 Paramagnetic Properties

The microwave absorption spectrum and relaxation times in natural orange ruby and pink ruby before and after x-irradiation were measured on the spectrometer which has been described earlier. The chromium concentrations in the two samples were 0.041% and 0.032% respectively, estimated spectrographically. Figure 6.3

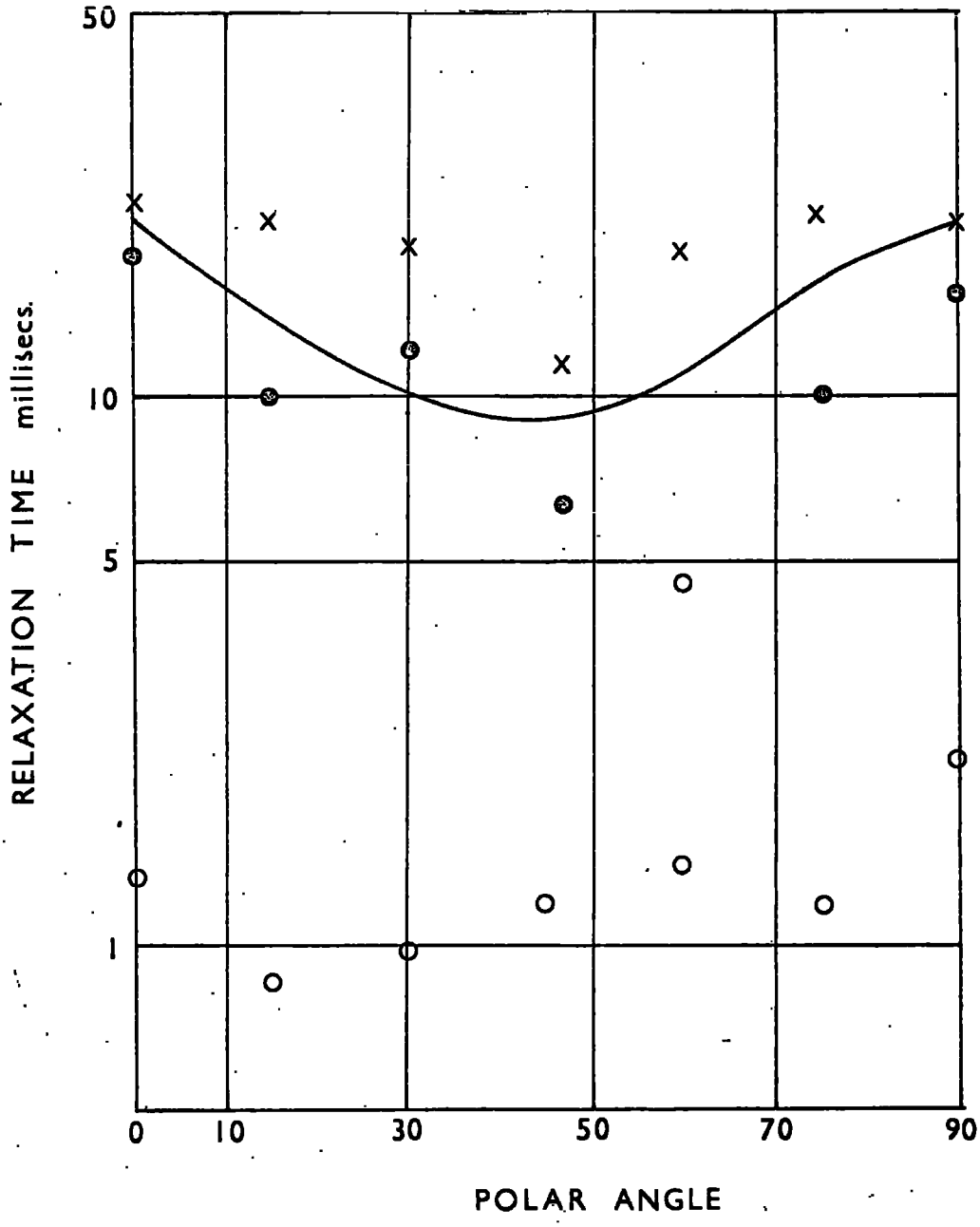

$+1/2$ to $-1/2$ transition at 4·2 °K

● pink ruby

○ after x-irradiation

X after x and u.v. irradiation

full line · theory $\left[1/6\right]$

Fig.6.3

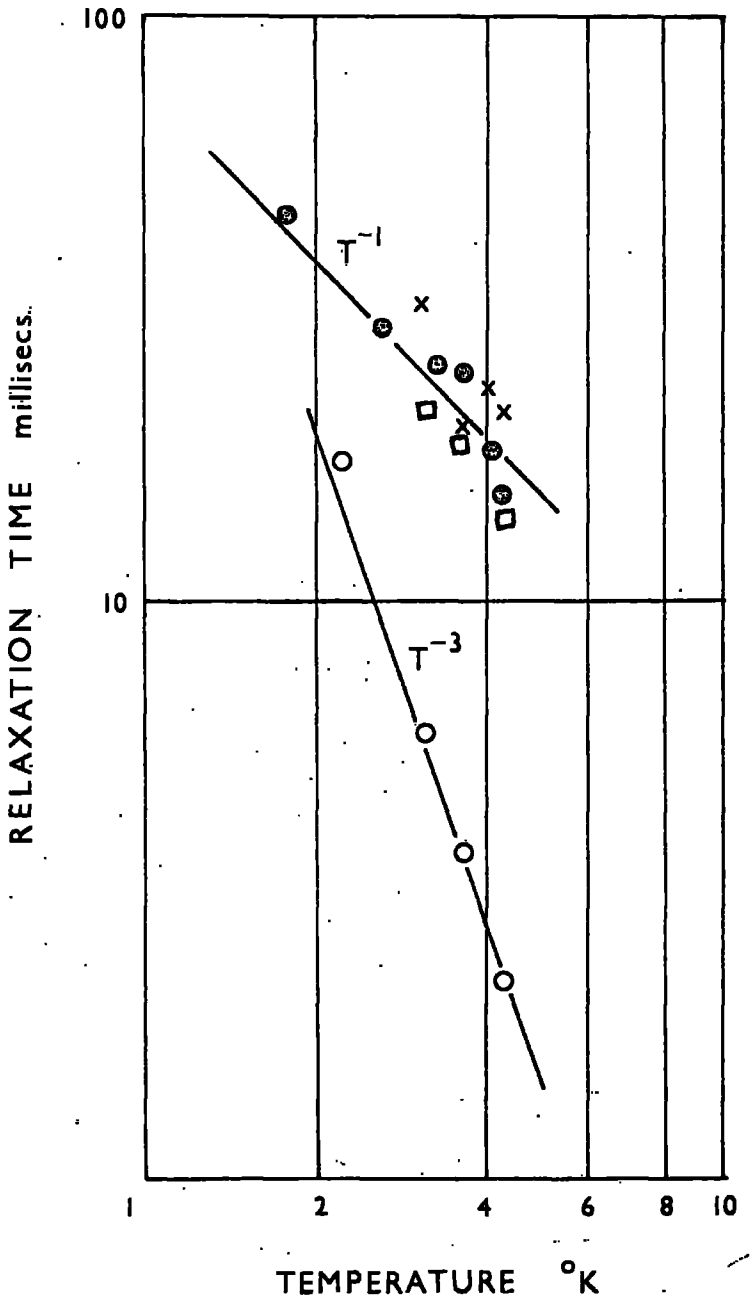

1/2 to -1/2 transition at $\theta = 90°$

● pink ruby ○ after x-irradiation

× after x and u.v. irradiation □ natural orange ruby

Fig. 6.4

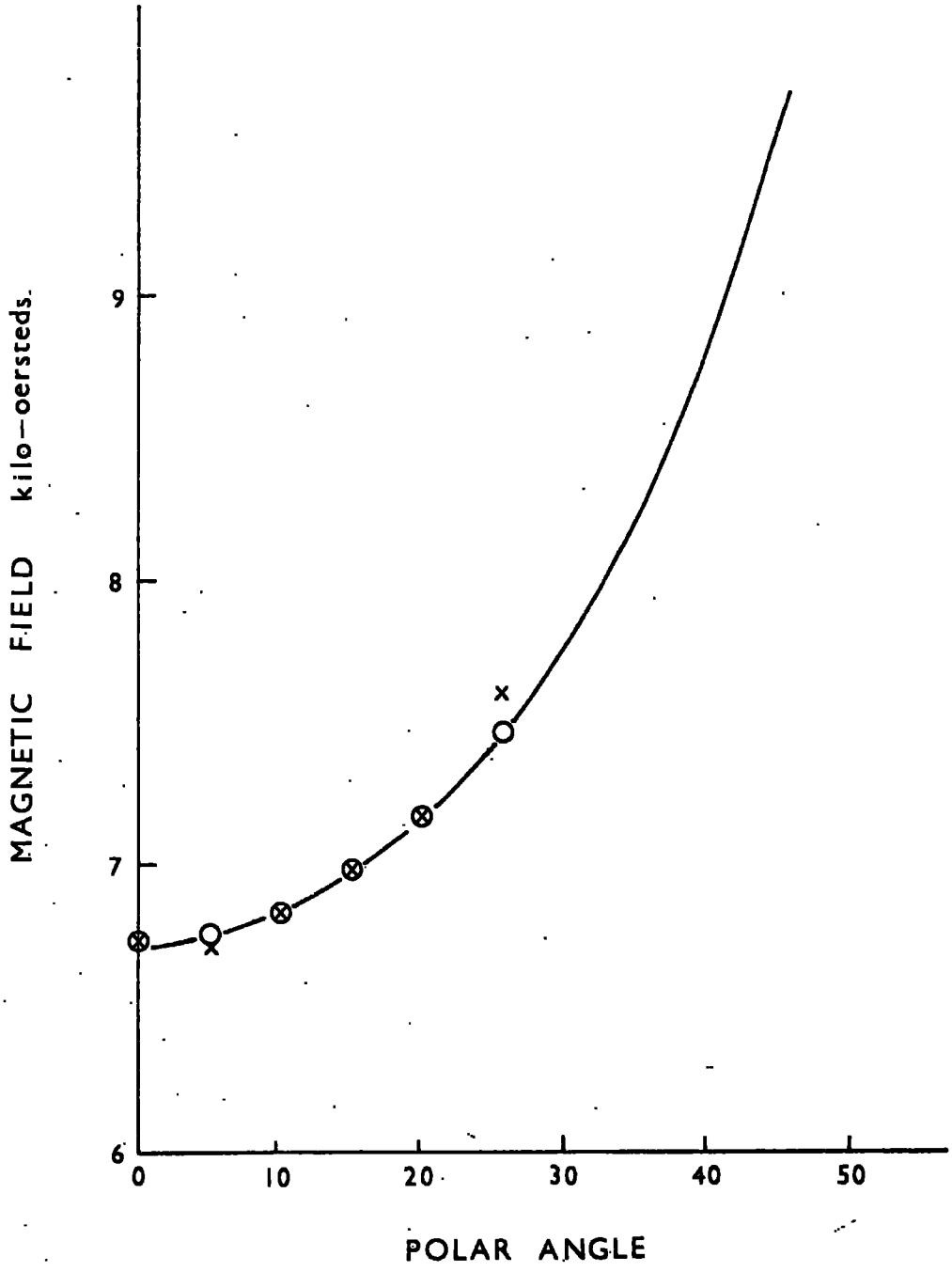
MAGNETIC FIELD kilo-oersteds.
9
8
7
6
0
10
20
30
40
50
POLAR ANGLE
O natural orange
x x-irradiated
full line Cr^{4+} predicted

Fig.6.5

shows the angular dependence of the relaxation time of the 1/2 to -1/2 transition in the pink ruby before and after x-irradiation. The angular dependence is also shown after the sample has been x-irradiated and then exposed to u.v. light until it had attained its original pink appearance. The temperature dependence of the relaxation time of the same transition at $\theta = 90^{o}$ is shown in figure 6.4 for natural orange ruby and pink ruby before and after x- and u.v. irradiation. The microwave absorption of natural orange ruby was identical to that of pink ruby except for an additional absorption line occurring at 6,700 oersteds at $\theta = 0^{o}$. A similar line was observed in the x-irradiated ruby, and the angular dependence of both lines is shown in figure 6.5 along with the predicted angular dependence of the $\Delta m = 2$ transition of Cr^{4+} in Al_2O_3 reported by Hoskins and Soffer.

6.4 Discussion

There is good agreement between the predicted angular dependence of the Cr^{4+} line and the experimentally observed line in both natural orange and irradiated ruby at $4.2^{o}K$. The absorption lines were undetectable at $1.7^{o}K$, and this would be expected as the probability of occupation will be low at these temperatures because the $M = \pm 1$ levels are 7 cm^{-1} above the ground state singlet.

The difference in angular dependence before and after x-irradiation is apparent. The values obtained from the natural orange sample were of the same order as the pink ruby, and some angular dependence was apparent. Both pink and natural orange ruby had relaxation times which were inversely proportional to temperature in the range 4.2°K to 1.6°K. Although it has been reported by Hoskins that Cr^{4+} has a short relaxation time at 4.2°K, its effect on the relaxation times of the Cr^{3+} ions in natural orange ruby is negligible. Recently Standley and Vaughan (1965) found that the Cr^{4+} ion had no serious influence on the Cr^{3+} relaxation even in the region where the absorption lines overlapped.

The noticeable reduction of the relaxation times in the irradiated sample and the apparently random angular variation is seen in figure 6.3. There is also a marked change in temperature dependence after irradiation and figure 6.4 shows this to be approximately T^{-3}. A comparable effect on the Cr^{3+} transitions has been reported by Zverev et al. (1963) following the introduction of vanadium into ruby. Approximately .1% of V^{3+} reduced the relaxation times of the Cr^{3+} transitions by approximately 100 times and changed the temperature dependence until it followed an approximate T^{-3} relationship below 4.2°K. As V^{3+} is isoelectronic with Cr^{4+}

$\frac{1}{2}$ to $-\frac{1}{2}$	$\frac{1}{2}$ to $\frac{3}{2}$	$-\frac{1}{2}$ to $-\frac{3}{2}$	Treatment
15.0 ms	15.0 ms	13.0 ms	As grown
2.1 ms	1.3 ms	4.1 ms	15 hrs. x-irrdn.
2.7 ms	3.5 ms	6.4 ms	14 days in dark
20.6 ms	16.2 ms	12.6 ms	21 hrs. U.V.

Relaxation Times for $\Delta m = 1$ transitions at

$\theta = 90^{\circ}$, $T = 4.2^{\circ}K$

Table 6.1

it would appear at first sight that the effect of irradiation of pink ruby is to generate enough Cr^{4+} to cause this effect. However, the intensity of the Cr^{4+} absorption line was approximately the same in natural orange and irradiated orange ruby, and was smaller by a factor of one hundred than that of the main Cr^{3+} absorption lines. Comparison of the relaxation times in pink and natural orange ruby shows that this amount of Cr^{4+} had little effect, thus the reduction of the relaxation times in irradiated ruby cannot be solely due to Cr^{4+}. High energy irradiation of undoped Al_2O_3 produces a resonance spectrum centred near g = 2 (Gamble et al.1965)which would undoubtedly affect the $+\frac{1}{2}$ to $-\frac{1}{2}$ transition. However, it was found that the relaxation times of transitions separated in magnetic field by several thousand oersteds were also reduced (see table 1). The $\Delta m = 1$ transitions for Cr^{3+} ions were affected by irradiation, and the absorption lines broadened, and sometimes split. This could also explain the reduction of the relaxation time, but it would not be expected to affect the temperature dependence. This is most easily explained by postulating the existence of a fast relaxing centre whose population is temperature dependent in the range 4 - 1.7^{o}K. If the coupling between the chromium ion and this centre was strong enough, the relaxation time would be strongly temperature dependent in the

range under consideration. The Cr^{2+} ion in Al_2O_3 would be expected to be tightly coupled to the lattice (Standley et al. 1965) giving a broad absorption line. If this were present in ruby, cross-relaxation with the Cr^{3+} transitions would reduce the relaxation times and remove the angular dependence. As the lowest level of the Cr^{2+} ion is a singlet (Gorter, 1947) the intensity of an absorption line originating in an upper doublet would be strongly temperature dependent at helium temperatures. Any cross-relaxation effects would be similarly affected, giving the Cr^{3+} transitions a strong temperature dependence. It is difficult to explain why the relaxation time is still several milliseconds, if the Cr^{2+} ion has a short relaxation time and is coupled tightly enough to the Cr^{3+} ion to give the strong temperature dependence. The generation of Cr^{2+} by the x-irradiation of Cr^{3+} in Al_2O_3 would be expected by comparison with similar experiments reported by Lambe and Kikuchi (1960). X-irradiation of V^{3+} in Al_2O_3 led to an appreciable increase in V^{2+} but no detectable increase in V^{4+}. It was assumed that there was some unknown centre in the lattice which could yield an electron and recent work by Gamble et al. indicates that such centres exist. The existence of Cr^{2+} in γ-irradiated ruby was postulated by Maruyama and Matsuda after measurements on the intensity of the

Cr^{3+} lines before and after irradiation. Further evidence seemed to appear when it was calculated that an optical absorption band due to a Cr^{2+} ion would occur at 4,750 Å. However, the presence of a similar band in the natural orange ruby which exhibits relaxation time phenomena similar to that of pink ruby seems to indicate that this band is due to a colour centre. Hoskins and Soffer point out that a helium-like doubly charged centre in Al_2O_3 would be expected to give a band peaking at 4,900 Å. A band appears in reactor irradiated Al_2O_3 at 4,750 Å as reported by Levy, and using data from annealing experiments this has been attributed to a defect centre. It is possible that the Cr^{2+} band predicted by Maruyama and Matsuda is present in the irradiated sample but it is of low intensity.

Figures 6.3 and 6.4 show that the relaxation times measured after the x-irradiated sample had been exposed to u.v. radiation are very similar to the original values, and show the original temperature and angular dependence. Hence it appeared that the effects of x-irradiation had been removed by u.v. bleaching. Maruyama and Matsuda reported that annealing at 350°C removed the effects of γ-irradiation and concluded that interstitials cannot have been formed as these would be

Sample 1	Sample 2	Sample 3	Treatment
18.0 ms	18.6 ms	13.0 ms	As grown
1.3 ms			15 hrs.x-irrdn.
22.4 ms	17.4 ms	12.0 ms	21 hrs. U.V.

Relaxation Times of $+\frac{1}{2}$ to $-\frac{1}{2}$ transition

at $\theta = 0^{o}$, $T = 4.2^{o}K$

Table 6.2

stable at such low annealing temperatures After x-irradiation we found that the relaxation time remains short if the sample is kept away from u.v. radiation (table 1). Table 6.2 shows corroborative results from additional specimens, samples 2 and 3 were of similar concentrations but the latter was grown by the Verneuil process, measurements were made at the beginning and end of the cyclic treatment only.

It must be concluded that the additional absorption bands in the natural orange and x-irradiated ruby are derived from colour centres. These centres are present in the samples from growth, and the x-rays change the electron distribution in the lattice. The low energy required to remove the effects of irradiation confirms this view. The increase of the intensity of the band attributed to defects in Al_2O_3 upon the introduction of chromium indicates that additional defects are introduced into the lattice with the chromium, probably to compensate for the difference in ionic radius of the Cr^{3+} and Al^{3+} ions.

The g = 2 line in natural orange ruby reported by Jolley and McLaughlan was not observed in our samples. An improved inversion ratio could however be obtained using the Cr^{4+} line. At the double pumping position the energy separation of the Cr^{4+} levels is almost the same as the idler transition energy. If cross-relaxation

occurred to the Cr^{4+} ion which has a short relaxation time, then the population inversion in the signal levels would be enhanced.

Footnote:

A majority of the contents in this chapter have appeared as a paper in Proc. Phys. Soc. 1966, Vol. 87, 49.

Chapter 7

Relaxation Mechanisms in Other Materials

7.1 Introduction

Measurements have been made on chromium doped spinel, rutile and alums and on iron doped alum. The available number of samples in each case has been limited, and so the values of τ are only indicative of the order of magnitude of the relaxation times that can be expected in these materials, which will now be discussed under separate headings.

7.2 Chromium doped Spinel

Dugdale (1965) has described the paramagnetic relaxation of Cr^{3+} in $MgAl_2O_4$ grown from a fluxed melt, measured at 9.2 Gc/s. Measurements have been made at Q-band on two of the samples kindly loaned by D.E. Dugdale.

The chromium ions can occupy one of four inequivalent sites in the lattice, each with a trigonal distortion along a body diagonal of a cube and a zero field splitting of 55.5 Gc/s. With the magnetic field parallel to one of these trigonal axes i.e. in the (111) direction, the 1/2 to -1/2 transition for the single site was observed at a magnetic field corresponding approximately to $g = 2$. A second broad absorption line was observed at a magnetic

field near 7,000 oersteds and this was attributed to the 1/2 to 3/2 transition of the single site which is coincident with the 1/2 to -1/2 transition of the three other sites.

The two samples measured had chromium concentrations of 0.2% and 0.05%, and at 4.2°K the relaxation times of the 1/2 to -1/2 transition of the single site were 210 μs. and 3.2 ms. respectively. These values were taken from the last part of the recovery curve which generally consisted of more than one exponential. The value of τ for the 0.2% sample was independent of temperature below 4.2°K, but the 0.05% sample had a temperature dependence of $T^{-0.6}$ which was greater than had been obtained at X-band. The relaxation time measured for the other sites at 7,000 oersteds was found to be linearly dependent on the temperature below 4.2°K in the high concentration sample, and the values of τ at 1.7°K were 50 μs. and 1.6 ms. in the 0.2% and 0.05% samples respectively.

The relaxation times of the 1/2 to -1/2 transition of the single site show an inverse square concentration dependence which indicates, as Dugdale points out, that cross-relaxation to the pair system is probably being observed. However, the ratio of the relaxation times measured at the two frequencies in the two samples is approximately equal to the ratio of the relaxation times

obtained if an Orbach process is assumed to occur via the upper ground state levels. This would not be expected unless the relaxation of the pair system was being observed.

Even if the relaxation of the single site is being dominated by the pair system, the relaxation of the other sites as they coincide at 7,000 oersteds may be unaffected by the pairs, as the ratio of the number of single ions to pairs is increased by a factor of 4. The observed temperature dependence of T^{-1} indicates that the relaxation of the single ions is being observed although a concentration dependence is still present.

The evidence given by these measurements tends to support the theory that the relaxation of the single site is determined predominantly by the pair relaxation, although it is not clear what the relaxation time that is being measured represents.

7.3 Chromium doped Rutile

The zero field splitting of the Cr^{3+} ion in TiO_2 is 43.3 Gc/s, and there are two inequivalent sites for the chromium ions. A piece of red rutile has been examined of unknown concentration, and numerous additional absorption lines were seen in the microwave spectrum compared with the known spectra of the Cr^{3+} ion. The value of τ for the 2 - 3 transition of ion (b) at $\theta=90^{o}$,

$\phi=0^{\circ}$ (see Pace et al. 1961 for nomenclature) was 93 μs. compared with 2.2 ms. in the comparison sample. The temperature dependence for the same transition at high magnetic field was T^{-3} compared with the usual approximate T^{-1} temperature dependence. Red rutile is thought to derive its colour from the presence of Cr^{2+} ions which are associated with an oxygen deficiency in the lattice (Maddock, private communication). If the sample is heated in an oxygen atmosphere at 700°C for five hours the usual dark violet colour is obtained. It is interesting to note the similar temperature dependence of red rutile and x-irradiated ruby which may both contain Cr^{2+} ions.

X-irradiation of a piece of chromium doped rutile which had measured relaxation times similar to those reported by Pace et al. (1961) at 4.2°K, reduced the values of τ by a factor of 2 and increased the temperature dependence from approximately T^{-1} to $T^{-1.6}$. The microwave spectrum of the irradiated rutile did not contain the numerous lines of the red rutile, and it appears that a far more detailed examination of oxygen deficient rutile is required to understand which mechanisms are limiting the relaxation times.

7.4 Alums

(1) Chromium Potassium Alum. In 1960 Kochelaev pointed out that one of the basic assumptions in Van Vleck's work (1940) was not always valid, namely, that the atoms surrounding the paramagnetic ion were bound with forces of the same order of magnitude as those of the ion. In particular in complexes XY_6 where the paramagnetic ion X is surrounded by an octahedron of diamagnetic ions Y, the complex may have vibrational frequencies (intramolecular vibrations) which differ considerably from the frequencies between neighbouring complexes (lattice vibrations). Kochelaev considered that the intra-molecular vibrations are an intermediate link in the transmission of energy from the spins to the lattice vibrations. In chromium potassium alum the chromium ion is surrounded by an octahedron of water molecules and is a good example of situation under discussion. Kochelaev calculated that τ at $77^{\circ}K$ was of the order of 5×10^{-7} sec., this is of order of magnitude agreement with experiment which indicate values of $\tau < 5 \times 10^{-6}$ sec.

Measurements have been made at helium temperatures on two samples, one with a chromium concentration of approximately 10% and the other with a concentration of 0.05%. One large absorption line at approximately g = 2

Ratio of $\frac{\tau_{alum}}{\tau_{ruby}}$	Van Vleck	Kochelaev	Experimental
1 phonon	10^{-3}	1	2.5×10^{-2}
2 phonon			
(a) $T \ll \theta_o$	10^{-6}	10^{-3}	10^{-2} ($77^{\circ}K$)
(b) $T \gg \theta_o$	10^{-3}	1	

Table 7.1

was observed with two small subsidiary lines on either side. Bleaney (1950) has explained the spectrum in terms of two zero field splittings. For the dominant line both samples gave a value of τ at 4.2°K of 0.5 ms., the high concentration sample had a temperature dependence of $T^{-1.8}$ and the lower one $T^{-0.8}$. These results are in agreement with Nisada (1964) who found at X-band that the value of τ was near 3 ms. and independent of concentration up to 11.7%. At this concentration the temperature dependence was reported to be $T^{-1.8}$.

Kochelaev has calculated the ratio of the relaxation of the chromium ion in chromium potassium alum and ruby and compared it with the ratio obtained using Van Vleck's original method. The ratios are shown in table 7.1 together with the experimentally determined values. It is difficult to know which theoretical value to use at higher temperatures (77°K), as Θ_o for the alum is 78°K (Kapadnis 1956). The experimental results seem to agree with the predictions of Kochelaev at higher temperatures, but the agreement is by no means convincing at helium temperatures.

(2) Methylamine Alum. Chromium and iron doped methylamine alum single crystals have been grown at room temperature from a solution of methylamine alum and the appropriate ammonium alum. Starting with methyl-ammonium chloride, the alum was produced by adding concentrated sulphuric acid and aluminium sulphate.

The reaction is described as follows:

$$2CH_3NH_3Cl + H_2SO_4 + Al_2(SO_4)_3 \rightarrow 2AlCH_3NH_3(SO_4)_2 + 2HCl$$

The spectrum of chromic methylamine alum has been examined in detail by Baker (1956), who concluded that at low temperatures the symmetry is rhombic, and that there are four sites in each unit cell. With the magnetic field parallel to the (111) direction 6 absorption lines were observed, 3 arising from a single site, the other 3 from the three other sites whose axes of distortion are equally inclined to the magnetic field. Samples with a concentration of 0.22% and 0.05% have been measured and the results were the same for both of them. The values of τ at $4.2^{o}K$ ranged from 0.38 ms. to 1 ms. for the different transitions and the temperature dependence below $4.2^{o}K$ in both samples for the same transition was T^{-2}.

A single crystal of ferric methylamine alum was grown with a concentration of 0.58% to see if the zero field transition at 34.5 Gc/s could be observed. This transition would be used in a zero field maser operating at a signal frequency of 12.3 Gc/s as suggested by Bogle and Symmons (1961). The number of absorption lines was greater than 30, Bleaney et al. 1954, have reported seeing as many as 60 ... which are unexplainable

using a simple energy level system. The zero field line was not observed, but this may have been due to the very low transition probability that would be expected from a $\Delta m = 2$ transition. Measurements of the relaxation times were made for the strongest absorption lines present and the values of τ were in the range 200 - 400 μs., although there were considerable cross-relaxation effects present. The temperature dependence was T^{-1} below $4.2^{o}K$.

If the water complex plays an important role in governing the relaxation times in the alums it would not be expected that the values of the relaxation times would be very different in the various alums, and this is the case. The lack of concentration dependence of τ is particularly significant.

7.5 Discussion

Mattuck and Strandberg (1960) have shown that for ions of the 'iron group' the transition probability between Kramer's doublets will be very small, and in zero magnetic field strictly zero. Thus for the Cr^{3+} ion in ruby and similar lattices the relaxation of the 1/2 to -1/2 transition is via a level of the upper Kramer's doublet by the Orbach process. The ratios of the relaxation times given by this process at Q and X-band is :

$$\frac{\tau_Q}{\tau_x} = \left[\frac{\Delta_x}{\Delta_Q}\right]^3 \frac{\exp.(\Delta_Q/kT) - 1}{\exp.(\Delta_x/kT) - 1}$$

where Δ for trigonal symmetry is given approximately by

$$\Delta \simeq 2D + \frac{3g\beta H}{2}$$

If the splitting $\Delta < kT$ then the exponential term in the Orbach process can be expanded to give the linear dependence in T as predicted by the direct process. The ratio of τ_Q/τ_x when D = 0 is H_X^2/H_Q^2, which is the Van Vleck result for multiple Kramer's doublets with no zero field splitting. For large values of D the ratio tends to unity until $\Delta > \theta_o$ and then the Orbach process cannot take place and the ratio becomes equal to H_X^4/H_Q^4, i.e. as for an isolated doublet.

Unless the texture and impurity of samples is known it is difficult to ensure any accuracy in taking ratios of relaxation times from published data. In the case of ruby it is known that similar samples were found by Standley et al. (1965) to the ones used in the present work. The ratio of the results at Q and X-band is approximately 0.1 compared with the Orbach ratio of 0.185. The ratios of the relaxation times for 0.02% Fe in sapphire using the X-band results of Kask et al. (1963) and the Q-band results of 0.02% Fe in ruby give 0.23 compared with the theoretical value of 0.33. As we

have mentioned earlier the spinel results agreed reasonably well with the Orbach ratio, but very little weight can be given to this result as it is unlikely that the relaxation of the single ion was measured. Using the X-band result of Manenkov et al. for the relaxation time of the lower doublet in rutile and the value obtained from the present work an experimental ratio of 0.3 is obtained compared with the theoretical prediction of 0.40. Lampe and Wagner (1965) have reported that the temperature dependence of this transition in rutile has been fitted to an expression of the Orbach form with Δ equal to the zero field splitting. The agreement between theory and experiment improves for increasing zero field splitting. This may have been expected as the degree of mixing of the states and the transition probability between the levels of +1/2 to -1/2 transitions will decrease with increasing zero field splitting. The experimental ratio may vary by a factor or 2 or more depending on the crystallographic and chemical properties of the samples chosen.

Thus the frequency dependence of the relaxation of the lowest Kramer's doublet in the materials examined in this thesis apart from the alums, can be explained to an order of magnitude by considering an Orbach process via an upper doublet. The behaviour of the alums seems

to depend on the waters of crystallization, and this may account for the high concentration that the samples can contain before exchange interaction limits the relaxation times.

Chapter 8

Conclusions

The Laue back reflection x-ray technique has given information on the perfection of the crystal structure in a simple and easily usable form. The accuracy of these results has not been high, but the use of a more sophisticated method e.g. 2 crystal x-ray spectrometer, would have necessitated undertaking far more measurements as the versatility of such techniques is less, and it is difficult to see what increased information would be gained. There have been two particular advantages in using the microwave spectrometer as it has been constructed. The elimination of a klystron to provide the local oscillator signal has allowed flexibility of operation, especially in variations of the tuning frequency. The inherent low Q properties of the system have allowed continuous temperature measurements to be made from $1.5^{o}K$ to $120^{o}K$ without any elaborate readjustment of the spectrometer. The use of a cavity would have increased the sensitivity and ease with which the spectrometer could have been operated. at the expense of this flexibility of application.

Rubies grown at high temperatures contain a large number of physical defects which mainly arise from the large thermal gradients present within the boule and furnace during growth. Samples grown from the vapour phase, and by the Verneuil and Czochralski technique had dislocation densities near $10^5/cm^2$, and mosaic and c-axis misorientations ranging from a few seconds of arc to several degrees. A detailed study of samples grown from the vapour phase has shown that a change of c-axis misorientation by 1^o can reduce the relaxation time by a factor of 2, and that there was no effect of the mosaic structure on the relaxation time. The temperature dependence of the relaxation time in the Raman region has suggested that the chromium ions occupy two types of lattice site. One is perfect, that is the surrounding lattice is regular and largely unaffected by dislocations, and the other site has associated crystal defects. These may be neighbouring isolated vacancies or dislocations and grain boundaries. Optical measurements have shown that the presence of Cr^{3+} ions in the lattice also increase the number of lattice defects compared with undoped Al_2O_3. Infrared absorption measurements have also shown that a large number of hydroxyl ions are present in the lattice

(Stephenson, private communication). The effects of lattice imperfections will increase as the measuring frequency increases, that is as the wavelength becomes comparable with the dimensions of the distorted regions.

The presence of impurities and other valence states of the chromium ion may also affect the relaxation time. Cr^{4+} ions have been detected in ruby but they have been found to have no effect on the relaxation of the Cr^{3+} ions. The Cr^{2+} ion has not been directly observed, although the change of relaxation behaviour produced by x-irradiation indicates that such an ion, or similar fast relaxing centre has been generated by irradiation. The similar temperature dependence of the relaxation times in chromium doped oxygen deficient rutile which is thought to contain Cr^{2+} ions, is an additional indication of the nature of the centre in x-irradiated ruby. Ferric ions do reduce the relaxation times of the chromic ion if a sufficient number are present. Although the two inequivalent sites lead to extensive cross-relaxation between the two ions at polar angles below 60^{o}, the effects are limited to a small range of energies near the coincidence positions. However, the divalent ion may be expected to have a considerable effect on the relaxation times of the chromic ions if it were present.

The frequency dependence of the relaxation times in some materials containing Kramer's ions, in particular for transitions across the lower Kramer's doublet, has been explained in terms of an Orbach relaxation process via upper levels. The effect is more important in materials with a large zero field splitting such as rutile and spinel.

The mechanism governing the relaxation of paramagnetic ions in the alums has been found to depend on the presence of waters of crystallization. These water complexes modify the rate of exchange of energy between the spins and the lattice vibrations, and similar relaxation times are found in various alums.

In the absence, at present, of perfect single crystals paramagnetically doped but containing no waters of crystallization or similar complexes, the relaxation times in nearly perfect crystals should yield very useful information. In particular, the temperature dependence in the Raman region should be particularly distinctive, especially if a material with a low Debye temperature is used. The use of this dependence on temperature to yield information concerning the perfection of the lattice site, leads to the possibility of the examination of the effect of the controlled introduction of defects into the lattice.

APPENDIX 1

Relaxation Times and Amplitudes for Ruby at 35 Gc/s calculated by P.L. Donoho.

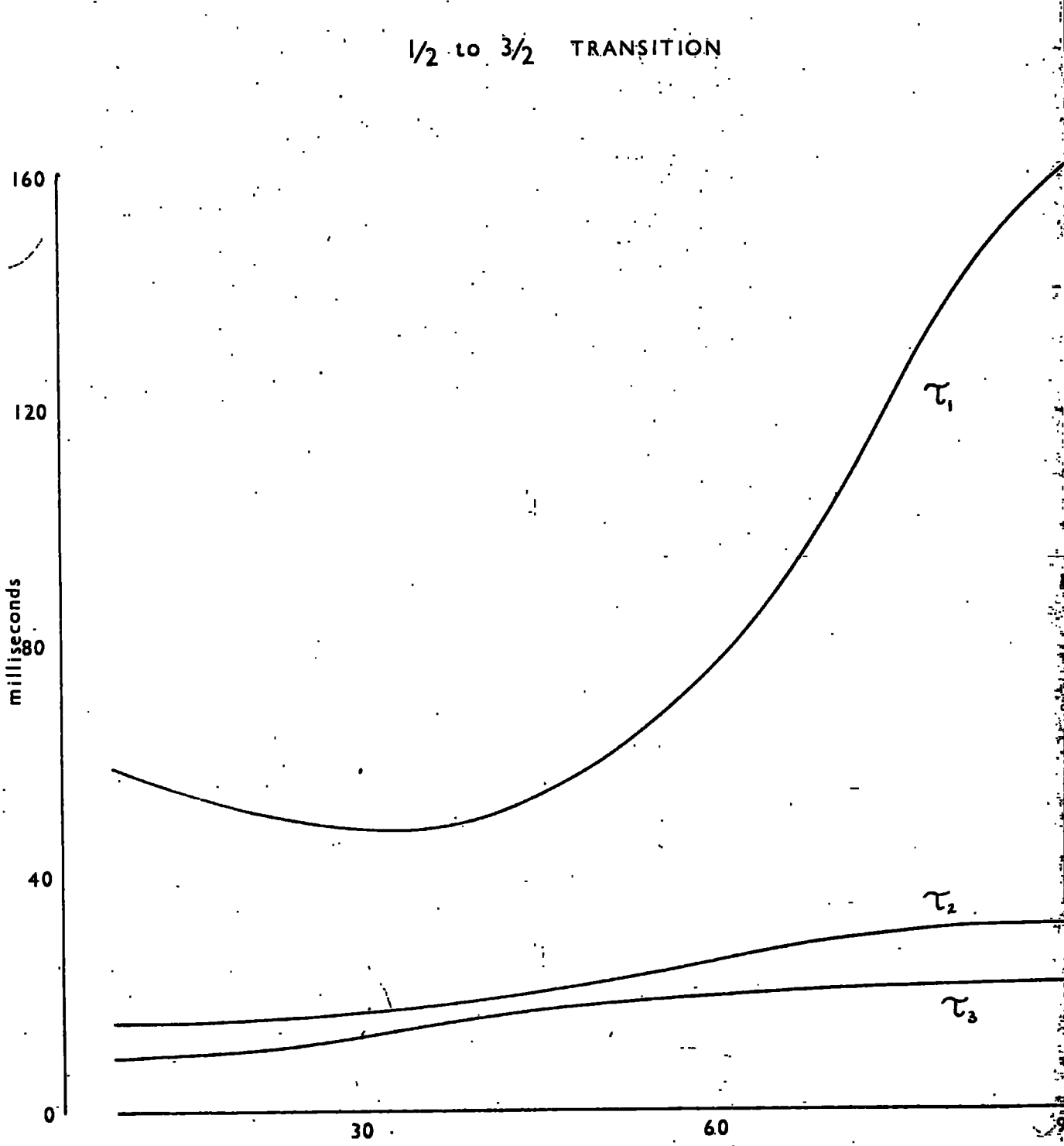
1/2 to 3/2 TRANSITION
160
120
80
40
0
milliseconds
30
60
POLAR ANGLE
τ1
τ2
τ3

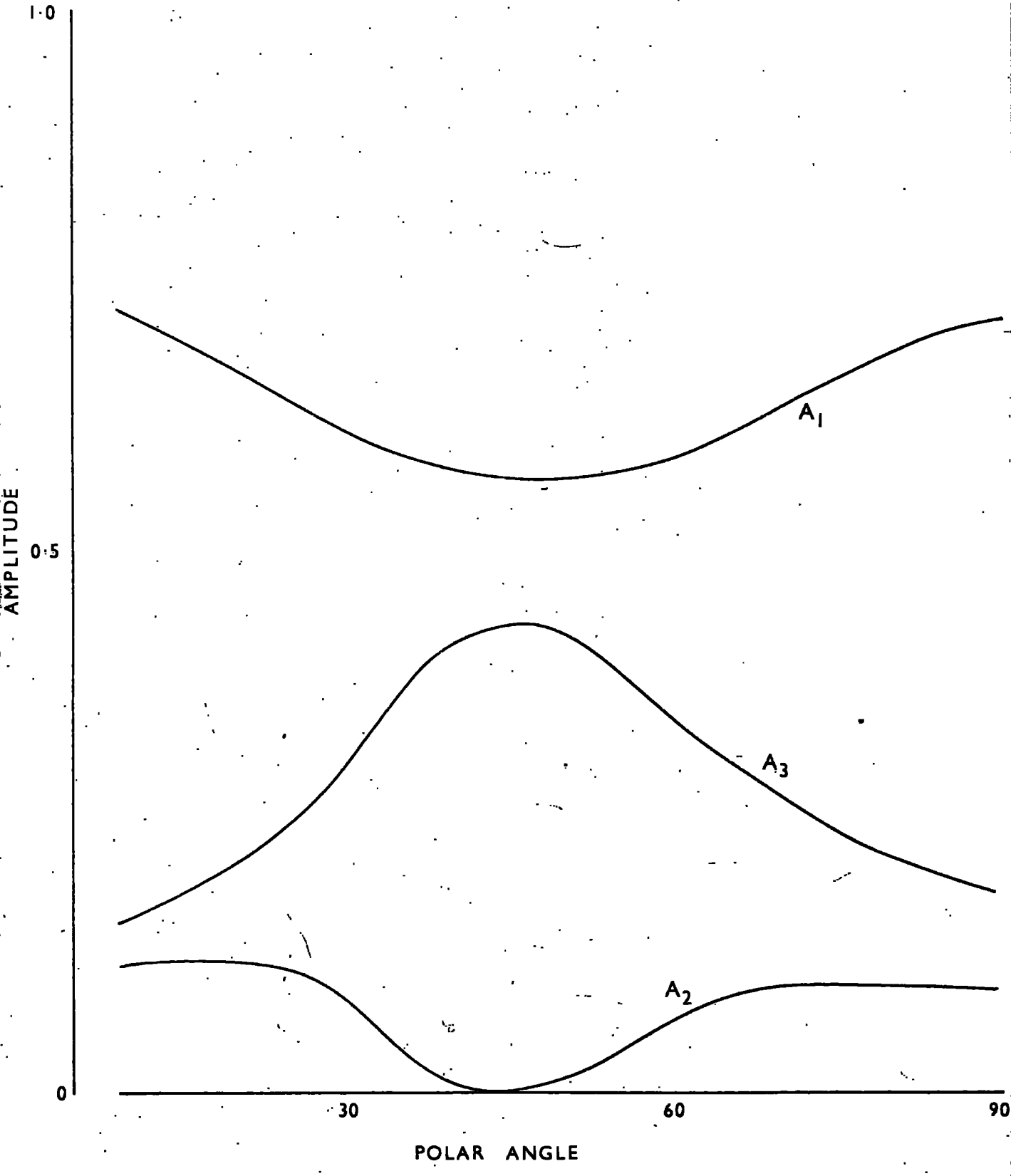
1·0
0·5
0
AMPLITUDE
A1
A3
A2
30
60
90
POLAR ANGLE

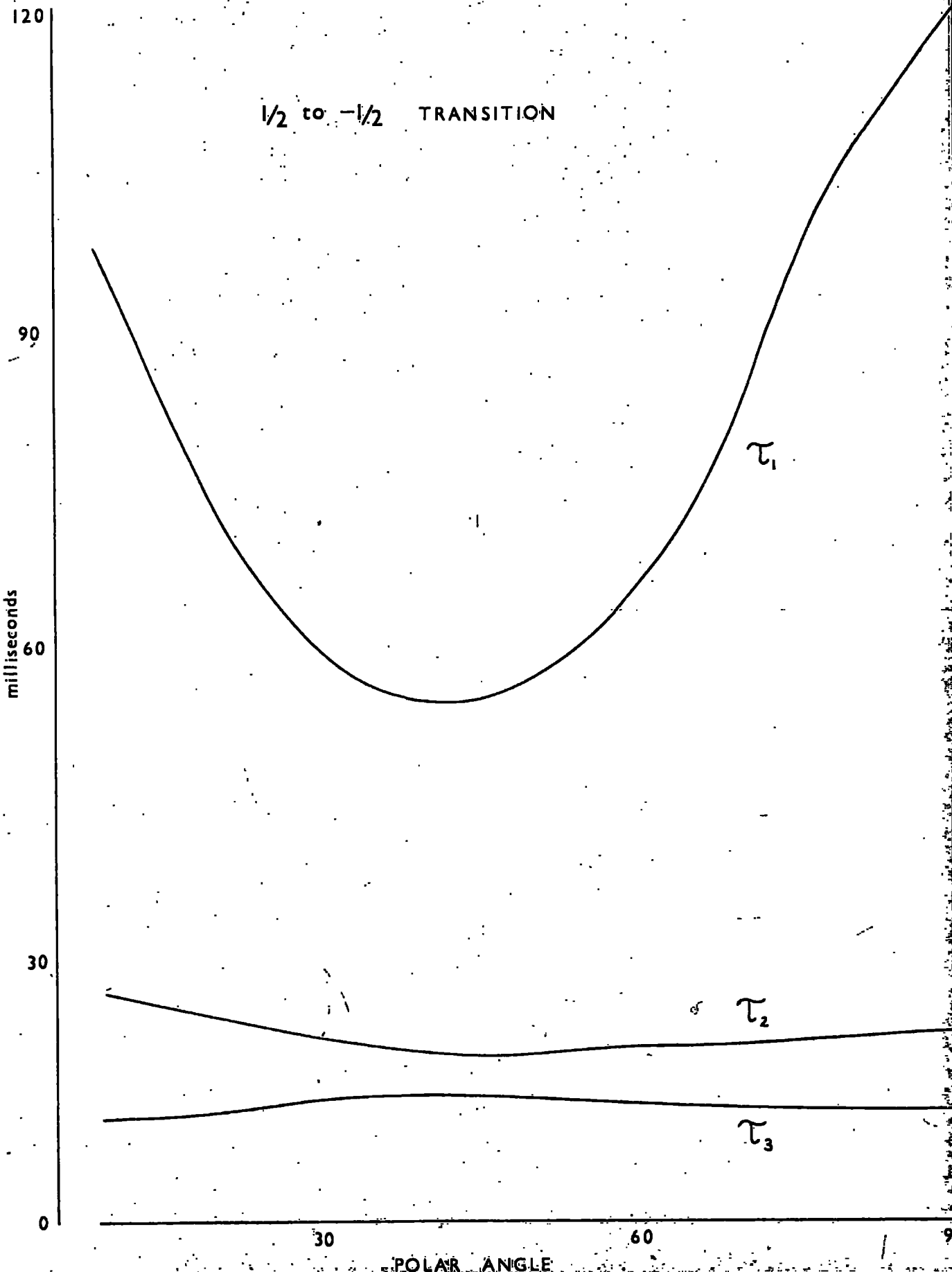
1/2 to −1/2 TRANSITION
120
90
60
30
0
milliseconds
τ_1
τ_2
τ_3
30
60
POLAR ANGLE

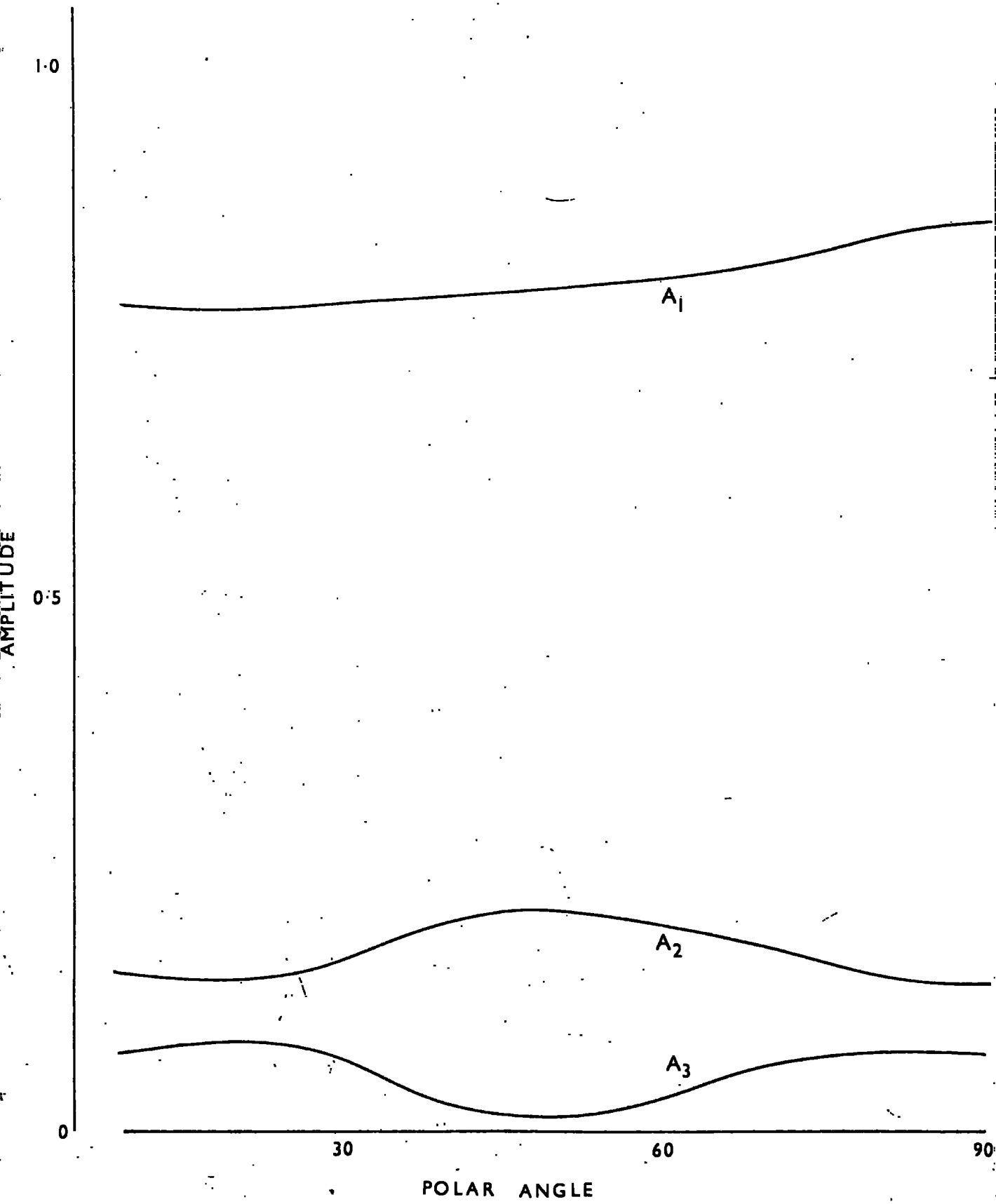
1·0
0·5
0
AMPLITUDE
A1
A2
A3
30
60
90
POLAR ANGLE

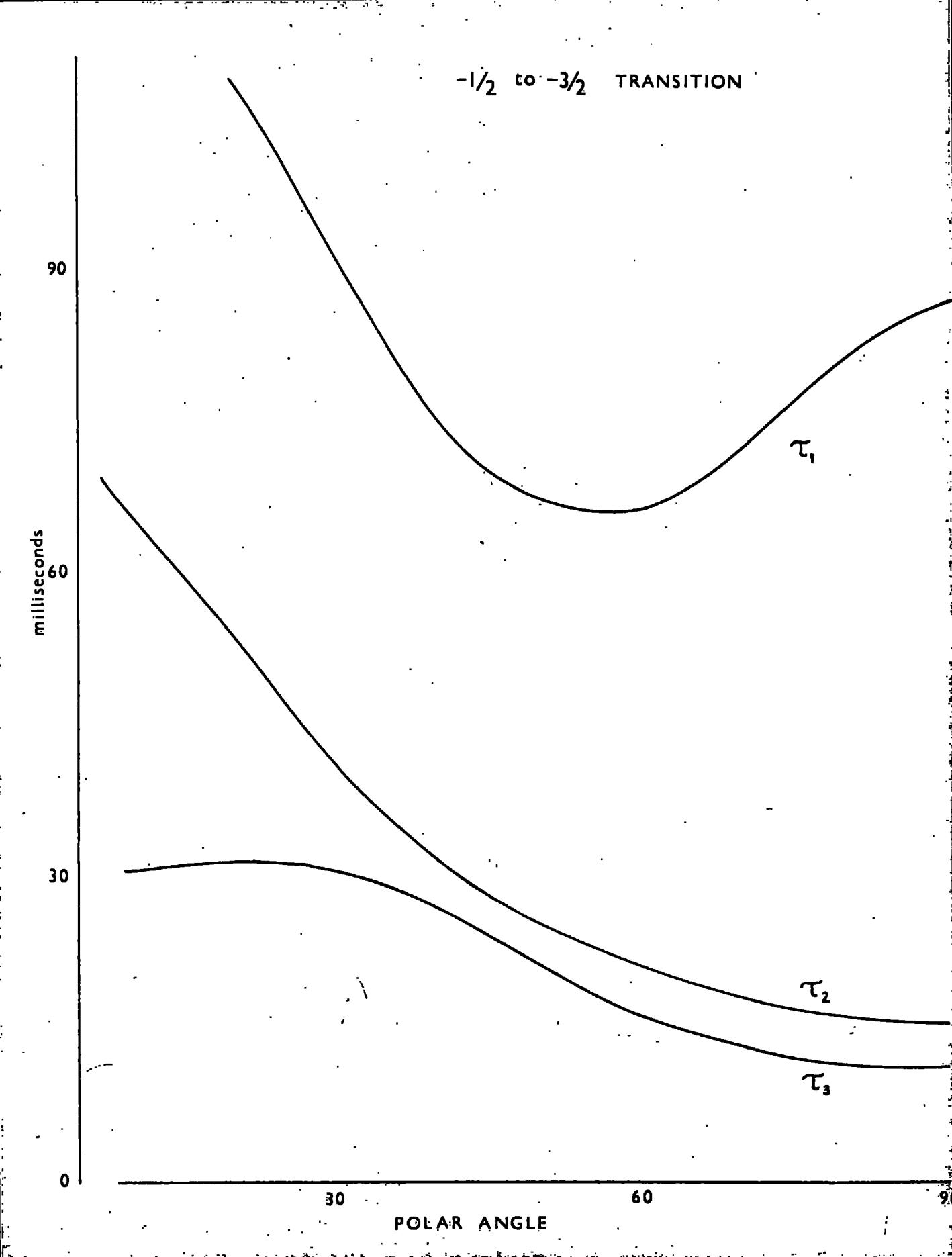
-1/2 to -3/2 TRANSITION
90
60
30
0
milliseconds
τ_1
τ_2
τ_3
30
60
POLAR ANGLE

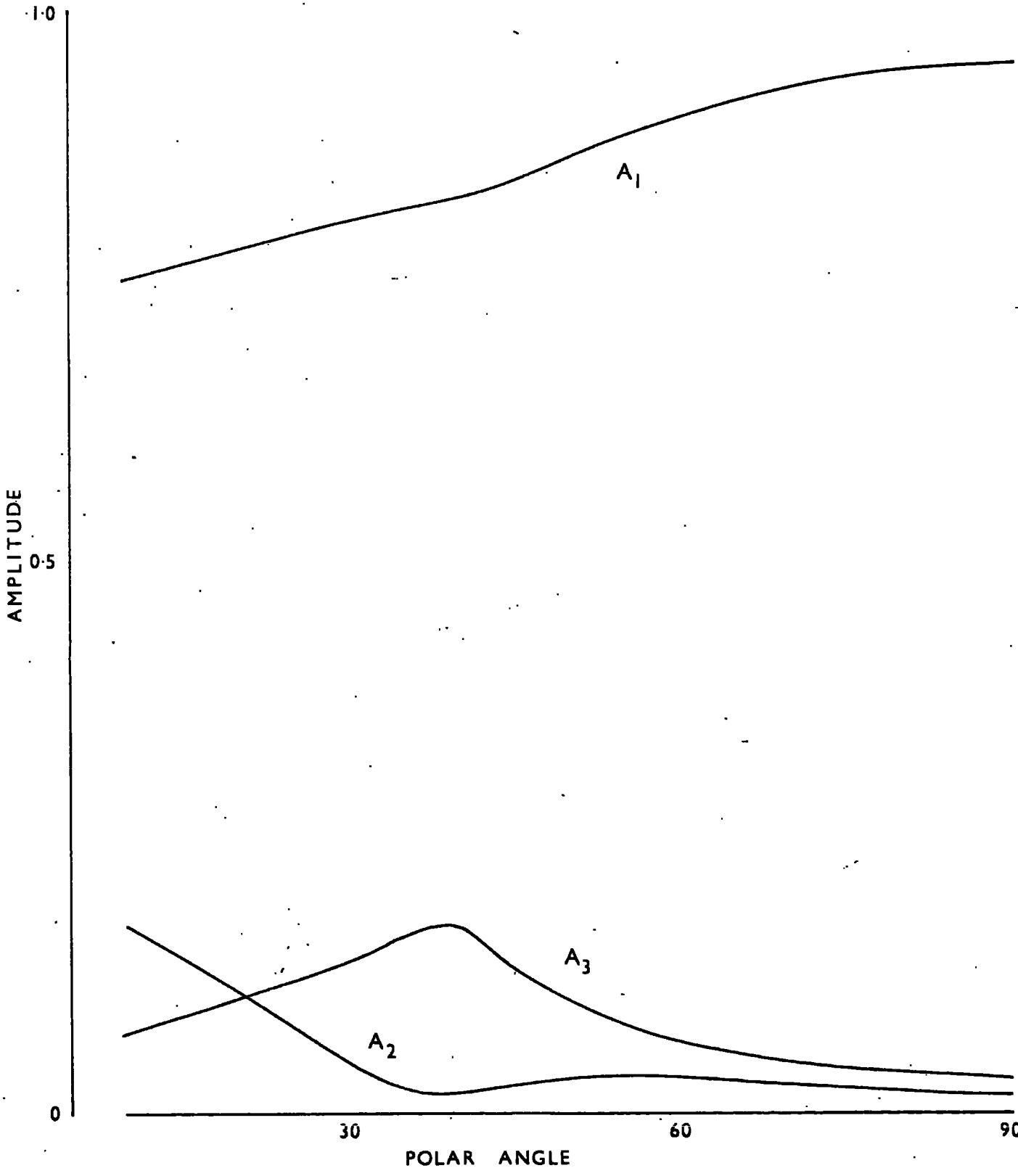
1·0
0·5
0
AMPLITUDE
A_1
A_2
A_3
30
60
90
POLAR ANGLE

APPENDIX 2

Research Note reprinted from

Journal of Scientific Instruments, 1965,

Vol. 42, 648.

Reprinted from the *Journal of Scientific Instruments*, Vol. 42, pp. 648–649, August 1965

A single-klystron superheterodyne receiver for use at millimetric wavelengths

G. BROWN, D. R. MASON and J. S. THORP
Department of Applied Physics, University of Durham
MS. received 12*th April* 1965, *in revised form* 12*th May* 1965

Abstract. A superheterodyne receiving system is described using a transmission crystal modulator instead of a separate klystron to generate the local oscillator signal. It has been used in paramagnetic resonance experiments at millimetric wavelengths. Instrumental line broadening is negligible and the signal-to-noise ratio is 30 db.

1. Experimental

The measurement of relaxation times in paramagnetic materials by the pulse saturation method (Davis *et al.* 1958) involves the use of at least two klystrons. A low-power klystron supplies the continuous monitor power, and a high-power klystron operating at the same frequency provides the saturating pulses. To enable weak transitions to be observed a superheterodyne receiver is usually used to amplify the resonance signal. Superheterodyne detection requires the presence of a local oscillator signal to beat with the incoming resonance signal, producing an intermediate-frequency oscillation in the balanced mixer. In conventional microwave superheterodynes a third klystron is used as the local oscillator; but, above about 35 Gc/s, maintaining a fixed frequency separation between three independent klystrons is an acute problem.

To overcome this difficulty a microwave signal is generated containing both the monitor and local oscillator frequencies. The transmission crystal modulator is driven at 45 Mc/s, amplitude-modulating the power incident from a 35 Gc/s reflex klystron, as shown in the figure. This produces low-power sidebands at 34955 Mc/s and 35045 Mc/s. The signal is then split, half going to the local oscillator input of the balanced mixer, the other half constituting the monitor signal. The transmission crystal modulator consists of a germanium point-contact diode (GEC type VX3136) mounted in the waveguide and fed from an external signal source. The intermediate frequency of 45 Mc/s is chosen to give minimum overall noise (Strum 1953). A similar method of generating sidebands in a microwave signal was used by Pound (1946) and others in connection with frequency stabilization circuits.

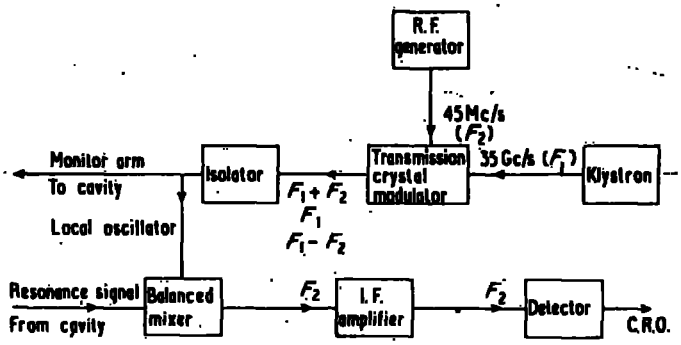

Block diagram of the receiving apparatus.

The signal returning from the microwave cavity consists of a 35 Gc/s carrier amplitude-modulated by both the resonance signal and a 45 Mc/s oscillation. In the balanced mixer this meets the local oscillator signal of 35 Gc/s amplitude-modulated at 45 Mc/s. The local oscillator sidebands beat with the incoming signal to produce, after detection in the balanced mixer, a 45 Mc/s i.f. carrier amplitude-modulated by the resonance signal. This is amplified by a conventional stagger-tuned circuit, and detected for cathode-ray oscilloscope presentation of the resonance.

2. Discussion

The presence in a microwave cavity of two additional frequencies 90 Mc/s apart will have the effect of broadening or splitting an absorption line of comparable frequency width. Examination of the line shape of the $+\frac{1}{2}$ to $-\frac{1}{2}$ transition in ruby with a 160 kc/s phase-sensitive detector system showed no detectable broadening. We therefore conclude from the sensitivity of this system that the power level of the sidebands is at least 30 db below carrier level. Placing the transmission crystal modulator in the local oscillator arm immediately before the balanced mixer removes the possibility of instrumental broadening due to the presence of sidebands in the cavity. However, it appears from present work that the efficiency of sideband generation is proportional to the incident 35 Gc/s power level over the range 5 to 20 mw. For this reason the transmission crystal modulator is placed as near the klystron as possible. The

power in the sidebands is dependent upon the level of 45 Mc/s drive to the modulator diode. At present the maximum available drive is 1 v r.m.s., the limit of the r.f. generator in use. Experiment suggests that this drive could be usefully increased.

The insertion loss of 3 db for the transmission crystal modulator was found to be independent of the r.f. generator output, and was almost entirely due to the modulator diode alone. Ideally it would be preferable to have a single frequency in the local oscillator arm. However, because the sideband power level is so low, the presence of F_1 serves to bias the balanced mixer crystals to the minimum noise condition.

3. Conclusion

The elimination of the local oscillator klystron simplifies the use of the microwave spectrometer for all forms of resonance experiments. The frequency separation of carrier and sidebands is constant, ensuring optimum performance of the superheterodyne at all times. The only bandwidth limitation of the present receiver is set by the highest frequency component of the resonance signal. This contrasts with the conventional superheterodyne in which the i.f. bandwidth is determined by the relative frequency instability of the monitor and local oscillator klystrons. The overall signal-to-noise ratio of the spectrometer and superheterodyne is 30 db, which compares favourably with conventional systems.

The modification described appears to be directly applicable to spectrometers operating at higher frequencies, where frequency instability is an even greater problem.

Acknowledgments

One of us (G. B.) wishes to thank the British Broadcasting Corporation for the award of a Research Scholarship, and the other (D. R. M.) wishes to thank the Department of Scientific and Industrial Research for the award of a maintenance grant.

References

Davis, C. F., Strandberg, M. W. P., and Kyhl, R. L., 1958, *Phys. Rev.*, **111**, 1268–72.

Pound, R. V., 1946, *Rev. Sci. Instrum.*, **17**, 490–505.

Strum, P. D., 1953, *Proc. Inst. Radio Engrs, N.Y.*, **41**, 875–89.

APPENDIX 3

Letter to Editor reprinted from

British Journal of Applied Physics 1964, 15, 775.

BRIT. J. APPL. PHYS., 1964, VOL. 15

Concentration and textural inhomogeneities in synthetic ruby

Abstract. Inhomogeneities of structure in synthetic ruby, grown by flame fusion from the vapour phase, have been studied by x-ray and etching techniques and correlated with chemically estimated variations in chromium concentration. The highest concentrations of chromium were found in those parts of the crystal where there was greatest mosaic misorientation and where the dislocation density was greatest.

1. Introduction

The ruby and sapphire boules examined were grown by flame fusion from the vapour phase (Jack and Stephenson unpublished) with the *c* axis along the growth direction. Specimens were cut perpendicular to the *c* axis having the boule outer surface and centre as ends. Concentration and texture comparisons were made on adjacent pairs of specimens.

2. Chemical analysis

Details of the methods used will be given separately (see also Dodson 1962). These enabled the chromium and iron contents to be determined in a series of volumes of about 10^{-3} cm^3 across the specimen. Although a very high chromium concentration was found near the boule outer surface (20 μg Cr per mg Al_2O_3) the concentration fell rapidly over a distance of about 2 mm towards the centre and thereafter remained approximately constant (0·35 μg Cr per mg Al_2O_3). Some iron was detected in a thin layer near the boule outer surface but in the central regions the concentration was generally less than 0·002 μg Fe per mg Al_2O_3. Similar variations in chromium concentration have been reported by Yonemitsu and Maruyama (1962) and by Dils *et al.* (1962).

3. Texture analysis

Crystalline textures of both ruby, Cr^{3+} in Al_2O_3, and sapphire, undoped Al_2O_3, were examined using x-ray methods (Thorp and Curtis 1964) and etching techniques (Scheuplein *et al.* 1960). Marked mosaic structures were found near the outside of the boules. The mosaic element volume was about 10^{-8} cm^3 and the relative misorientation between mosaic elements was as high as three degrees (figure 1†). The mosaic imperfection decreased over a few millimetres towards the centre and the remainder was of comparatively uniform single crystal texture. However, some fine scale mosaic structure was observed near the centre as shown by the split diffraction spots of figure 2.

Etch pit counts near the outer edges of the boules gave densities of up to $2·8 \times 10^5$ pits per cm^2, whereas in the central regions (figure 3), values of about $0·6 \times 10^5$ pits per cm^2 were found. The linear dimensions of the grains were about 10^{-2} cm which is of the same order as those of the mosaic elements, 10^{-2}–10^{-3} cm, obtained from the x-ray photographs.

4. Conclusions

The results suggest that variations in chromium concentration correspond to departures from crystalline perfection. The highest chromium concentrations coincide with the greatest dislocation densities occurring in these rubies near the outsides of the boules. In the more perfect central regions localized mosaic imperfections may cause occasional high chromium concentrations.

As sapphire and ruby show very similar mosaic distributions it appears that in ruby the chromium accumulates in the highly misoriented regions rather than that the imperfections

† Figures printed as a plate at end of issue.

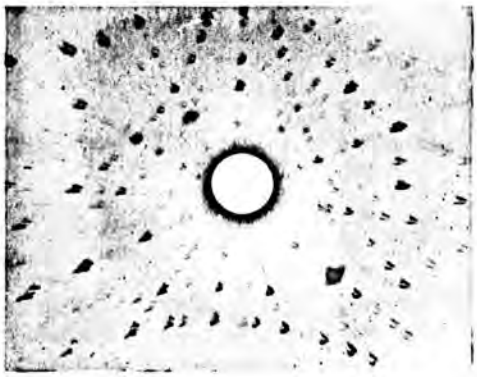

Figure 1. Specimen 1. Outer region of ruby boule (concentration 20 μg Cr per mg Al_2O_3). Back reflection photograph taken 0·5 mm from boule outer surface. Beam parallel to *c* axis, CuKα radiation.

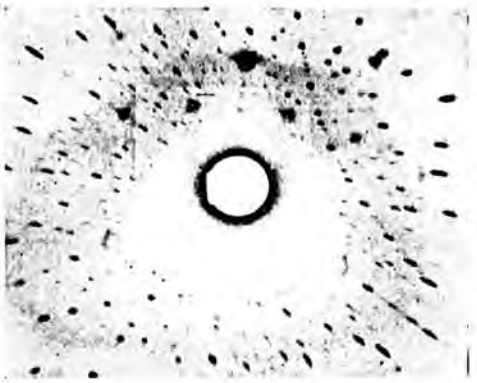

Figure 2. Specimen 1. Central region of ruby boule (concentration 0·35 μg Cr per mg Al_2O_3). Back reflection photograph taken 4·5 mm from boule outer surface. Beam parallel to *c* axis, CuKα radiation.

Figure 3. Etch pit pattern on (0001) face in central region of boule. Magnification ×160.

are caused by local high concentrations of chromium. Thus to achieve better homogeneity of doping the mosaic imperfection should be reduced, for example by better control of the temperature gradients occurring in the growing crystal.

Similar arguments apply to the distribution of iron impurity concentrations.

Acknowledgments

We wish to acknowledge the co-operation received from The Thermal Syndicate Ltd. throughout this work.

Two of us (D. A. C. and D. R. M.) also wish to thank the Department of Scientific and Industrial Research for its award of maintenance grants.

Department of Applied Physics,
University of Durham.

J. S. THORP
D. A. CURTIS
D. R. MASON

29th January 1964, *in revised form* 18*th March* 1964

DILS, R. R., MARTIN, G. W., and HUGGINS, R. A., 1962, *Appl. Phys. Letters*, **1**, 75.
DODSON, E. M., 1962, *Analyt. Chem.*, **34**, 966.
SCHEUPLEIN, R., and GIBBS, P., 1960, *J. Amer. Ceram. Soc.*, **43**, 458.
THORP, J. S., and CURTIS, D. A., 1964, *3rd International Symposium on Quantum Electronics, Paris* 1963. (New York: Columbia University Press), in the press.
YONEMITSU, H., and MARUYAMA, T., 1962, *J. Chem. Soc. Japan*, **65**, 1729.

References

Andrew, E.R., 1958, 'Nuclear Magnetic Resonance' p.14 (C.U.P.)

Baker, J.M., 1956, Proc.Phys.Soc., 69B., 633.

Basov, N.G., Prokhorov, A.M.,1955, Zh.Eksper,Teor.Fiz.,28,249.

Barron, T.H.K., Morrison, J.A., 1959, Phys.Rev. 115, 1439.

Betts, D.D., Bhatia, A.B., Horton G.K., 1956,Phys.Rev.104,42.

Bhimasenacker, J., 1950, Proc.Nat'l.Inst.Sci.India, 16, 241.

Bleaney, B., 1950., Proc.Roy.Soc., A.204, 203.

Bleaney B., Trenham, R.S., 1954, Proc.Roy.Soc., A.223, 1.

Bloch, F., 1946, Phys. Rev. 70, 460.

Bloembergen, N., Shapiro, S., Pershan, P.S., Artman, J.O., 1959, Phys.Rev., 114, 445.

Bogle, G.S., Symmons, H.F., 1959, Aust.J.Phys., 12, 1.

1961, Proc. Phys.Soc., 78, 812.

Brice, J.C., 1965,"The Growth of Crystals from the Melt" p.13 (North-Holland).

Brown, G., Mason D.R., Thorp, J.S., 1965, J.Sci.Inst.42, 648.

Brout R., Visscher, W., 1962, Phys. Rev. Lett. 9, 54.

Casimir, H.B.G., du Pre, F.K., 1938, Physica, 5, 507.

Castle, J.G., Chester P.F., Wagner, P.E., 1960,Phys.Rev.119,953.

Castle J.G., Feldman D.W., Klemens, P.G., 1961, Quantum Electronics (Columbia), 414.

Castle J.G., Feldman, D.W., Klemens, P.G., Weeks, R.A., 1963, Phys. Rev., 130, 577.

Chang, W.S.C., 1960, Quantum Electronics, (Columbia) 346.

Curtis, D.A., 1964, Ph.D. Thesis, Durham.

Davis, C.F., Strandberg, M.W.P., Kyhl, R.L., 1958, Phys. Rev. 111, 1268.

Dils, R.R., Martin, G.W., Huggins, R.A., 1962, Appl.Phys.Lett., 1, 75.

Dobrov, W.I., Browne, M.E., 1963, Paramagnetic Resonance, 447.

Dodd, D.M., Wood, D.L., Barns, R.L., 1964, J.A.P., 35, 1183.

Donoho, P.L., 1964, Phys.Rev. 133, A.1080.

Dugdale, D.E., 1965, Phys. Lett., 16, 226.

Einstein, A., 1917, Phys. Z., 18, 121.

Eschenfelder, A.H., Weidner, R.T., 1953, Phys. Rev., 92, 869.

Feng, S., Bloembergen, N., 1963, Phys. Rev., 130, 531.

Furukawa, G.T., Douglas, T.B., McCoskey, R.E., Ginnings, D.C., 1956, J. Res. Nat. Bur. Stand., 57, 67.

Gamble, F.T., Bartram, R.H., Young C.G., Gilliam, O.R., Levy, P.W. 1965, Phys. Rev., 138, A. 577.

Gorter, C.J., 1947, 'Paramagnetic Relaxation' (New York : Elsevier) p. 19.

Grant, W.J.C., 1964, Phys. Rev., 134, A.1554 et seq.

Grilly, E.R., 1962, Cryogenics, 226.

Heitler, W., Teller, E., 1936, Proc. Roy. Soc., 155, 629.

Hemphill, R.B., Donoho, P.L., 1963, See Donoho 1964.

Hoskins, R.H., Soffer, B.H., 1964, Phys. Rev., 133, A.490.

Jolley, D.G., McLaughlan, S.D., 1963, Nature, 199, 898.

Kapadnis, D.G., 1965, Physica, 22, 159.

Kask, N.E., Kornienko, L.S., Smirnov, A.I., 1963, Soviet Physics - Solid State 5, 1212.

Kiel A., Phys. Rev., 120, 137.

Klemens, P.G., 1962, Phys. Rev., 125, 1795.

Klemens, P.G., Castle, J.G., Feldman, D.W., 1963, Proc. 8th Int. Conf. on Low Temps. (Butterworth), 292.

Kochelaev, B.I., 1960, S.P. Doklady, 5, 349.

1961, S.P. Solid State 2, 1294.

Lambe, J., Kikuchi, C., 1960, Phys. Rev., 118, 71.

Lampe, D.R., Wagner, P.E., 1965, Bull. Am. Phys. Soc., 10, 488.

Lehman, H.W., Gunthard, H.H., J. Phys. Chem. Sol., 25, 941.

Levy, P.W., 1961, Disc. Faraday Soc., 31, 118.

Linares, R. C., 1965, J. Phys. Chem. Sol., 26, 1817.

Maiman, T.H., 1961, Phys. Rev., 123, 1145 et seq.

Manenkov, A.A., Milyaev, V.A., Prokhorov, A.M., 1962, S.P.-Solid State, 4, 280.

Mason, D.R., Thorp, J.S., 1966, Proc. Phys. Soc., 87, 49.

Maruyama, T., Matsuda, Y., 1964, J.Phys. Soc. Japan, 19, 1096.

Mattuck, R.D., Strandberg, M.W.P., 1960, Phys. Rev. 119, 1204.

Michel, R.E., 1960, J. Phys. Chem. Sol., 13, 164.

Mills, D.L., 1965, Phys. Rev., 1 A.1623.

Montroll, E.W., Potts, R.B., 1955, Phys. Rev., 100, 525.

Nisada, Y., 1964, J. Phys. Soc., Japan, 19, 2273.

1965, J. Phys. Soc., Japan, 20, 1390.

Orbach, R., 1961, Proc. Phys. Soc., 77, 821.

Orbach, R., Blume, M., 1962, Phys. Rev. Lett. 8, 478.

Pace, J.H., Sampson, D.F., Thorp, JωS., 1961, Proc. Phys. Soc., 77, 257.

Powell, R.L., Bunch, M.D., 1959 "Problems of Low Temperature Physics and Thermodynamics", p. 129.

Purcell, E.M., 1946, Phys. Rev., 69, 881.

Purcell, E.M., Pound, R.V., 1951, Phys. Rev., 81, 279.

Rogers, W. M., Powell, R.L., 1958, Nat. Bureau of Standards Circular No. 535.

Roitsin, A.B., 1962, S.P. - Solid State, 3, 2102.

1966, S.P. - Solid State, 7, 2566.

Rosenstock, H.B., 1962, J. Phys. Chem. Sol., 23, 659.

Scheuplein, R., Gibbs, P., 1960, J. Am. Ceram. Soc., 43, 458.

Schultz, G.V., 1964, Phys. Lett., 9, 301.

Schultz - du Bois, E.O., 1959, Bell Syst. Tech. J., 38, 271.

Schumacher, R.T., 1958, Phys. Rev. 112, 837.

Scovil, H.E.D., Feher, G., Seidel, H., 1957, Phys.Rev.105, 762.

Siegman, A.E., 1964, 'Microwave Solid-State Masers'.

Standley, K.J., Vaughan, R.A., 1965, Phys.Rev., 139, A1275.

1965, Proc.Phys.Soc.,86, 861.

Sugano, S., Tanabe, Y., 1958, J. Phys. Soc., Japan, 13, 880.

Thorp, J.S., Curtis, D.A., Mason, D.R., 1964, B.J.A.P.15, 775.

Topping, J., 1959, "Errors of Observation and their Treatment".

Van Vleck, J.H., 1940, Phys. Rev., 57, 426.

Vereschagin, L.F., Stardubstev, S.V., Ionusov, N.S., 1965, S.P. - Doklady, 9, 983.

Wachtman, J.B., Tefft, W.E., Lam., D.G., 1960, J.Res.Nat.Bur. Stand., 64A., 213.

Wachtman, J.B., Scuderi, T.G., Cleek, G.W., 1962, J.Am.Ceram. Soc., 45, 319.

Waller, J., 1932, Z. Phys., 79, 370.

Watkins, G.D., Feher, E., 1962, Bull. Am. Phys. Soc., 7, 29.

Weber, J., 1953, Trans. Inst. Radio. Engin. PGED - 3.

Zeverev, G.M., Prokhorov, A.M., Schevchenko, A.K., 1963, S.P. - Solid State, 4, 2297.

Ziman, J.M., 1954, Proc. Roy. Soc., A226, 436.

1959, ' Electrons and Phonons " O.U.P.

20 OCT 1966
LIBRARY